Electronic Supplementary Material (ESI) for Dalton Transactions.

Supporting information for:

Reactions of cyclonickelated complexes with hydroxylamines and TEMPO: isolation of new TEMPOH adducts of Ni(II) and their reactivities with nucleophiles and oxidants

*Rajib K. Sarker, and Davit Zargarian**

Département de chimie, Université de Montréal, Montréal (Québec), Canada H3C 3J7

zargarian.davit@umontreal.ca

RECEIVED DATE (to be automatically inserted after your manuscript is accepted if required according to the journal that you are submitting your paper to)

Table of Contents

1. General experimental considerations

All manipulations were carried out under a nitrogen atmosphere using standard Schlenk techniques and an inert-atmosphere box. The transfer/addition of all liquid reagents/reactants was performed with BRAND Transferpette® micropipettes (20-200 µL and 100-1000µL). Reported volumes should be considered to be within ±7 µL (for > 200 µL transfers) and ±3 µL (for < 200 µL transfers) of the measurements, with a >99% confidence level.[1] Solvents (CH_2Cl_2, DCM, tetrahydrofuran, THF, acetonitrile, MeCN, toluene, etc.) were dried by passage over a column of activated alumina, collected under nitrogen, and stored over 3 Å molecular sieves inside transfer/storage flasks equipped with high vacuum valves (Straus flasks). Et_3N was dried over CaH_2. The Ni^{II} precursor $[(i\text{-PrCN})NiBr_2]_n$ used throughout this study was prepared as reported previously.[2,3] Other reagents were purchased from Sigma-Aldrich or FisherSci and used without further purification.

The NMR spectra were recorded at 500 MHz (^1H), 125.72 MHz (^{13}C), and 202.4 MHz (^{31}P). Chemical shift values are reported in ppm (δ) and referenced internally to the residual solvent signals (^1H and ^{13}C: 1.94 and 118.26 ppm for CD_3CN; 7.26 and 77.16 for $CDCl_3$; 7.16 and 128.06 for C_6D_6) or externally (^{31}P: H_3PO_4 in D_2O, δ = 0). The minimal precision of the NMR spectra was found to be 0.3 Hz for ^1H, 0.7 Hz for ^{13}C and 2 Hz for ^{31}P.

Single crystals of complexes **3a**-**3d** and **7a** were grown from Et_2O solutions cooled to -35 °C. Whereas complex **5a** was grown from DCM-Hexane mixture and complex **6a** was grown from DCM-Et_2O mixture. The crystallographic data for all structures were collected on either a Bruker Microsource (Cu radiation) or a Bruker Venture Metaljet (Ga radiation) via the Bruker APEX II or APEX III[4] software packages. Cell refinement and data reduction were performed using SAINT.[5] An empirical absorption correction, based on multiple measurements of equivalent reflections, was applied using the program SADABS or TWINABS.[6] The space group was confirmed by the XPREP[7] routine in APEX. The structures were solved in OLEX[8] using the SHELX[9] suite and refined by full-matrix least squares with SHEXL. All non-hydrogen atoms were refined with anisotropic displacement parameters, whereas hydrogen atoms were set in calculated positions and refined via the riding model, with thermal parameters being 1.5 times that of the carbon bearing the H in question. All Thermal ellipsoid plots were drawn using OLEX.

2. Procedures for the synthesis of Ni-TEMPOH complexes **3a**-**3d**

[{κ^P,κ^C-(*i*-Pr)$_2$PO-(C$_6$H$_4$)}Ni(Br)(TEMPOH)], 3a. A 25 mL Schlenk flask containing 10 mL of DCM was charged with dimer [{κ^P,κ^C-(*i*-Pr)$_2$PO-C$_6$H$_4$}Ni(μ-Br)]$_2$ (95 mg, 0.137 mmol, 1.00 equiv) and Et$_2$NOH (27.5 µL, 0.273 mmol, 2.00 equiv). The resulting mixture was stirred overnight under inert atmosphere at room temperature. To this mixture was added TEMPO (43 mg, 0.273 mmol, 2 equiv) and the stirring was continued under the same conditions for 3 h. The final reaction mixture was placed under vacuum to remove all volatiles, and the resulting sticky yellow solid residue was treated with ca. 1 mL of Et$_2$O, filtered and the filtrate kept at -35 ˚C overnight. Brown crystals were separated and washed with cold hexane. Yield: 106 mg, 0.211 mmol, 77%. ^{1}H NMR (400 MHz, 20 °C, C$_6$D$_6$): δ 1.10 (s, 6H, CC*H*$_3$), 1.11 (br s, 6H, C*H*$_2$), 1.25(dd, 6H,$^3J_{HP}$ =14.3, $^3J_{HH}$ =7.0, CHC*H*$_3$), 1.54 (dd, 6H,$^3J_{HP}$ =17.1, $^3J_{HH}$ =7.2, CHC*H*$_3$), 1.75 (s, 6H, CC*H*$_3$), 2.24 (sept, 2H, PC*H*, J_{HH} = 7.1), 6.91 (dd, 1H, C3$_{Ar}$-*H*, $^3J_{HH}$ = 7.7, $^4J_{HH}$ = 1.1), 7.03 (t, 1H, $^3J_{HH}$ = 7.4, C4$_{Ar}$-*H*),), 7.09 (t, 1H,$^3J_{HH}$ = 7.3, C5$_{Ar}$-*H*),7.93 (d, 1H, C6$_{Ar}$-H, $^3J_{HH}$=7.6), 8.48 (br s, 1H, NH). ^{13}C{^{1}H} NMR (125.72 MHz, 20 °C, C$_6$D$_6$): δ 16.06 (s, 1C, CH*C*H$_3$), 17.16 (d, 2C, J_{PC} = 1.5, CH*C*H$_3$), 18.71 (d, 1C, J_{PC} = 3.9, CH*C*H$_3$), 20.69 (s, 2C, C*C*H$_3$), 28.81 (d, 2C, J_{PC} = 26.5, P*C*H) , 30.14 (s, 2C, C*C*H$_3$), 37.21 (s, 3C, *C*H$_2$), 66.27 (s, 2C, *C*CH$_3$), 110.05 (d, 1C, J_{PC} = 13.0, C3$_{Ar}$), 120.48 (d, 1C, J_{PC} = 2.3, C4/5$_{Ar}$), 126.64 (s, 1C, C5/4$_{Ar}$), 134.28 (d, 1C, J_{PC} = 35.8, C1/6$_{Ar}$), 134.83 (d, 1C, J_{PC} = 3.9, C6/1$_{Ar}$), 167.64 (d, 1C, J_{PC} = 13.4, C2$_{Ar}$). ^{31}P{^{1}H} NMR (202.4 MHz, 20 °C, C$_6$D$_6$): δ 201.49 (s, 1P). Anal. calc. for C$_{21}$H$_{37}$BrNNiO$_2$P: C, 49.94; H, 7.38, N, 2.77. Found: C, 49.72; H, 7.32; N, 2.72.

[{κ^P,κ^C-(*i*-Pr)$_2$PO-(5-Cl-C$_6$H$_3$)}Ni(Br)(TEMPOH)], 3b. A 25 mL Schlenk flask containing 10 mL of DCM was charged with TEMPO (36 mg, 0.230 mmol, 2.00 equiv) and Et$_2$NOH (23.1 µL, 0.230 mmol, 2.00 equiv). The resulting mixture was stirred for 20 min under inert atmosphere at room temperature, followed by addition of the dimeric precursor [{κ^P,κ^C-(*i*-Pr)$_2$PO-(5-Cl-C$_6$H$_3$)}Ni(μ-Br)]$_2$ (88 mg, 0.115 mmol, 1 equiv) and continued stirring for 2 h under the same conditions. The final reaction mixture was placed under vacuum to remove all volatiles, and the resulting sticky dark brown solid residue was treated with ca. 1 mL of Et$_2$O, filtered and the filtrate kept at -35 ˚C overnight. Brown crystals were separated and washed with cold hexane. Yield: 57 mg, 0.106 mmol, 46%. ^{1}H NMR (400 MHz, 20 °C, C$_6$D$_6$): δ 1.03 (s, 6H, CC*H*$_3$), 1.08 (br s, 6H, C*H*$_2$), 1.18 (dd, 6H, $^3J_{HP}$ =14.5, $^3J_{HH}$ =6.9, CHC*H*$_3$), 1.48 (dd, 6H,$^3J_{HP}$ =17.2, $^3J_{HH}$ =7.3, CHC*H*$_3$), 1.70 (s, 6H,CC*H*$_3$), 2.16 (ps oct, 2H, PC*H*, $^3J_{HH}$ = 7.0), 6.95 (d, 1H, C6$_{Ar}$-*H*, $^4J_{HH}$ = 2.0), 7.05 (d,

1H,$^{3}J_{HH}$ = 8.3, C3$_{Ar}$-*H*),), 7.74 (dd, 1H,$^{3}J_{HH}$ = 8.3, $^{4}J_{HH}$ = 1.6, C4$_{Ar}$-*H*), 8.35 (br s, 1H, N-*H*). ^{13}C{^{1}H} NMR (125.72 MHz, 20 °C, C_6D_6): δ16.00 (s, 1C, CH*C*H$_3$), 17.02 (d, 1C, $^{2}J_{PC}$= 1.7, CH*C*H$_3$), 18.55 (d, 2C, $^{2}J_{PC}$= 3.7, CH*C*H$_3$), 20.59 (s, 2C, C*C*H$_3$), 28.79 (d, 1C, $^{2}J_{PC}$= 26.4, P*C*H) , 30.10 (s, 2C, C*C*H$_3$), 37.17 (s, 1C, CH$_2$), 66.32 (s, 2C, *C*CH$_3$), 110.65 (d, $^{2}J_{PC}$= 26.4, 1C, C6$_{Ar}$), 120.45 (d, 1C, $^{2}J_{PC}$ = 2.1, 1C, C3$_{Ar}$), 131.90 (s, 1C, C5$_{Ar}$), 132.69 (d, J_{PC} = 36.1, 1C, C1$_{Ar}$), 135.41 (d, 1C, J_{PC} = 4.07, 1C, C4$_{Ar}$), 167.56 (d, J_{PC} = 14.4, 1C, C2$_{Ar}$) . ^{31}P{^{1}H} NMR (202.4 MHz, 20 °C, C_6D_6): δ203.02 (s, 1P). Anal. calc. for $C_{21}H_{36}BrClNNiO_2P$: C, 46.75; H, 6.73; N, 2.60. Found: C, 46.57; H, 6.81; N, 2.53.

[{κ^P,κ^C-(*i*-Pr)$_2$PO-(5-OMe-C$_6$H$_3$)}Ni(Br)(TEMPOH)], 3c. A 25 mL Schlenk flask containing 10 mL of DCM was charged with TEMPO (29 mg, 0.186 mmol, 2.00 equiv) and Et_2NOH (18.7 µL, 0.186 mmol, 2.00 equiv). The resulting mixture was stirred for 20 min under inert atmosphere at room temperature, followed by addition of the dimeric precursor [{κ^P,κ^C-(*i*-Pr)$_2$PO-(5-OMe-C$_6$H$_3$)}Ni(μ-Br)]$_2$ (70 mg, 0.093 mmol, 1 equiv) and continued stirring for 2 h under the same conditions. The final reaction mixture was placed under vacuum to remove all volatiles, and the resulting sticky dark brown solid residue was treated with ca. 1 mL of Et_2O, filtered and the filtrate kept at -35 ˚C overnight. Brown crystals were separated and washed with cold hexane. Yield: 44 mg, 0.082 mmol, 43%. ^{1}H NMR (400 MHz, 20 °C, C_6D_6): δ 1.10 (s, 6H, CC*H*$_3$), 1.12 (br s, 6H, C*H*$_2$), 1.27 (dd, 6H, $^{3}J_{HP}$ =14.4, $^{3}J_{HH}$ = 7.0, CHC*H*$_3$), 1.57 (dd, 6H, $^{3}J_{HP}$ = 17.0, $^{3}J_{HH}$ =7.2, CHC*H*$_3$), 1.77 (s, 6H, CC*H*$_3$), 2.25 (ps oct, 2H, $^{3}J_{HH}$ = 7.1, PC*H*), 3.39 (s, 3H, OCH$_3$), 6.65 (d, 1H, C3$_{Ar}$-*H*, $^{4}J_{HH}$ = 2.6), 6.73 (dd, 1H, $^{3}J_{HH}$ = 8.5, $^{4}J_{HP}$ = 2.0, C6$_{Ar}$-*H*), 7.78 (dd, 1H, $^{3}J_{HH}$ = 8.6, $^{4}J_{HH}$ = 1.7, C4$_{Ar}$-*H*), 8.48 (s, 1H, N-*H*). ^{13}C{^{1}H} NMR (125.72 MHz, 20 °C, C_6D_6): δ 16.07 (s, 1C, CH*C*H$_3$), 17.17 (d, 1C, $^{2}J_{PC}$= 1.5, CH*C*H$_3$), 18.71 (d, 2C, $^{2}J_{PC}$ = 3.9, CH*C*H$_3$), 20.66 (s, 2C, C*C*H$_3$), 28.75 (d, 1C, $^{2}J_{PC}$= 26.3, P*C*H) , 30.17 (s, 2C, C*C*H$_3$), 37.21 (s, 3C, *C*H$_2$), 54.86 (s, 1C, O*C*H$_3$), 66.25 (s, 2C, *C*CH$_3$), 97.06 (d, $^{2}J_{PC}$ = 13.9, 1C, C3$_{Ar}$), 106.77 (s, 1C, C6$_{Ar}$), 123.30 (d, 1C, $^{2}J_{PC}$ = 37.7, 1C, C5$_{Ar}$), 134.67 (d, J_{PC} = 4.3, C4$_{Ar}$), 160.42 (s, 1C, C1$_{Ar}$), 167.69 (d, J_{PC} = 14.9, 1C, C2$_{Ar}$) . ^{31}P{^{1}H} NMR (202.4 MHz, 20 °C, C_6D_6): δ 200.80 (s, 1P). Anal. calc. for $C_{22}H_{39}BrNNiO_3P.Et_2O$: C, 51.26; H, 8.11, N, 2.30. Found: C, 51.06; H, 7.61; N, 2.62.

[{κ^P,κ^C-(*i*-Pr)$_2$PO-(4-MeO-C$_{10}$H$_5$)}Ni(Br)(TEMPOH)], 3d. A 25 mL Schlenk flask containing 10 mL of DCM was charged with TEMPO (26 mg, 0.167 mmol, 2.00 equiv) and Et_2NOH (16.8 µL, 0.167 mmol, 2.00 equiv). The resulting mixture was stirred for 20 min under inert atmosphere

at room temperature, followed by addition of the dimeric precursor [{κ^P,κ^C-(*i*-Pr)$_2$PO-(OMe-1-Nap)}Ni(μ-Br)]$_2$ (71 mg, 0.083 mmol, 1 equiv) and continued stirring for 2 h under the same conditions. The final reaction mixture was placed under vacuum to remove all volatiles, and the resulting sticky dark brown solid residue was treated with ca. 1 mL of Et_2O, filtered and the filtrate kept at -35 °C overnight. Brown crystals were separated and washed with cold hexane. (Yield: 50 mg, 0.086 mmol, 51%). ^{1}H NMR (400 MHz, 20 °C, C_6D_6): δ 1.12 (s, 6H, CC*H*$_3$), 1.14 (br s, 6H, C*H*$_2$), 1.28 (dd, 6H, $^3J_{HP}$ =14.3, $^3J_{HH}$ =7.0, CHC*H*$_3$), 1.58 (dd, 6H, $^3J_{HP}$ = 17.2, $^3J_{HH}$ = 7.2, CHC*H*$_3$), 1.79 (s, 6H, CC*H*$_3$), 2.29 (ps oct, 2H, PC*H*, $^3J_{HH}$ = 7.1), 3.86 (s, 3H, OC*H*$_3$), 7.33 - 7.38 (m, 2H, C_{Ar}-*H*), 7.46 (d, 1H, $^3J_{HH}$ = 1.5, C_{Ar}-*H*),), 8.15 - 8.19 (m, 1H, C_{Ar}-*H*), 8.54 (br s, 1H, N-*H*), 8.59 - 8.64 (m, 1H, C_{Ar}-*H*). ^{13}C{^{1}H} NMR (125.72 MHz, 20 °C, C_6D_6): δ 16.09 (s, 1C, C*C*H$_3$), 17.20 (d, 1C, $^2J_{PC}$= 1.7, CH*C*H$_3$), 18.74 (d, 2C, $^2J_{PC}$= 3.9, CH*C*H$_3$), 20.53 (s, 2C, C*C*H$_3$), 28.94 (d, 1C, $^2J_{PC}$= 26.3, P*C*H), 30.24 (s, 2C, *C*H$_2$), 37.22 (s, 1C, *C*CH$_3$), 55.32 (s, 1C, O*C*H$_3$), 66.36 (s, 2C, C), 109.47 (d, $^2J_{PC}$ = 4.3, 1C, C6$_{Ar}$), 122.07 (d, 1C, $^2J_{PC}$ = 12.4, 1C, C_{Ar}), 122.41 (s, C_{Ar}), 122.73 (s, C_{Ar}), 124.08 (s, C_{Ar}), 125.52 (s, C_{Ar}), 126.16 (s, C_{Ar}), 148.20 (d, J_{PC} = 3.0, C_{Ar}), 156.03 (d, 1C, J_{PC} = 13.8, C2$_{Ar}$). ^{31}P{^{1}H} NMR (202.4 MHz, 20 °C, C_6D_6): δ 199.38 (s, 1P). Anal. calc. for $C_{26}H_{41}BrNNiO_3P$: C, 53.36; H, 7.06; N, 2.39. Found: C, 53.26; H, 7.10; N, 2.38.3.

3. Procedures for the synthesis of complexes **5a**, **6a**, & **7a**.

[{κ^P,κ^C-(*i*-Pr)$_2$PO-(C$_6$H$_4$)}Ni(Br)(C$_4$H$_9$NO)], 5a. Method A: A 25 mL Schlenk flask containing 10 mL of DCM was charged with TEMPO (43 mg, 0.274 mmol, 2 equiv) and Et_2NOH (27.6 µL, 0.274 mmol, 2 equiv). The resulting mixture was stirred for 20 min under inert atmosphere at room temperature, followed by addition of the dimeric precursor [{κ^P,κ^C-(*i*-Pr)$_2$PO-C$_6$H$_4$}Ni(μ-Br)]$_2$ (95 mg, 0.137 mmol, 1 equiv), continued stirring for 20 min under the same conditions before adding morpholine (236 µL, 2.74 mmol, 20 equiv) and continued stirring for 2 h as before. The final reaction mixture was placed under vacuum to remove all volatiles, and the resulting sticky solid residue was treated with ca. 1 mL of DCM and filtered. The filtrate was layered with hexane and finally the filtrate was kept at -35 °C overnight. Brown crystals were separated and washed with cold hexane. **Method B:** A 25 mL Schlenk flask containing 10 mL of DCM was charged with the dimeric precursor [{κ^P,κ^C-(*i*-Pr)$_2$PO-C$_6$H$_4$}Ni(μ-Br)]$_2$ (95 mg, 0.137 mmol, 1 equiv) and morpholine (236 µL, 2.74 mmol, 20 equiv). This mixture was stirred for 2 h and then placed under vacuum to remove all volatiles. The resulting sticky solid residue was treated with ca. 1 mL of DCM and filtered. The filtrate was layered with hexane and finally the filtrate was kept at -35 °C

overnight. Brown crystals were separated and washed with cold hexane. Yield: 58 mg, 0.132 mmol, 48%.

^{1}H NMR (400 MHz, 20 °C, C_6D_6): δ 1.21 (dd, 6H, $^{3}J_{HP}$ = 14.6, $^{3}J_{HH}$ = 7.0, CHCH_3), 1.53 (dd, 6H,$^{3}J_{HP}$ = 17.1, $^{3}J_{HH}$ = 7.2, CHCH_3), 2.19 - 2.36 (m, 3H, overlap of N-*H* and PC*H*), 2.45 (br s, 2H, CH_2), 2.76 (br s, 2H, CH_2), 3.28 (br s, 2H, CH_2), 3.50 (br s, 2H, CH_2) 6.68 (d, 1H, $^{3}J_{HH}$ = 7.6, C3$_{Ar}$-*H*), 6.87 (tt, 1H, $^{3}J_{HH}$ = 6.2, $^{4}J_{HH}$ = 1.2, C4/5$_{Ar}$-*H*), 6.91 (dd, 1H, $^{3}J_{HH}$ = 7.9, $^{4}J_{HH}$ = 1.3, C6$_{Ar}$-*H*,), 7.05 (tt, 1H, $^{3}J_{HH}$ = 7.5, $^{4}J_{HH}$ = 1.4, C5/4$_{Ar}$-*H*). ^{13}C{^{1}H} NMR (125.72 MHz, 20 °C, C_6D_6): δ17.10 (d, 2C, J_{PC} = 1.8, CH*C*H$_3$), 18.81 (d, 2C, J_{PC} = 3.3, CH*C*H$_3$), 28.9 (d, 1C, J_{PC} = 27.1, P*C*H), 47.37 (s, 2C, *C*H$_2$), 68.01 (s, 2C, *C*H$_2$) , 111.24 (d, 1C, J_{PC} = 12.6, *C*4/5$_{Ar}$), 121.46 (d, 1C, J_{PC} = 2.3, *C*5/4$_{Ar}$), 127.29 (s, 1C, *C*6$_{Ar}$), 133.43 (d, 1C, J_{PC} = 3.2, *C*3$_{Ar}$), 135.05 (d, 1C, J_{PC} = 32.1, C1$_{Ar}$), 168.29 (d, 1C, J_{PC} = 12.9, C2$_{Ar}$). ^{31}P{^{1}H} NMR (202.4 MHz, 20 °C, C_6D_6): δ 196.03 (s, 1P), 193.06 (s, 1P); integration ratio 100:8. Anal. calc. for $C_{16}H_{27}Br_{0.93}Cl_{0.07}NNiO_2P$: C, 44.49; H, 6.25; N, 3.22. Found: C, 44.29; H, 6.19; N, 3.28.

NB: We believe that the minor ^{31}P singlet at 193.06 ppm is due to the presence of the Ni-Cl analogue of **5a** that originates from the presence of the corresponding Ni-Cl analogue in the specific batch of dimeric precursor **1a** used for this synthesis. Previous experience with this family of complexes has shown that the dimeric precursors **1** obtained from the C-H nickelation of the aryl phosphinite ligands R_2OPAr often contain variable amounts of its Ni-Cl analogues if R_2OPAr are contaminated with HCl•NEt_3 generated during their preparation from ArOH, $ClPR_2$, and NEt_3.

[{κ^P,κ^C-(*i*-Pr)$_2$PO-(C$_6$H$_4$)}Ni(imidazole)$_2$][Br], 6a. Method A: A 25 mL Schlenk flask containing 10 mL of DCM was charged with TEMPO (34 mg, 0.219 mmol, 2 equiv) and Et_2NOH (22.0 µL, 0.219 mmol, 2 equiv). The resulting mixture was stirred for 20 min under inert atmosphere at room temperature, followed by addition of the dimeric precursor [{κ^P,κ^C-(*i*-Pr)$_2$PO-C$_6$H$_4$}Ni(μ-Br)]$_2$ (76 mg, 0.110 mmol, 1 equiv), continued stirring for 20 min under the same conditions before adding imidazole (30 mg, 0.439 mmol, 4 equiv) and continued stirring for 1 h as before. The final reaction mixture was placed under vacuum to remove all volatiles, and the resulting sticky yellow solid residue was treated with ca. 1 mL of DCM and Et_2O mixture, filtered and the filtrate kept at -35 ˚C overnight. Brown crystals were separated and washed with cold hexane. **Method B:** A 25 mL Schlenk flask containing 10 mL of DCM was charged with the dimeric precursor [{κ^P,κ^C-(*i*-Pr)$_2$PO-C$_6$H$_4$}Ni(μ-Br)]$_2$ (76 mg, 0.110 mmol, 1 equiv) and imidazole

(30 mg, 0.439 mmol, 4 equiv). This mixture was stirred for 2 h and then placed under vacuum to remove all volatiles. The resulting sticky yellow solid residue was treated with ca. 1 mL of DCM and Et_2O mixture, filtered, and the filtrate kept at -35 ˚C overnight. Brown crystals were separated and washed with cold hexane. Yield: 66 mg, 0.137 mmol, 62%.

^{1}H NMR (400 MHz, 20 °C, C_6D_6): δ 1.30 (dd, 6H,$^3J_{HP}$ = 14.5, $^3J_{HH}$ = 7.0, CHCH_3), 1.63 (dd, 6H,$^3J_{HP}$ = 17.2, $^3J_{HH}$ = 7.2, CHCH_3), 2.40 (ps oct, 2H, PC*H*, $^3J_{HH}$ = 7.1), 5.96 (br s, C_{Ar}-*H*), 6.30 (td, 1H, C3$_{Ar}$-*H*, $^3J_{HH}$ = 7.7, $^4J_{HH}$ = 1.3), 6.68 (tt, 1H,$^3J_{HH}$ = 7.3, J_{HH} = 1.1, C4/5$_{Ar}$-*H*), 6.92 (dd, 1H, $^3J_{HH}$ = 7.9, $^4J_{HH}$ = 1.3, C6$_{Ar}$-*H*), 7.00 (tt, 1H, $^3J_{HH}$ = 7.8, $^4J_{HH}$ = 1.4, C5/4$_{Ar}$-H), 7.13 (br s, C_{Ar}-*H*), 7.20 (br s, C_{Ar}-*H*), 8.56 (br s, 1H, N-*H*). ^{13}C{^{1}H} NMR (125.72 MHz, 20 °C, C_6D_6): δ17.16 (d, 2C, J_{PC} = 1.8, CH*C*H$_3$), 18.87 (d, 2C, J_{PC} = 3.4, CH*C*H$_3$), 28.82 (d, 2C, J_{PC} = 27.1, P*C*H), 110.48 (d, C, J_{PC} = 12.9, *C*6$_{Ar}$) , 115.80 (s, C, C_{Ar}), 121.11 (d, C, J_{PC} = 2.3, *C*4/5$_{Ar}$), 126.88 (s, C, *C*5/4$_{Ar}$), 128.84 (s, C, C_{Ar}), 135.72 (d, C, J_{PC} = 33.9, C1$_{Ar}$), 136.87 (s, C, C_{Ar}), 138.95 (d, C, J_{PC} = 2.6, C3$_{Ar}$), 168.38 (d, 1C, J_{PC} = 13.3, C2$_{Ar}$). ^{31}P{^{1}H} NMR (202.4 MHz, 20 °C, C_6D_6): δ 194.93 (s, 1P).

[{κ^P,κ^C-(*i*-Pr)$_2$PO-(C$_6$H$_4$)}Ni(OCOCF$_3$)(TEMPOH)], 7a: A 50 mL Schlenk flask containing 10 mL of DCM was charged with TEMPO (42.8 mg, 0.274 mmol, 2 equiv) and Et_2NOH (27.6 µL, 0.274 mmol, 2 equiv). The resulting mixture was stirred for 20 min under inert atmosphere at room temperature, followed by addition of the dimeric precursor [{κ^P,κ^C-(*i*-Pr)$_2$PO-C$_6$H$_4$}Ni(μ-Br)]$_2$ (95 mg, 0.137 mmol, 1 equiv),), continued stirring for 20 min under the same conditions before adding $AgOCOCF_3$ (60.5 mg, 0.274 mmol, 2 equiv) and continued stirring for 2 h as before. The final reaction mixture was placed under vacuum to remove all volatiles, and the resulting sticky yellow solid residue was treated with ca. 1 mL of Et_2O, filtered and the filtrate kept at -35 ˚C overnight. Yellow crystals were separated and washed with cold hexane. Yield: 57.5 mg, 0.107 mmol, 39%) ^{1}H NMR (400 MHz, 20 °C, C_6D_6): δ 1.05 (s, 6H, CCH_3), 1.15 (br m, 6H, CH_2), 1.19 (dd, 6H,$^3J_{HP}$ =13.2, $^3J_{HH}$ =7.0, CHCH_3), 1.49 (dd, 6H,$^3J_{HP}$ =18.5, $^3J_{HH}$ =7.3, CHCH_3), 1.52 (s, 6H, CCH_3), 2.48 (dm, 2H, PC*H*, $^2J_{HH}$ = 7.1, J_{HH} = 2.3), 6.78 (dd, 1H, C3$_{Ar}$-*H*, $^3J_{HH}$ = 7.6, $^4J_{HH}$ = 1.5), 6.97 (pstpst, 1H,$^3J_{HH}$ ~ $^3J_{HH}$ ~ 7.4, $^4J_{HH}$ ~ J_{PH} = 1.1, C4/5$_{Ar}$-*H*), 7.03 (pstpst, 1H,$^3J_{HH}$ ~ $^3J_{HH}$ ~ 7.3, $^4J_{HH}$ ~ J_{PH} = 1.6, C5/4$_{Ar}$-*H*), 7.74 (pstd, 1H, $^3J_{HH}$ ~ $^3J_{HH}$ ~ 7.6, J_{PH}=1.6, C6$_{Ar}$-H), 7.86 (br s, 1H, NH). ^{13}C{^{1}H} NMR (125.72 MHz, 20 °C, C_6D_6): δ15.91 (s, 1C, CH*C*H$_3$), 16.95 (d, 2C, J_{PC} = 3.5, CH*C*H$_3$), 19.00 (d, 1C, J_{PC} = 5.7, CH*C*H$_3$), 19.74 (s, 2C, C*C*H$_3$), 29.16 (d, 2C, J_{PC} = 24.4, P*C*H) , 29.59 (s, 2C,

C*C*H$_3$), 37.46 (s, 3C, *C*H$_2$), 65.60 (s, 2C, *C*CH$_3$), 110.08 (d, 1C, J_{PC} = 12.0, C3$_{Ar}$), 120.41 (d, 1C, J_{PC} = 2.2, C4/5$_{Ar}$), 127.03 (s, 1C, C5/4$_{Ar}$), 134.90 (d, 1C, J_{PC} = 3.3, C6$_{Ar}$), 160.59 (d, 1C, J_{PC} = 35.8, C1$_{Ar}$), 168.47 (d, 1C, J_{PC} = 12.0, C2$_{Ar}$). ^{19}F{^{1}H} NMR spectrum of **7a** (C_6D_6): -74.3 (s). ^{31}P{^{1}H} NMR (202.4 MHz, 20 °C, C_6D_6): δ 199.84 (s, 1P). Anal. calc. for $C_{23}H_{37}F_3NNiO_4P$: C, 51.33; H, 6.93; N, 2.60. Found: C, 50.46; H, 7.45; N, 2.56.

4. NMR spectra of characterized compounds

Complex **3a**

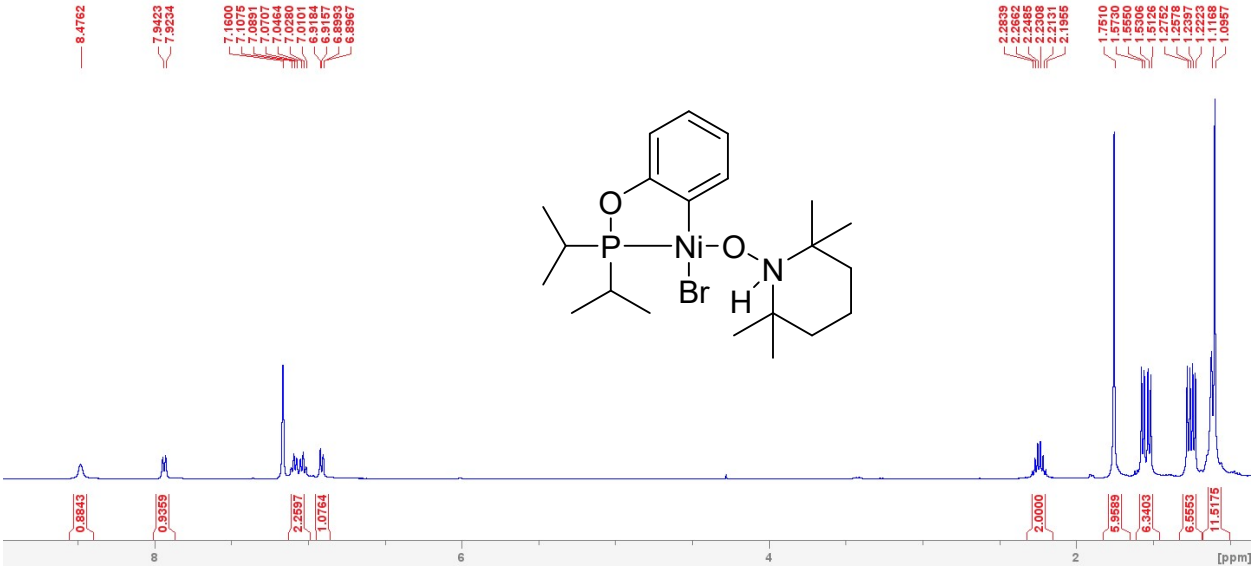

Figure S1. Full ^{1}H NMR spectrum of **3a** in C_6D_6.

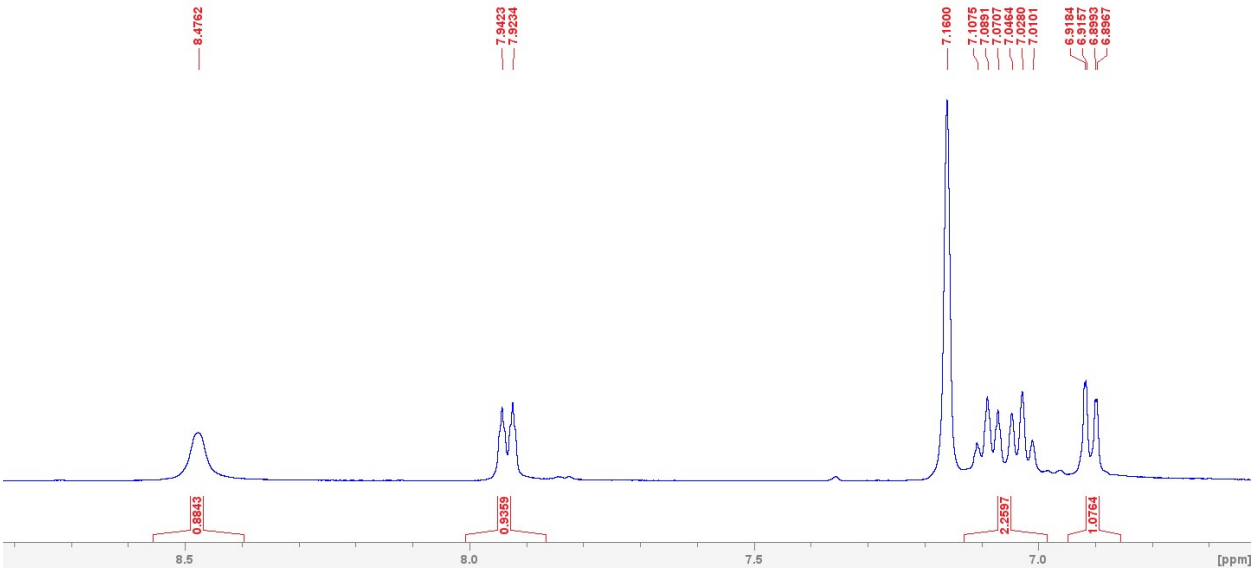

Figure S2. The expanded aliphatic region of the ^{1}H NMR spectrum of **3a** in C_6D_6.

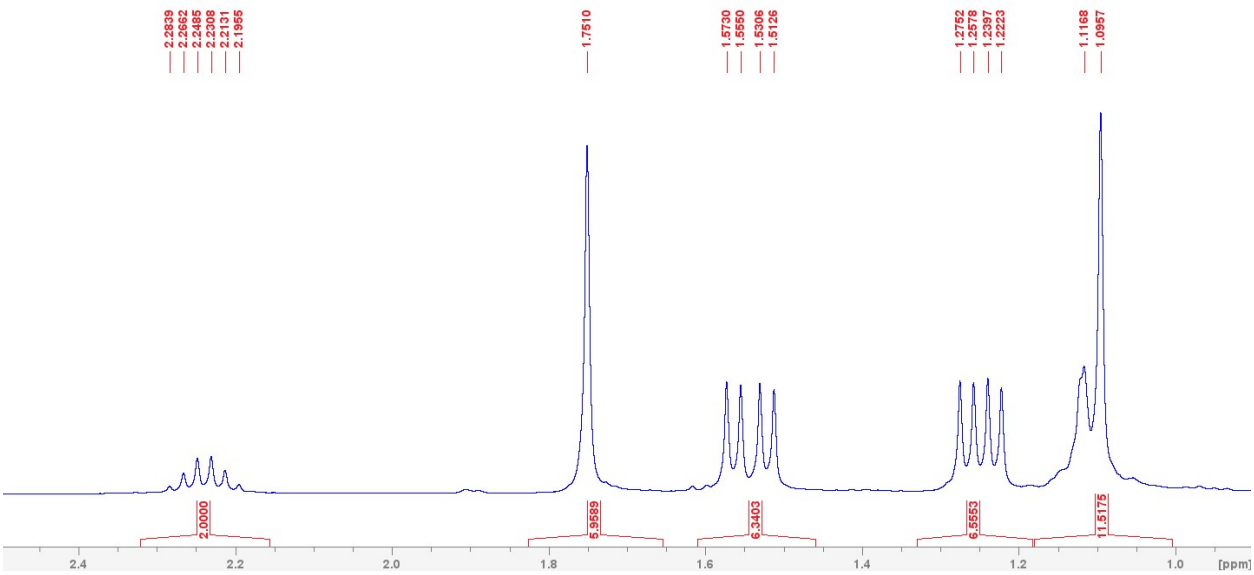

Figure S3. The expanded aromatic region of the ^{1}H NMR spectrum of **3a** in C_6D_6.

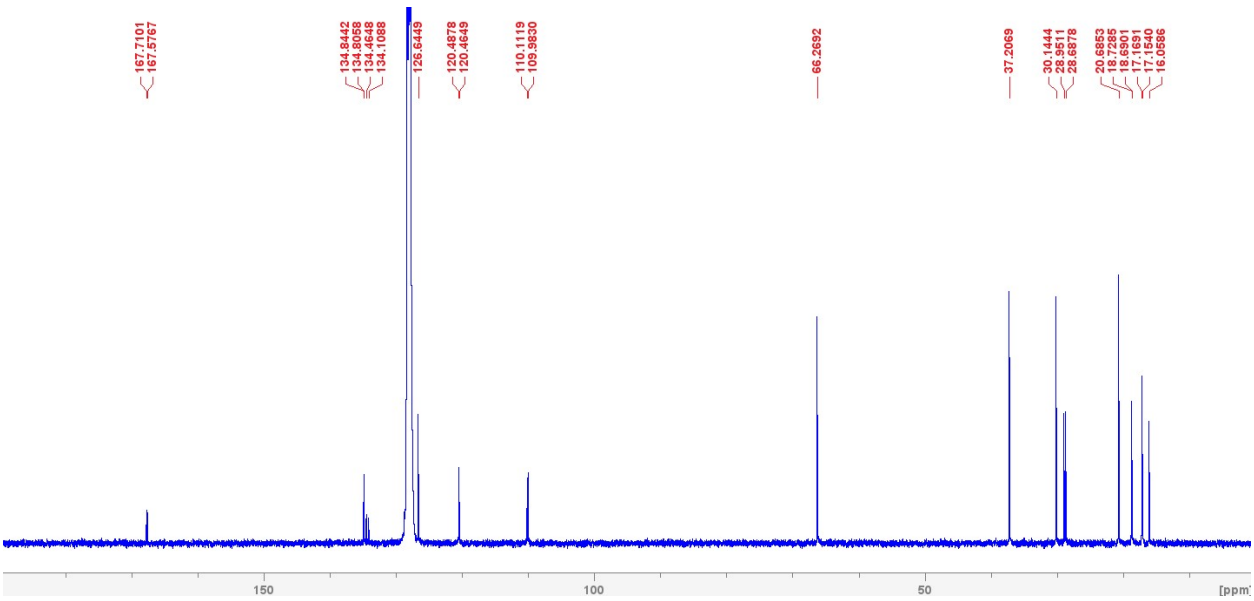

Figure S4. Full $^{13}C\{^{1}H\}$ NMR spectrum of **3a** in C_6D_6.

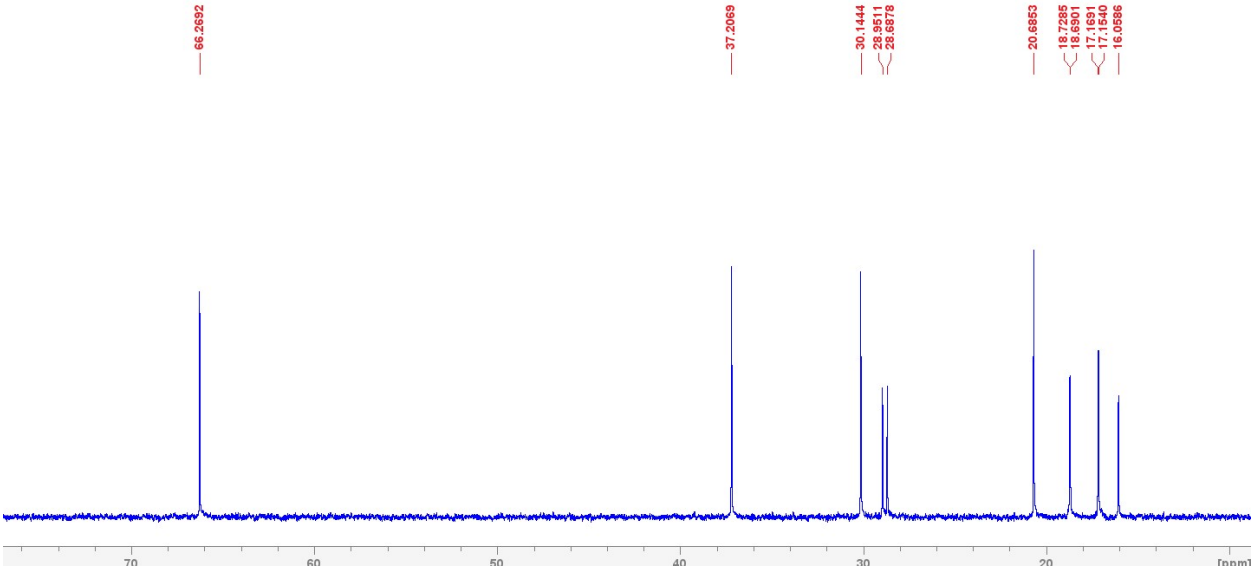

Figure S5. The expanded aliphatic region of the $^{13}C\{^{1}H\}$ NMR spectrum of **3a** in C_6D_6.

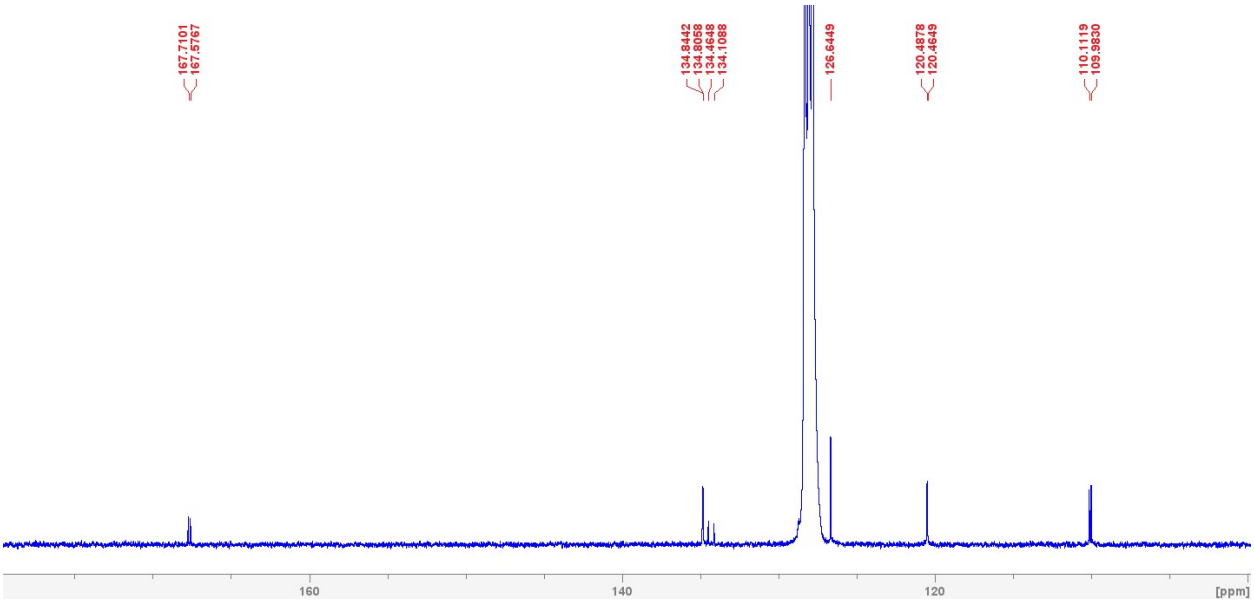

Figure S6. The expanded aromatic region of the $^{13}C\{^{1}H\}$ NMR spectrum of **3a** in C_6D_6.

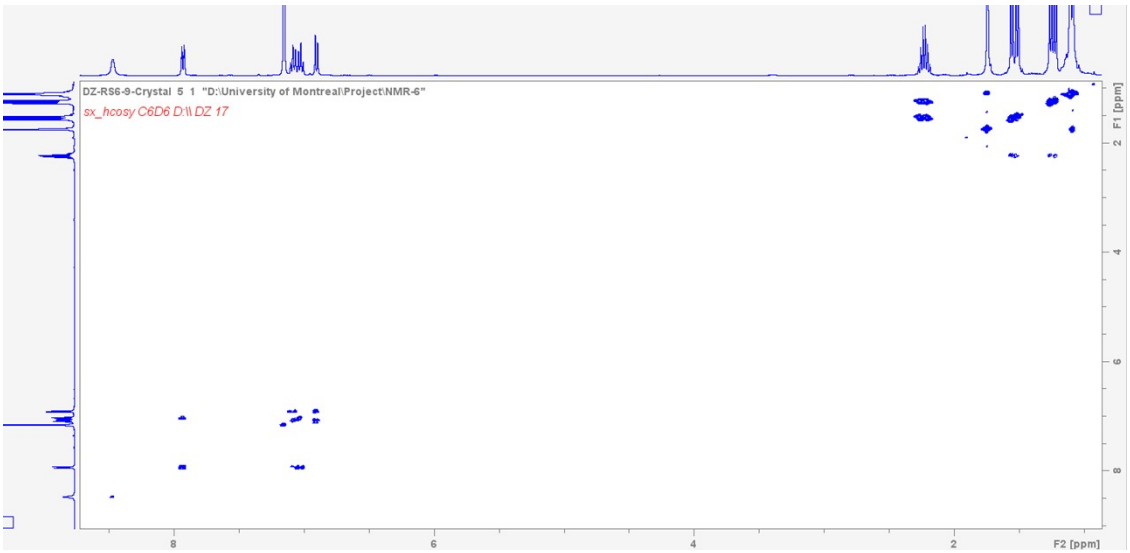

Figure S7. Full ^{1}H-^{1}H COSY NMR spectrum of **3a** in C_6D_6.

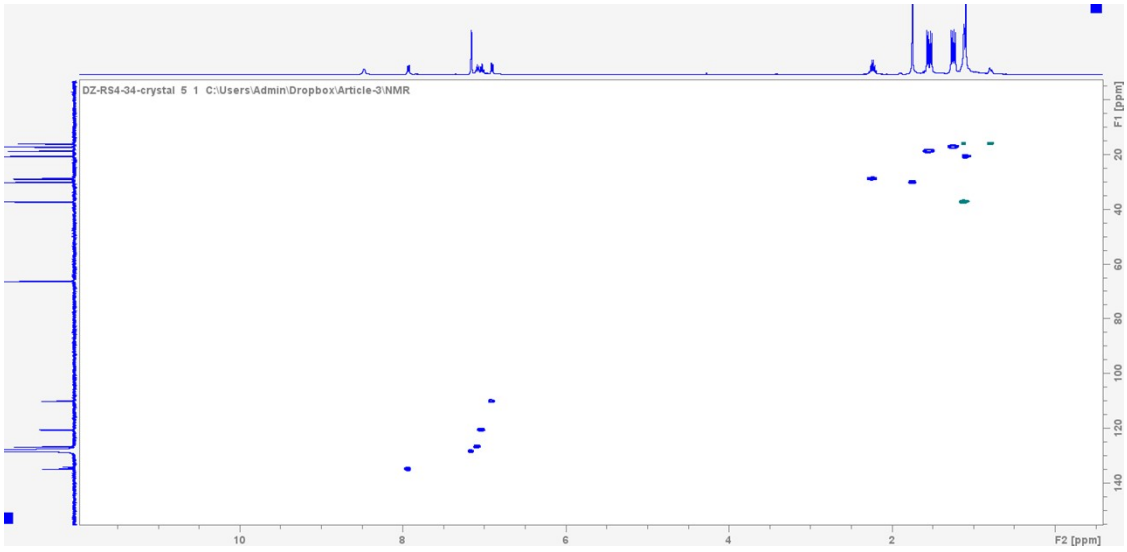

Figure S8. Full HSQC-edited NMR spectrum of **3a** in C_6D_6.

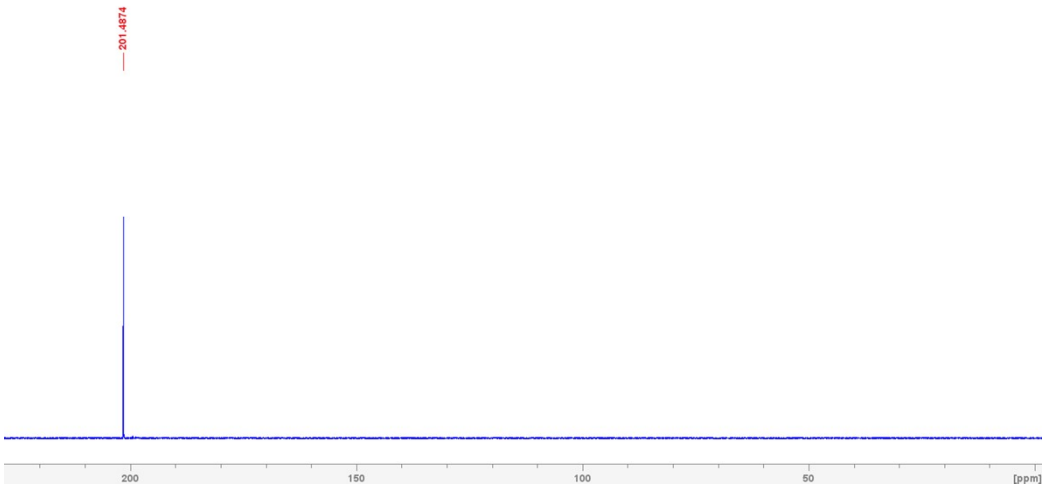

Figure S9. $^{31}P\{^{1}H\}$ NMR spectrum of **3a** in C_6D_6.

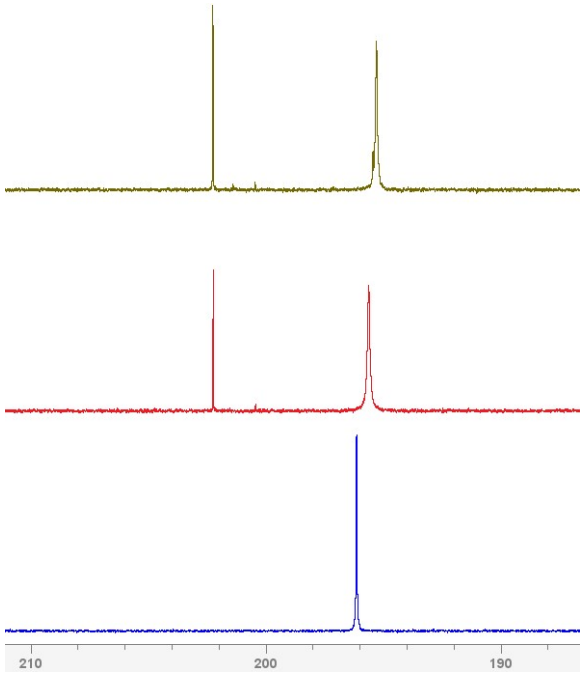

Figure S10. $^{31}P\{^{1}H\}$ NMR spectra of an acetonitrile solution of **1a** containing (from bottom to top) 0, 2, and 3 equiv of added TEMPOH (Ni:TEMPOH= 1:0, 1:1, 1:2).

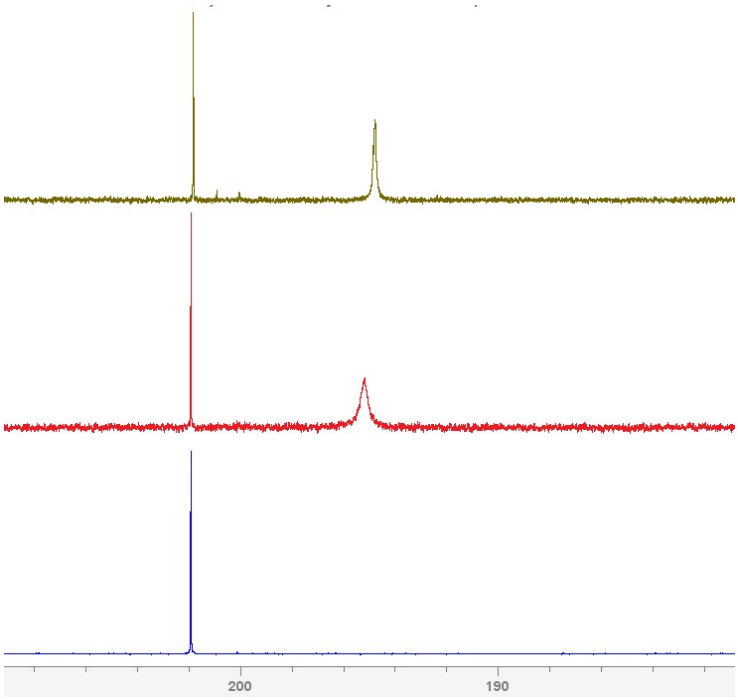

Figure S11. $^{31}P\{^{1}H\}$ NMR spectra of a DCM solution of **1a** to which were added, successively, 2 equiv of added TEMPOH (blue trace, Ni:TEMPOH:NCMe= 1:1:0), 600 equiv of MeCN (red trace, Ni:TEMPOH:NCMe= 1:1:300) and 2 more equiv of TEMPOH (brown trace, overall Ni:TEMPOH:NCMe= 1:2:300).

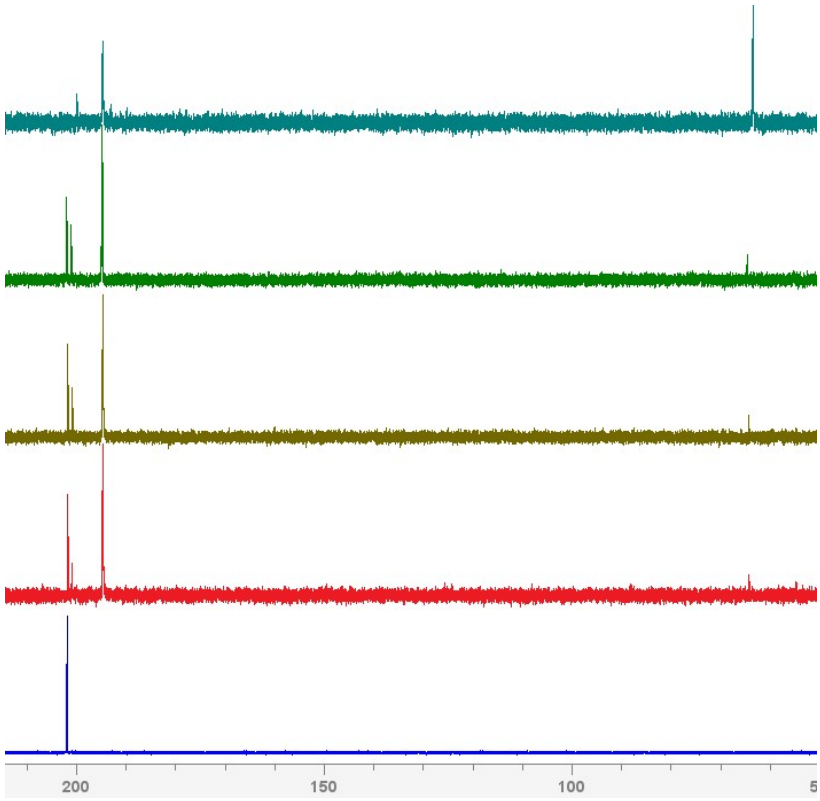

Figure S12. $^{31}P\{^{1}H\}$ NMR spectra of a DCM solution of **1a** to which were added, successively, 10 equiv of TEMPOH (blue trace, Ni:TEMPOH:NCMe = 1:5:0), 600 equiv of MeCN (red trace, Ni:NCMe = 1:5:300), 2 more equiv of TEMPOH (brown trace, Ni:TEMPOH:NCMe = 1: 6:300), and 4 more equiv of TEMPOH (green trace, Ni:TEMPOH:NCMe= 1:8:300). The sample was then allowed to stand for 3 days before a final spectrum was recorded (gray-blue trace).

Complex **3b**

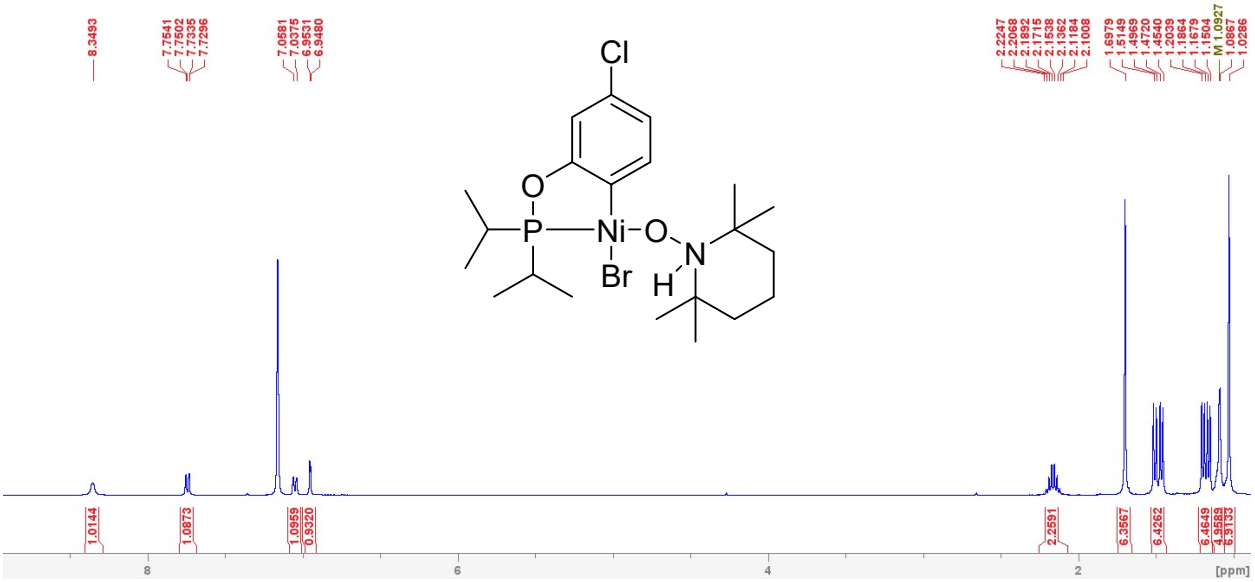

Figure S13. Full ^{1}H NMR spectrum of **3b** in C_6D_6.

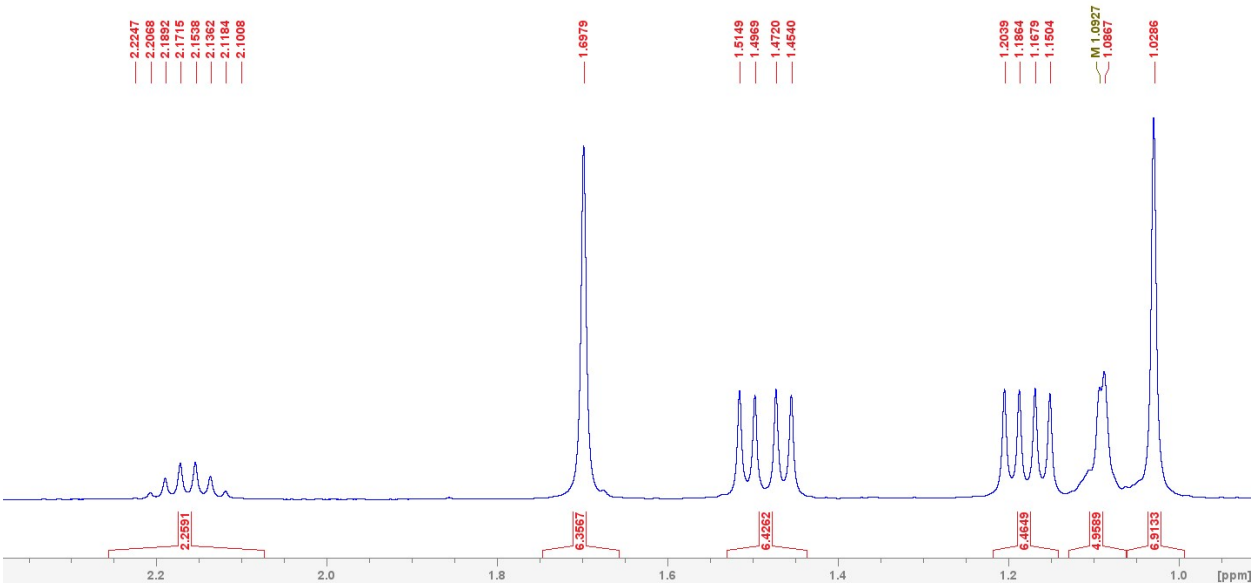

Figure S14. The expanded aliphatic region of the ^{1}H NMR spectrum of **3b** in C_6D_6.

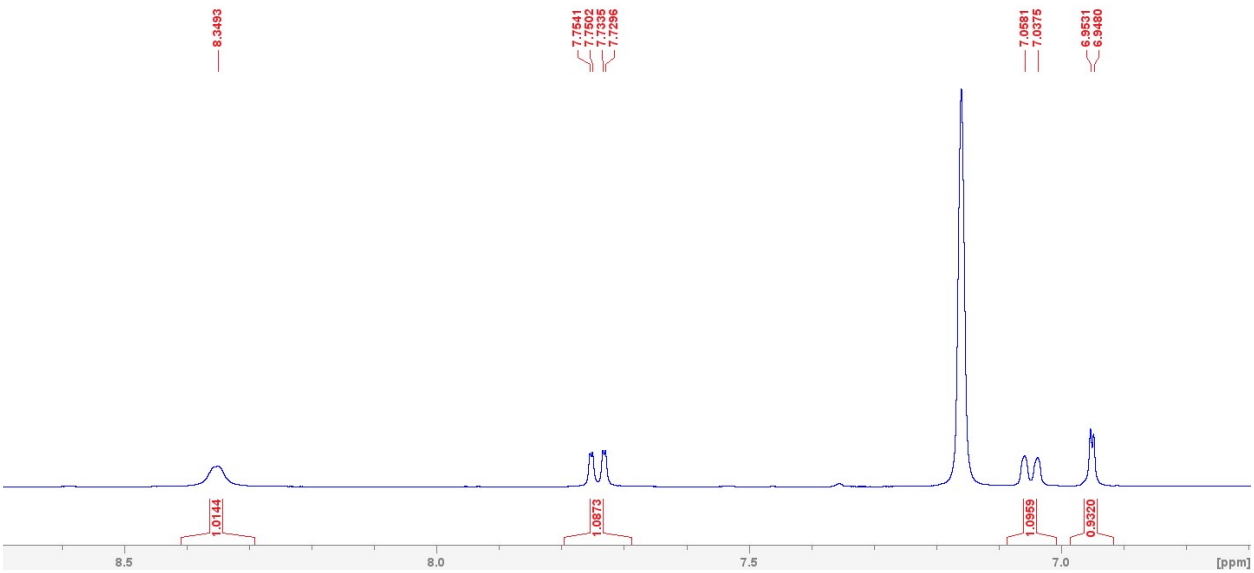

Figure S15. The expanded aromatic region of the ^{1}H NMR spectrum of **3b** in C_6D_6.

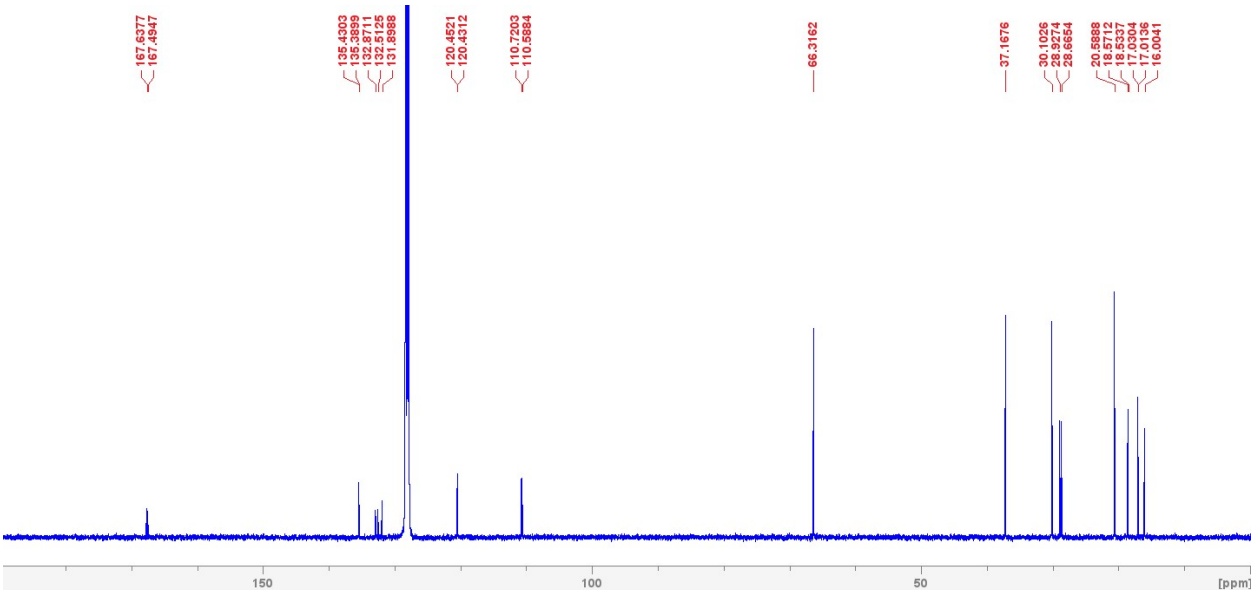

Figure S16. Full $^{13}C\{^{1}H\}$ NMR spectrum of **3b** in C_6D_6.

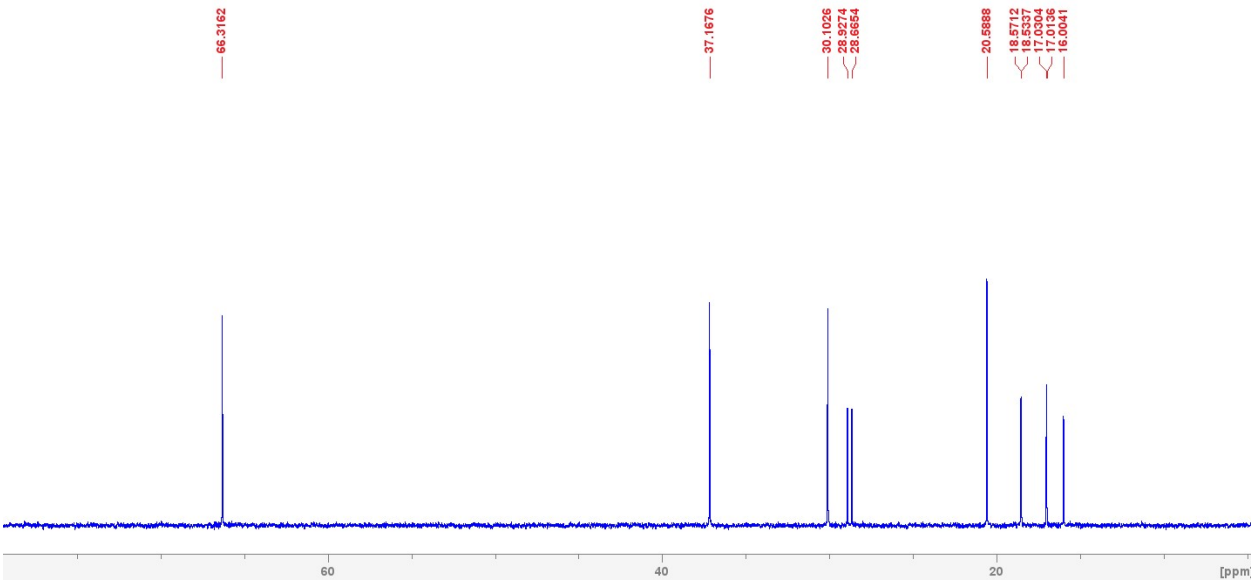

Figure S17. The expanded aliphatic region of the $^{13}C\{^{1}H\}$ NMR spectrum of **3b** in C_6D_6.

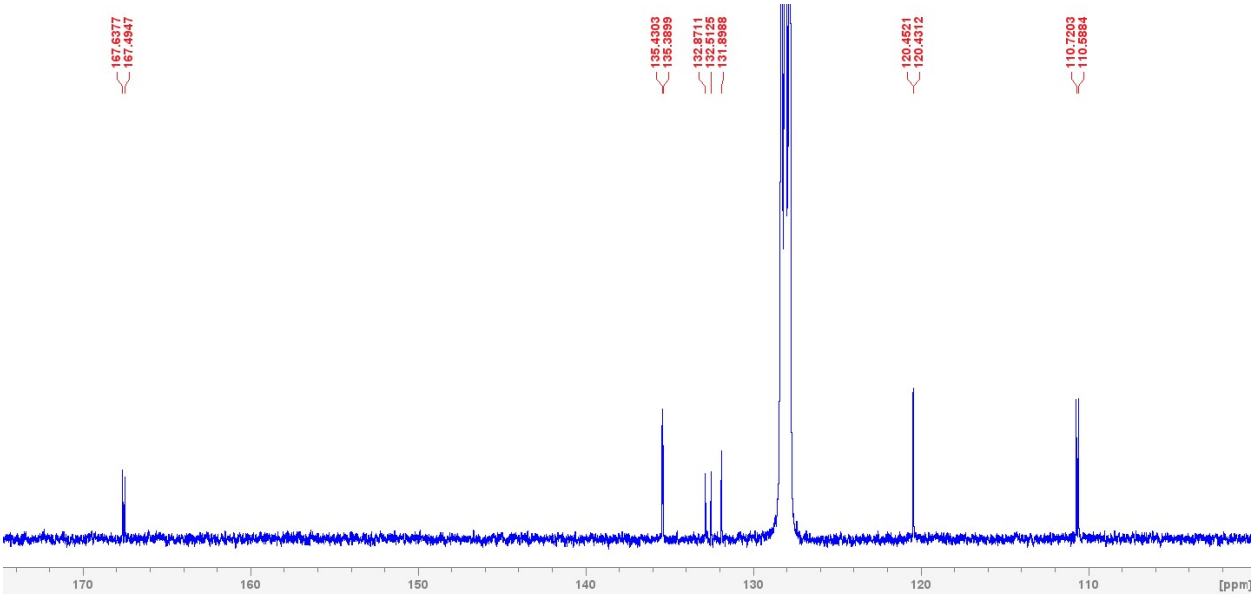

Figure S18. The expanded aromatic region of the $^{13}C\{^{1}H\}$ NMR spectrum of **3b** in C_6D_6.

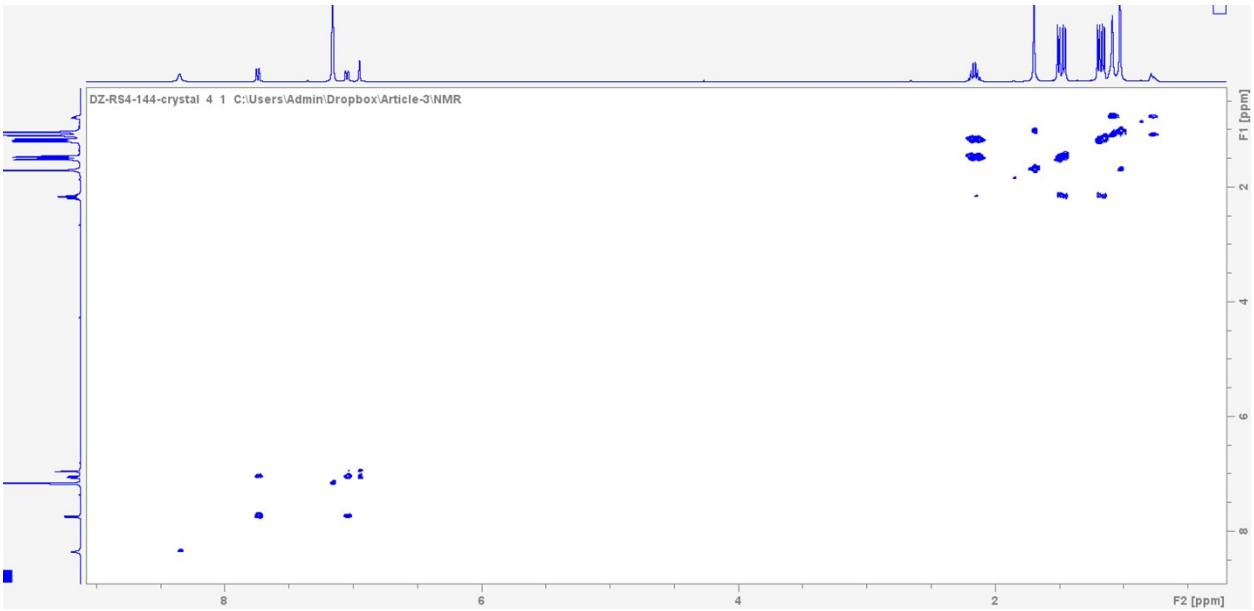

Figure S19. Full ^{1}H-^{1}H COSY NMR spectrum of **3b** in C_6D_6.

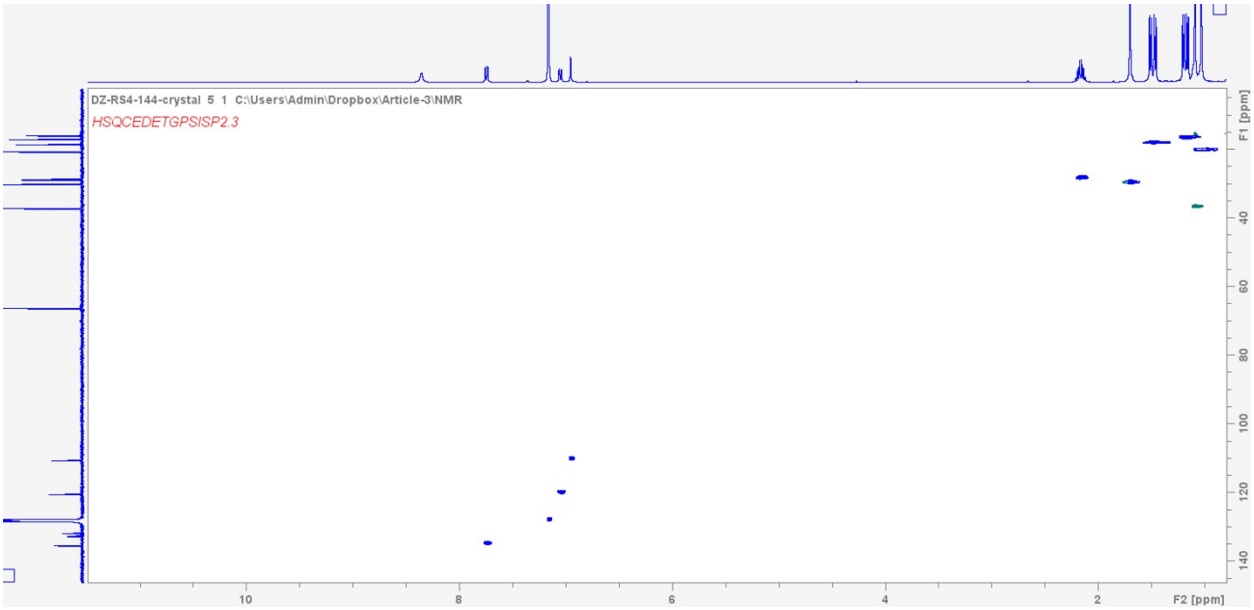

Figure S20. Full HSQC-Edited NMR spectrum of **3b** in C_6D_6.

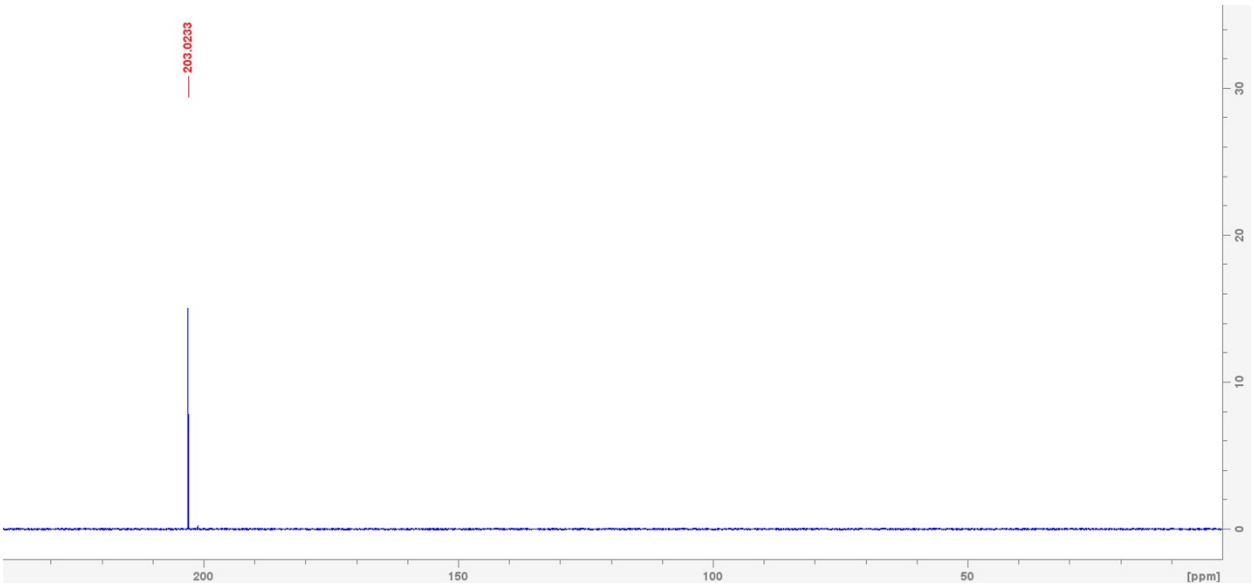

Figure S21. $^{31}P\{^{1}H\}$ NMR spectrum of **3b** in C_6D_6.

Complex **3C**

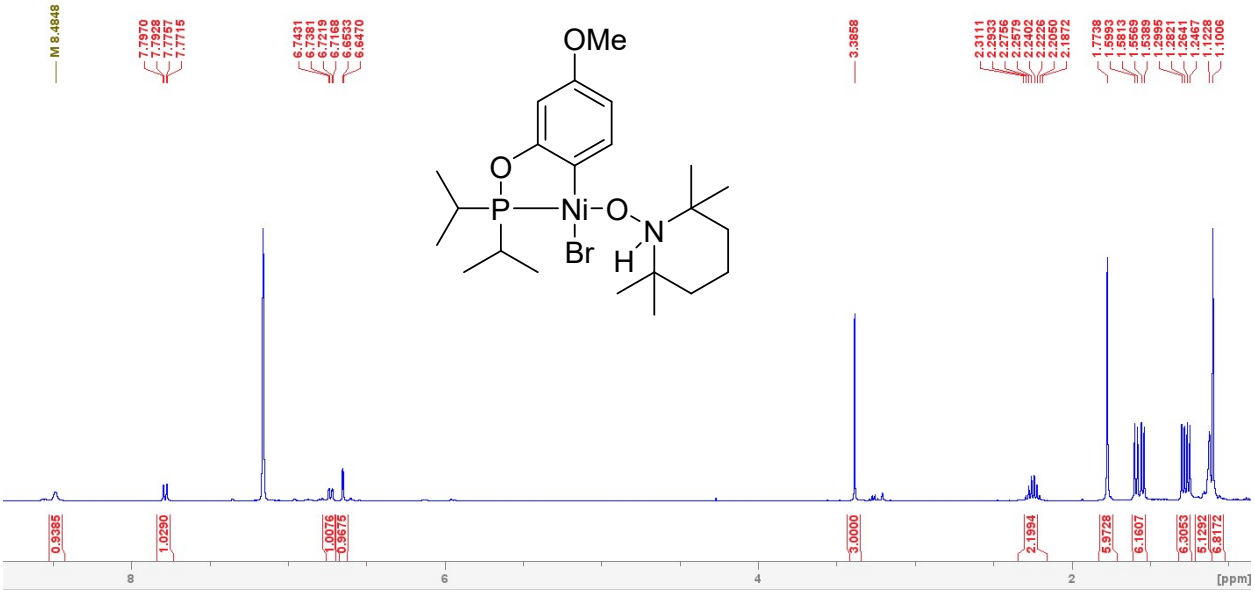

Figure S22. Full ^{1}H NMR spectrum of **3c** in C_6D_6.

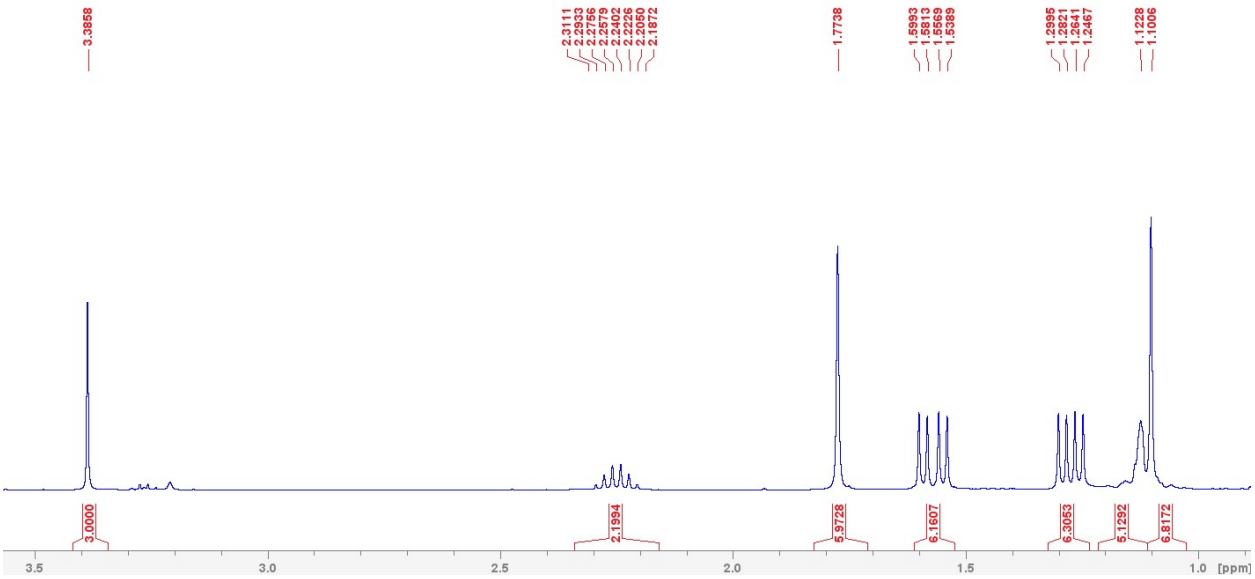

Figure S23. The expanded aliphatic region of the ^{1}H NMR spectrum of **3c** in C_6D_6.

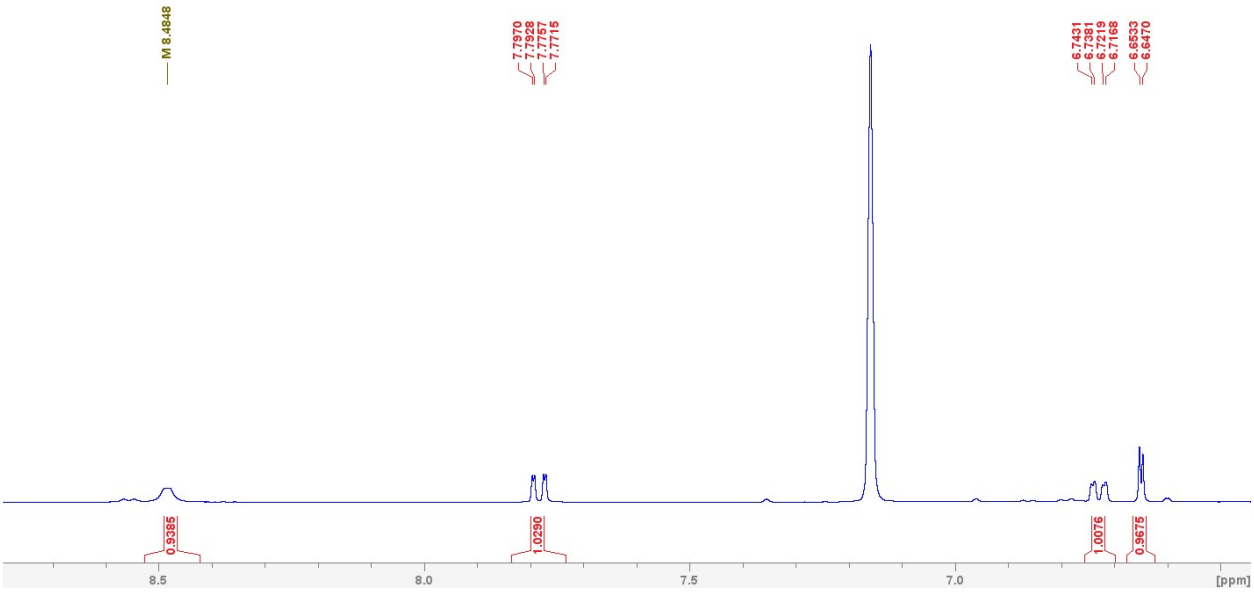

Figure S24. The expanded aromatic region of the ^{1}H NMR spectrum of **3c** in C_6D_6.

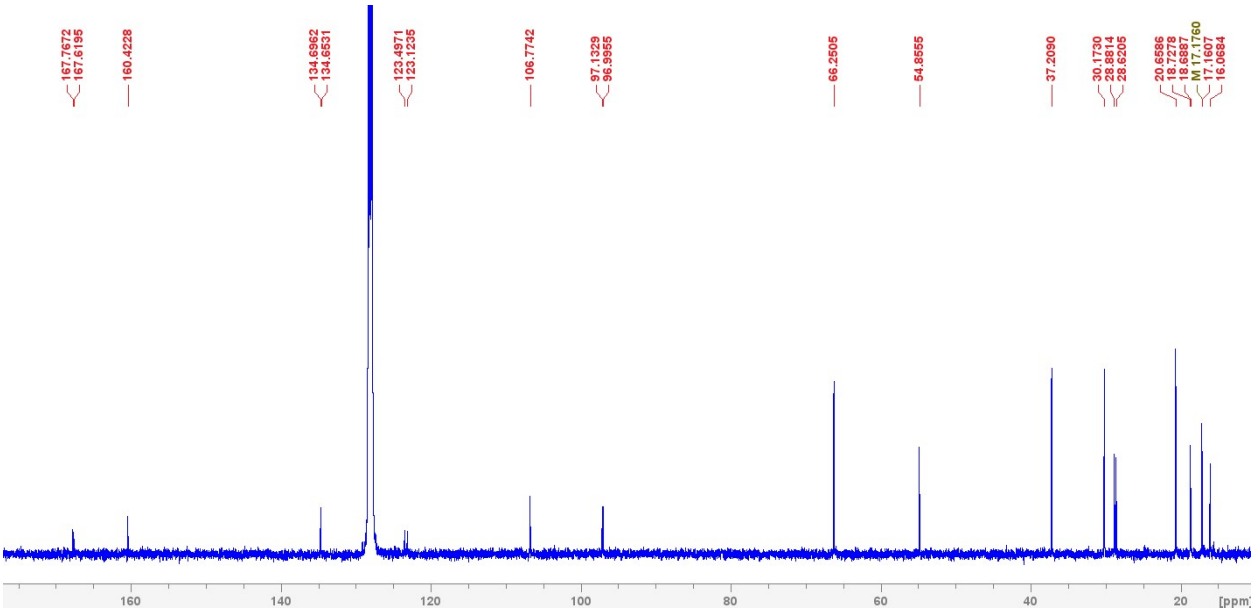

Figure S25. Full $^{13}C\{^{1}H\}$ NMR spectrum of **3c** in C_6D_6.

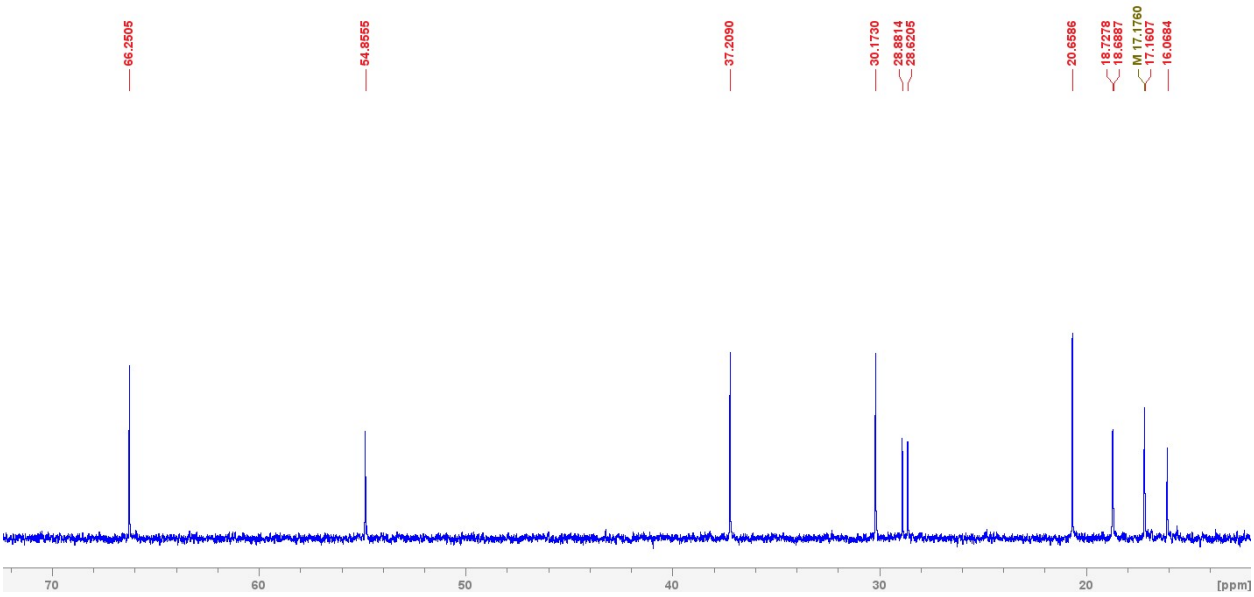

Figure S26. The expanded aliphatic region of the$^{13}C\{^{1}H\}$ NMR spectrum of **3c** in C_6D_6.

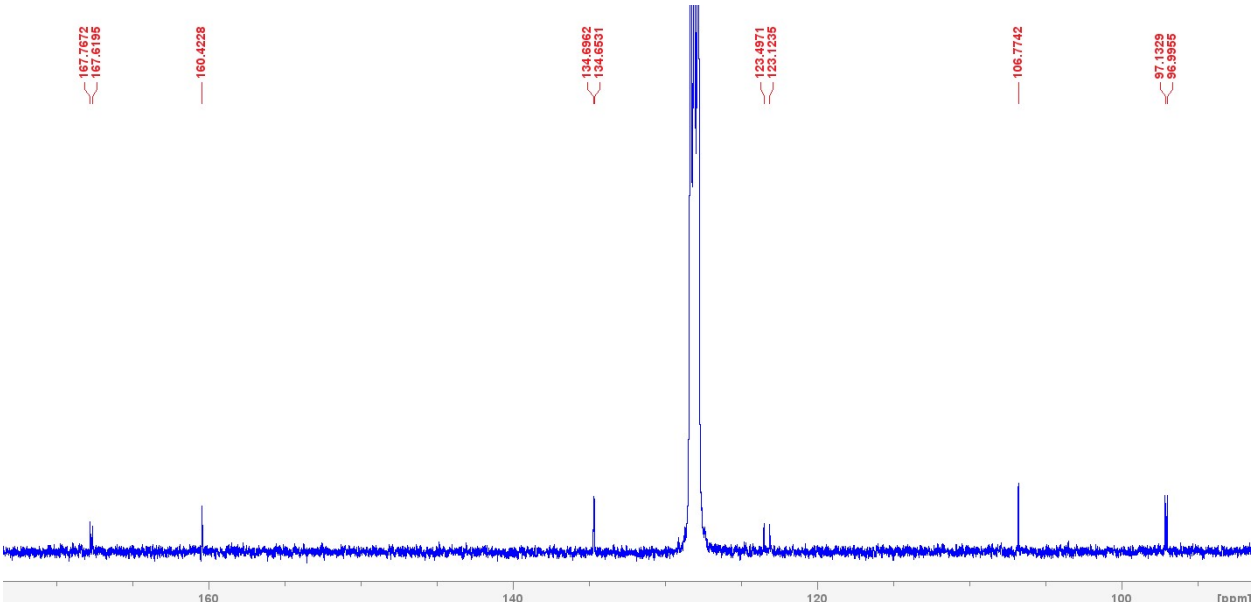

Figure S27. The expanded aromatic region of the $^{113}C\{^{1}H\}$ NMR spectrum of **3c** in C_6D_6.

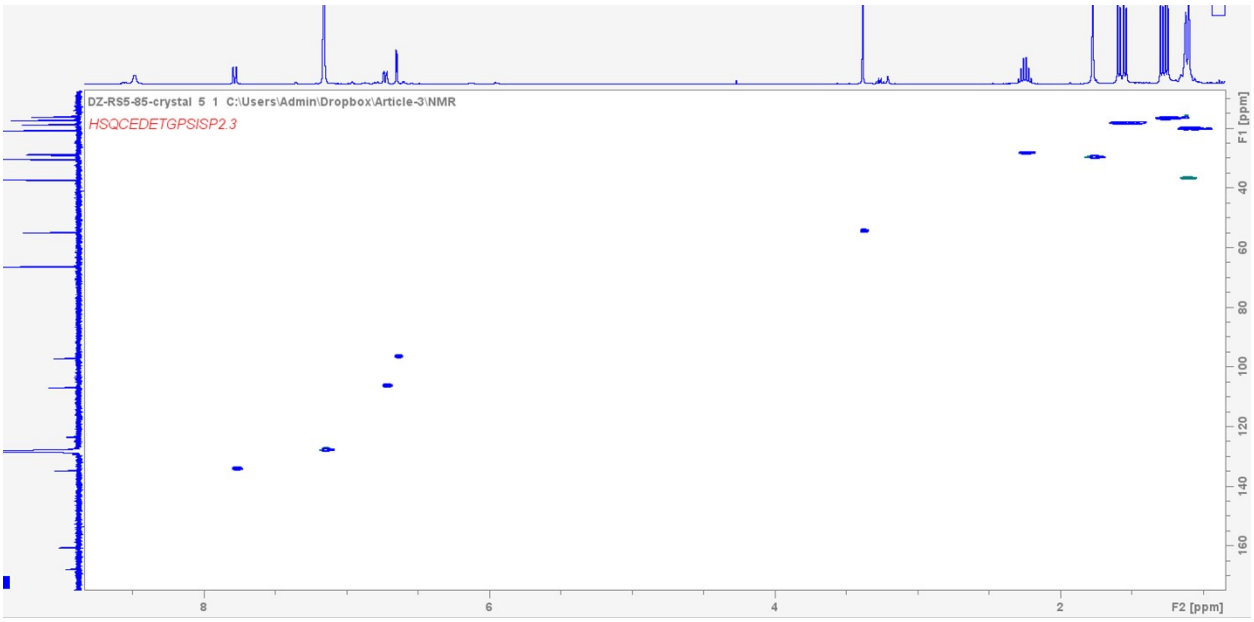

Figure S28. Full HSQC-Edited NMR spectrum of **3c** in C_6D_6.

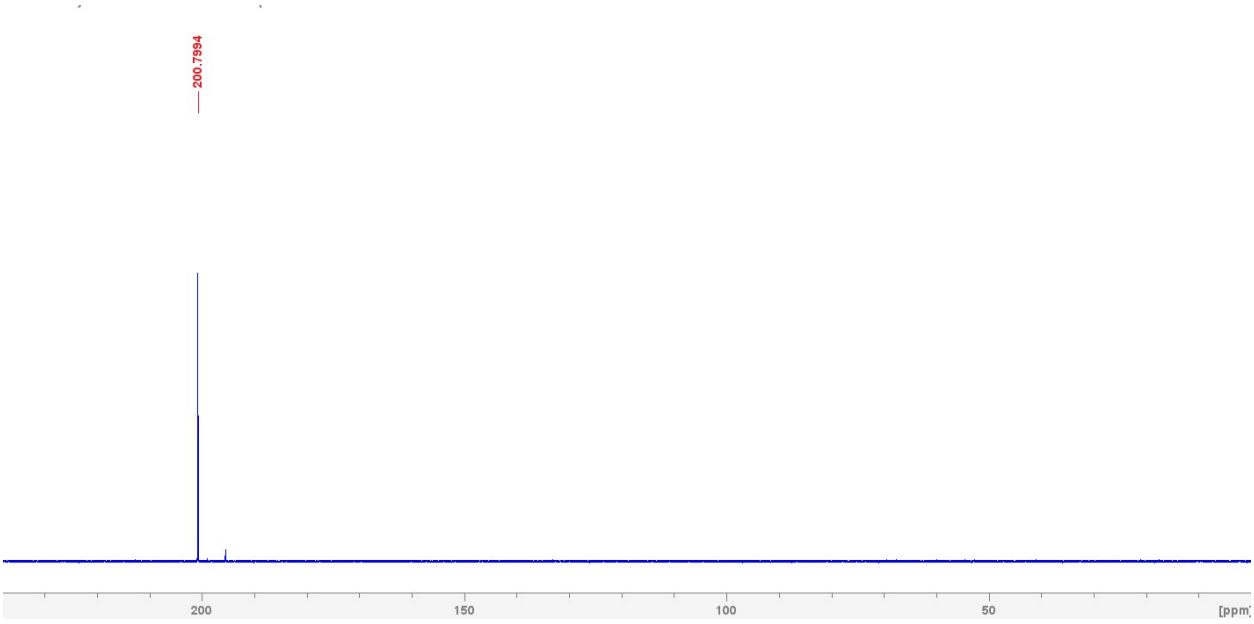

Figure S29. $^{31}P\{^{1}H\}$ NMR spectrum of **3c** in C_6D_6.

Complex **3d**

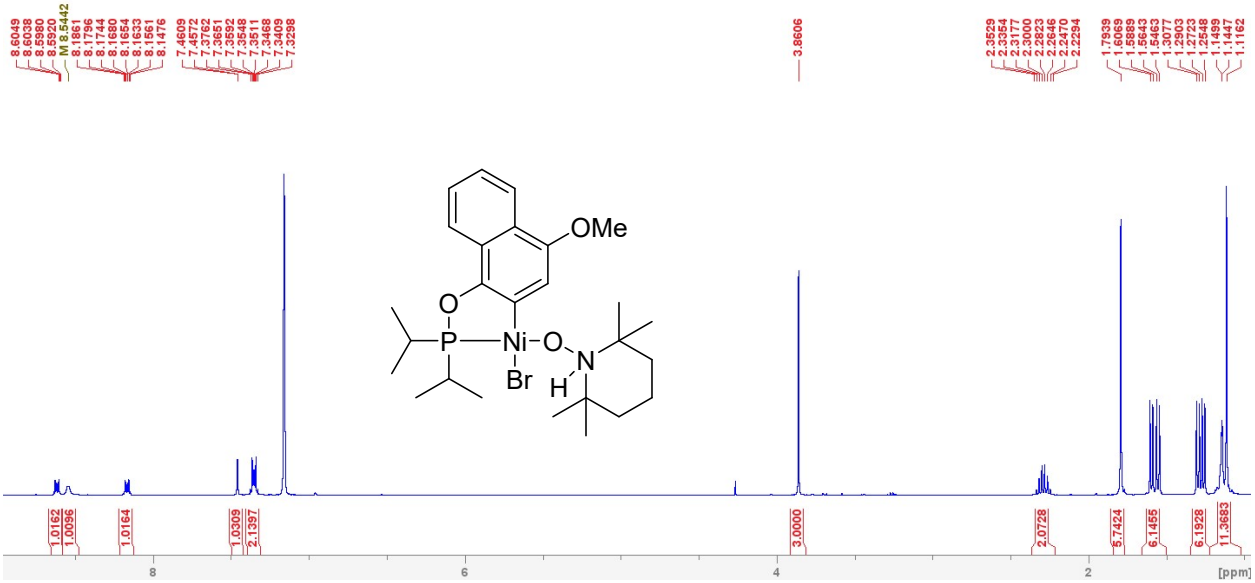

Figure S30. Full ^{1}H NMR spectrum of **3d** in C_6D_6.

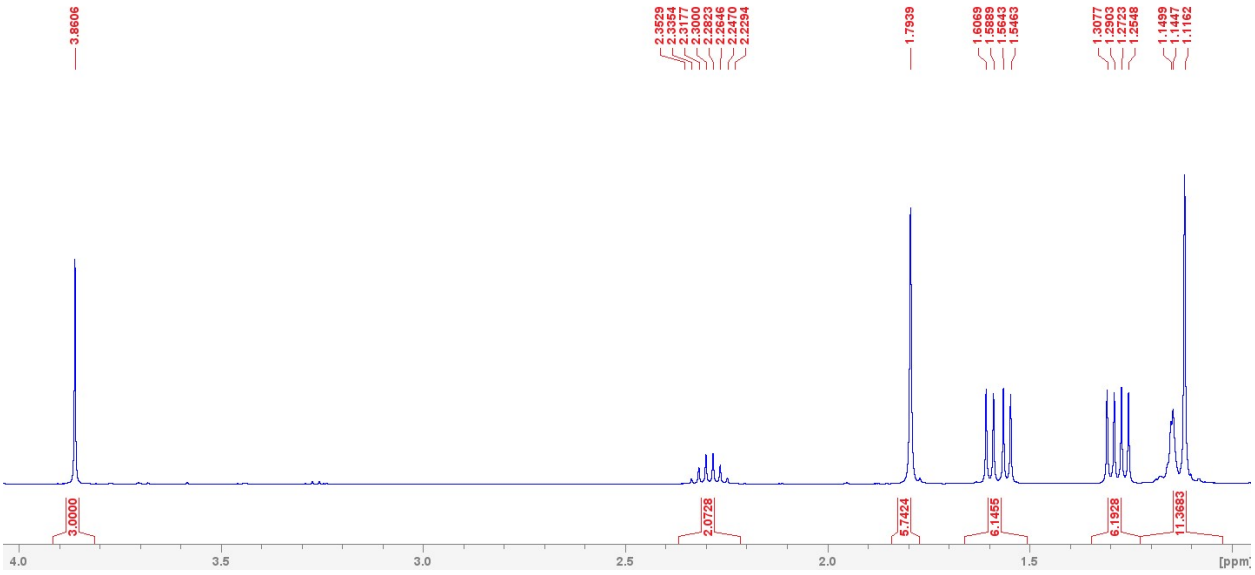

Figure S31. The expanded aliphatic region of the ^{1}H NMR spectrum of **3d** in C_6D_6.

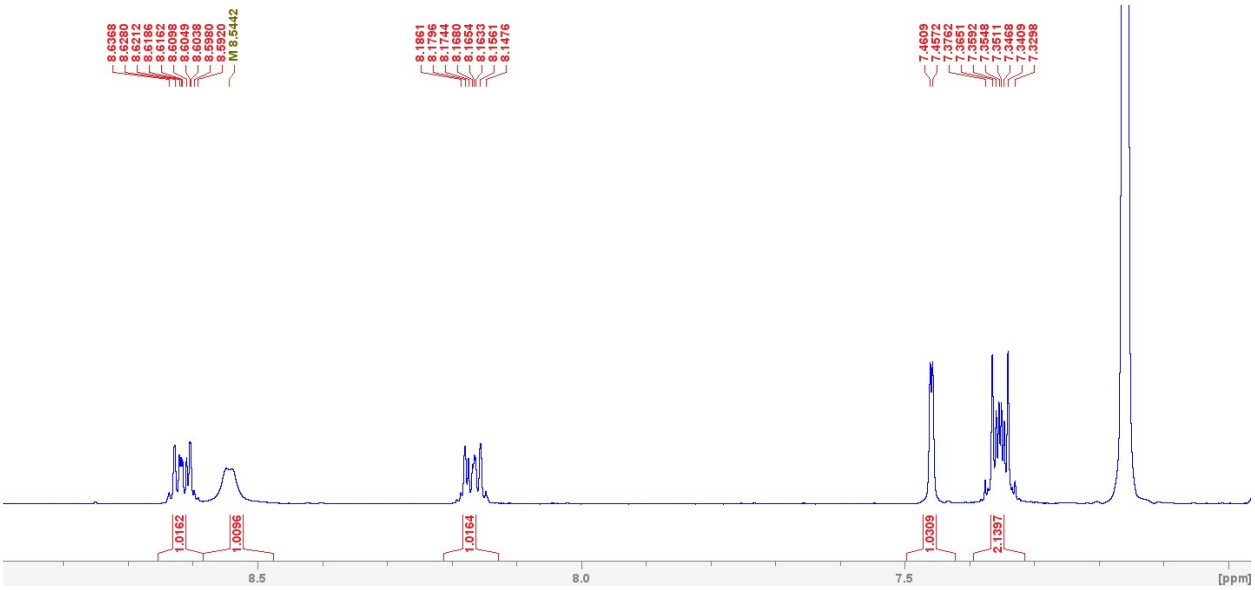

Figure S32. The expanded aromatic region of the ^{1}H NMR spectrum of **3d** in C_6D_6.

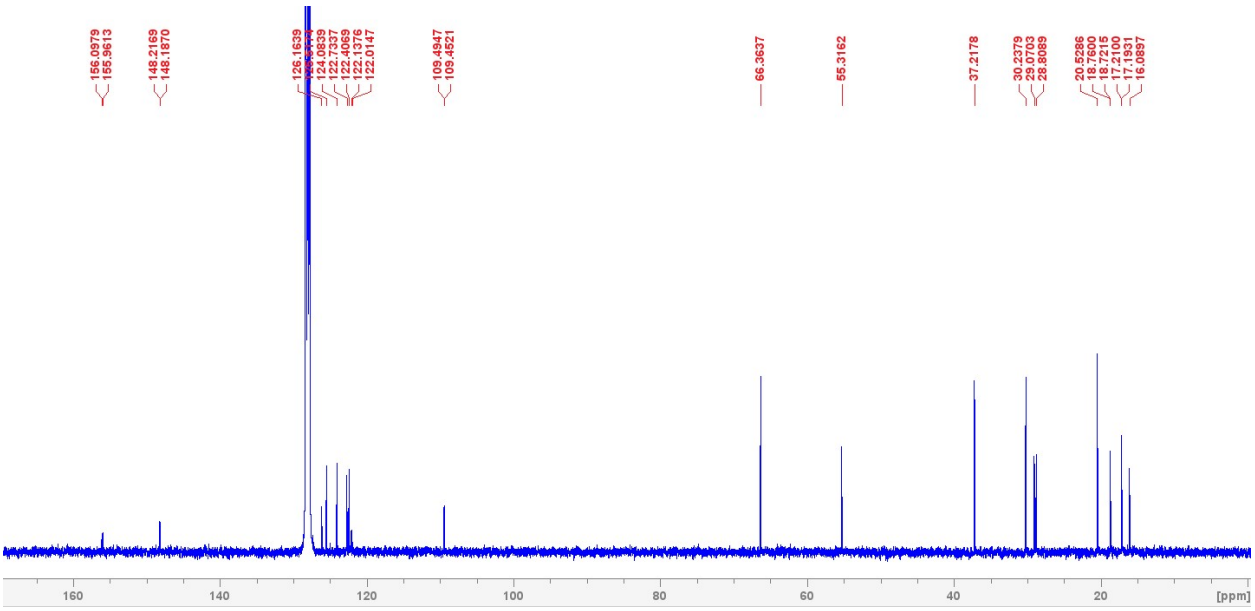

Figure S33. Full $^{13}C\{^{1}H\}$ NMR spectrum of **3d** in C_6D_6.

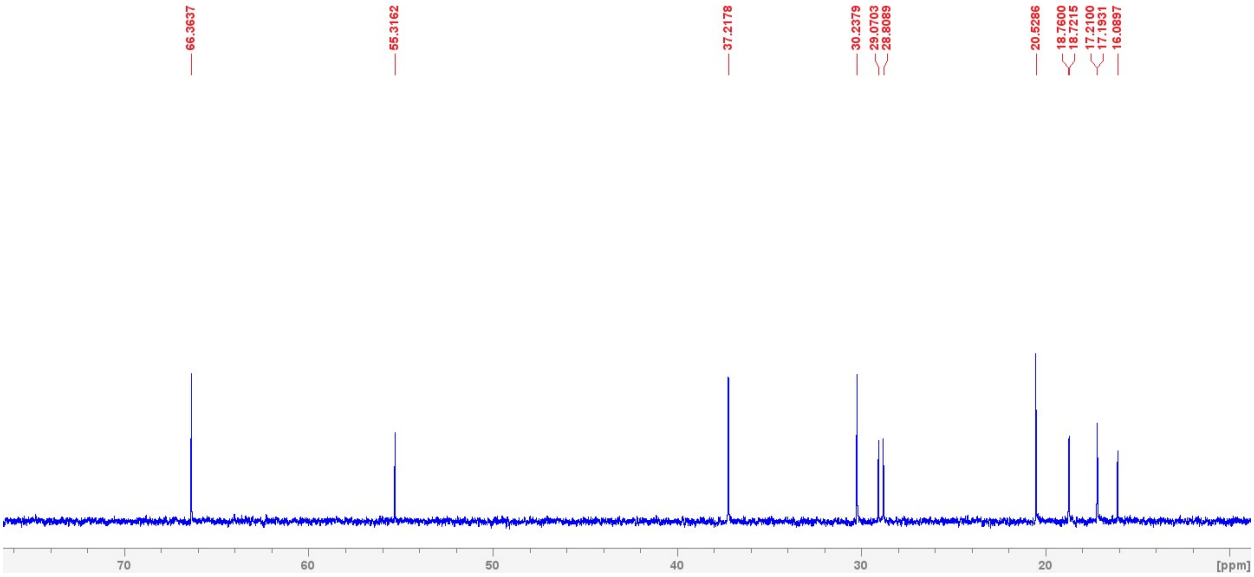

Figure S34. The expanded aliphatic region of the $^{13}C\{^{1}H\}$ NMR spectrum of **3d** in C_6D_6.

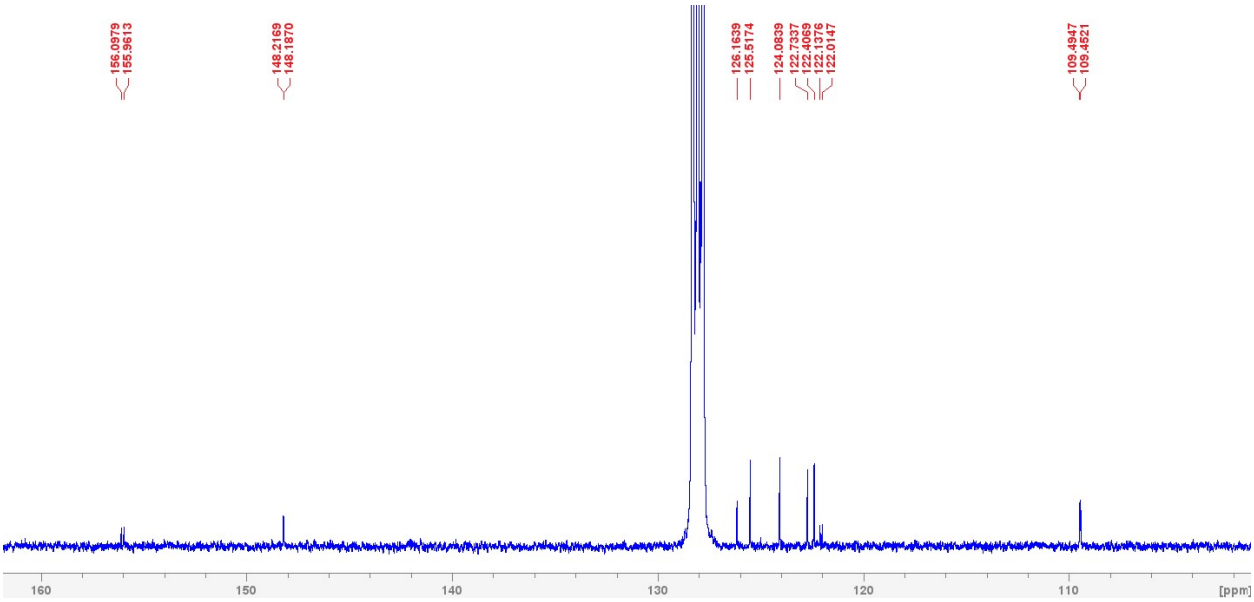

Figure S35. The expanded aromatic region of the $^{13}C\{^{1}H\}$ NMR spectrum of **3d** in C_6D_6.

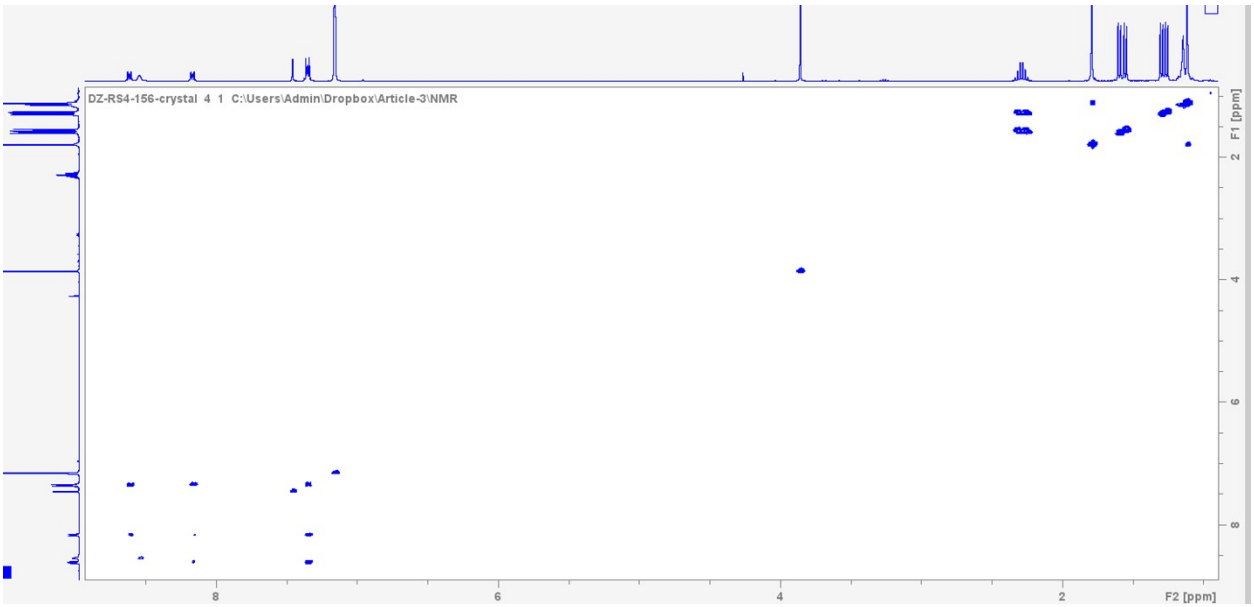

Figure S36. Full ^{1}H-^{1}H COSY NMR spectrum of **3d** in C_6D_6.

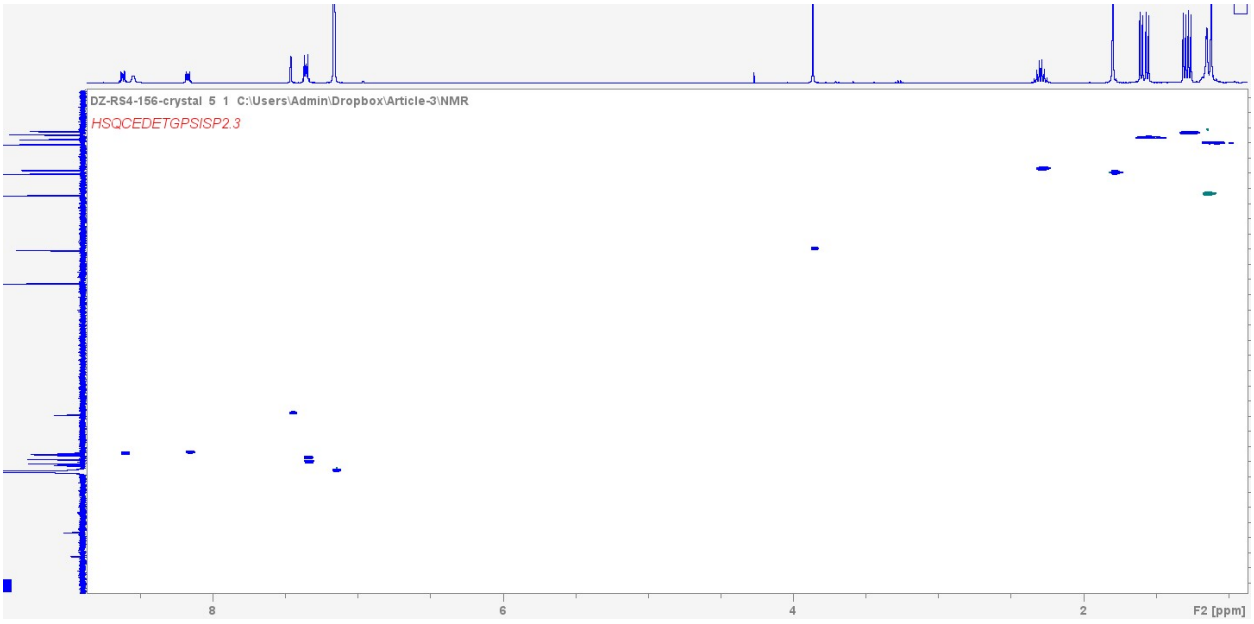

Figure S37. Full HSQC-Edited NMR spectrum of **3d** in C_6D_6.

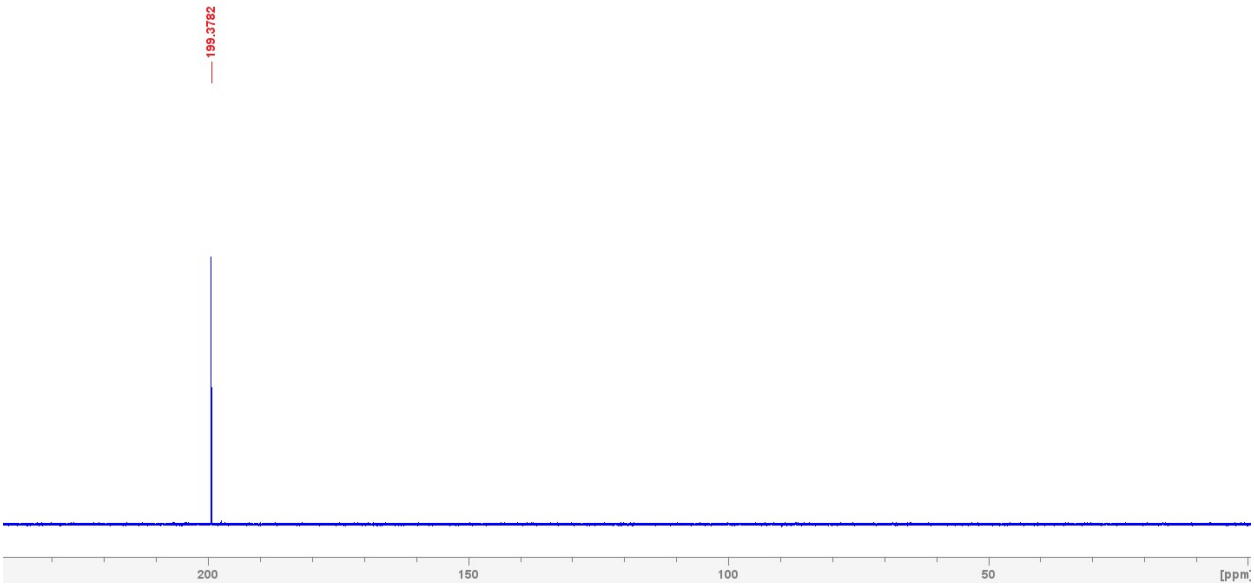

Figure S38. $^{31}P\{^{1}H\}$ NMR spectrum of **3d** in C_6D_6.

Complex **5a**

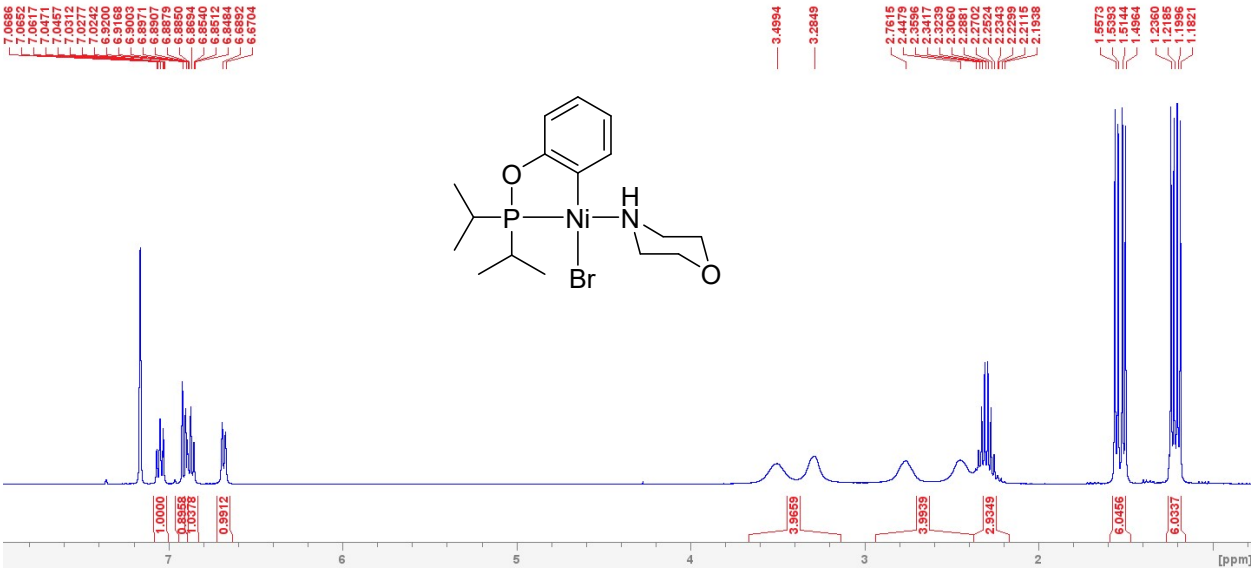

Figure S39. Full ^{1}H NMR spectrum of **5a** in C_6D_6.

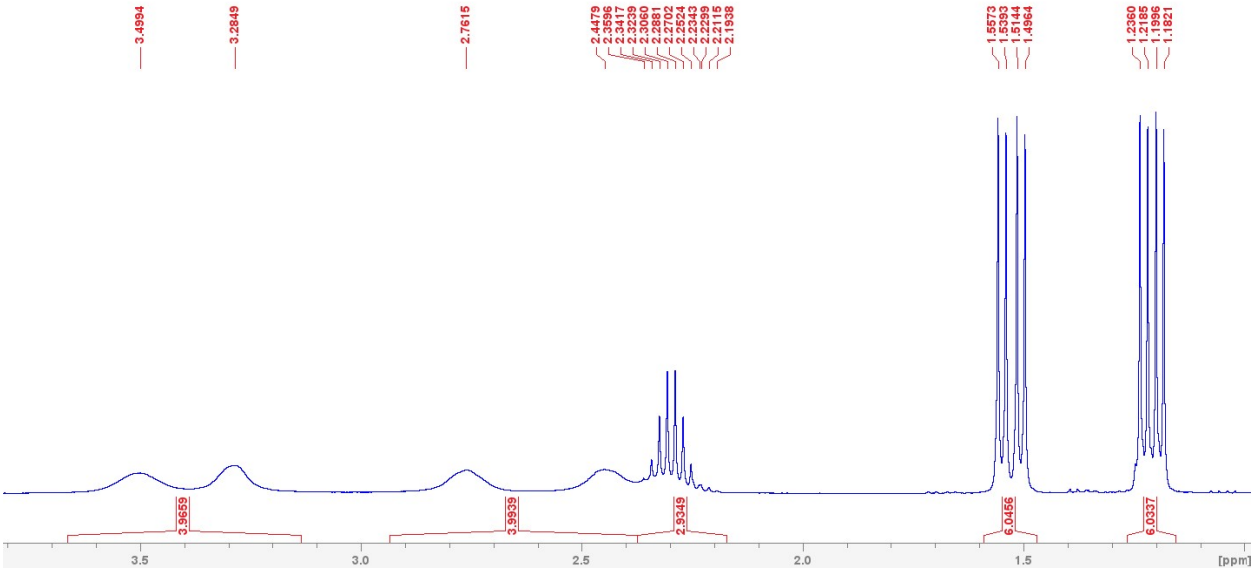

Figure S40. The expanded aliphatic region of the ^{1}H NMR spectrum of **5a** in C_6D_6.

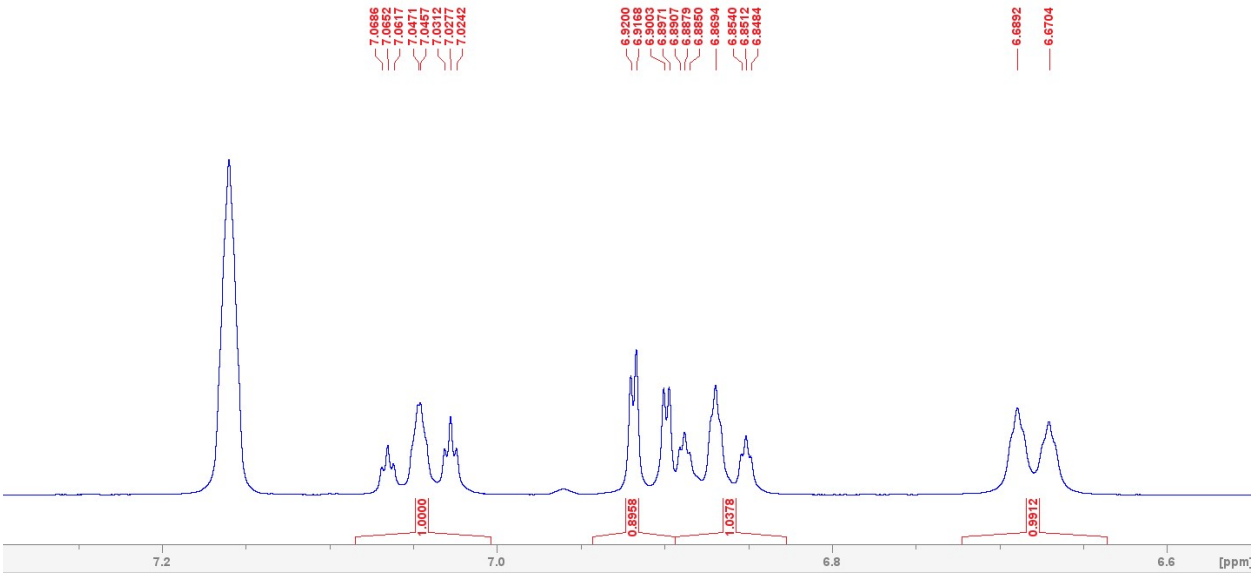

Figure S41. The expanded aromatic region of the ^{1}H NMR spectrum of **5a** in C_6D_6.

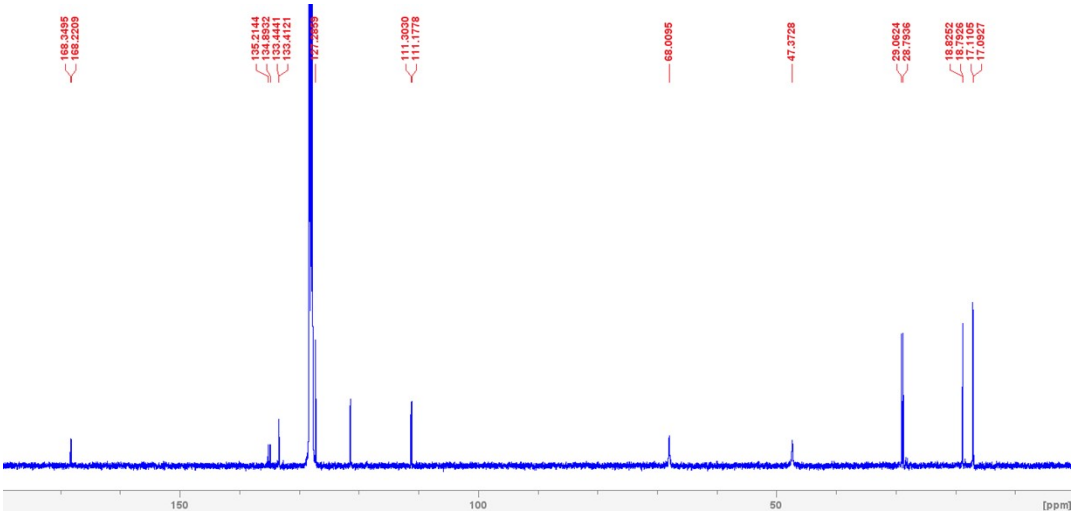

Figure S42. Full $^{13}C\{^{1}H\}$ NMR spectrum of **5a** in C_6D_6.

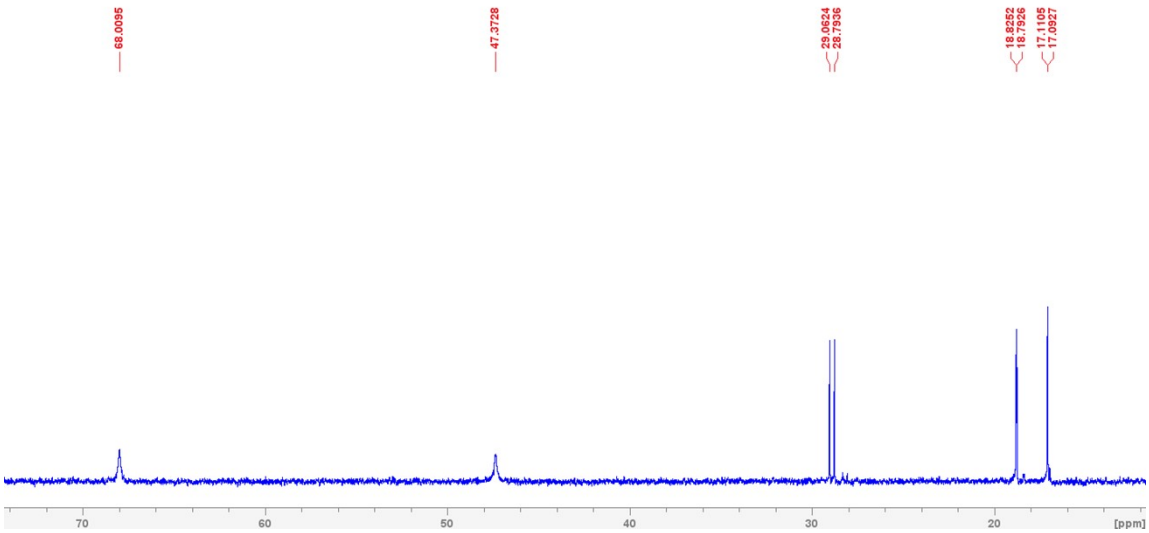

Figure S43. The expanded aliphatic region of the $^{13}C\{^{1}H\}$ NMR spectrum of **5a** in C_6D_6.

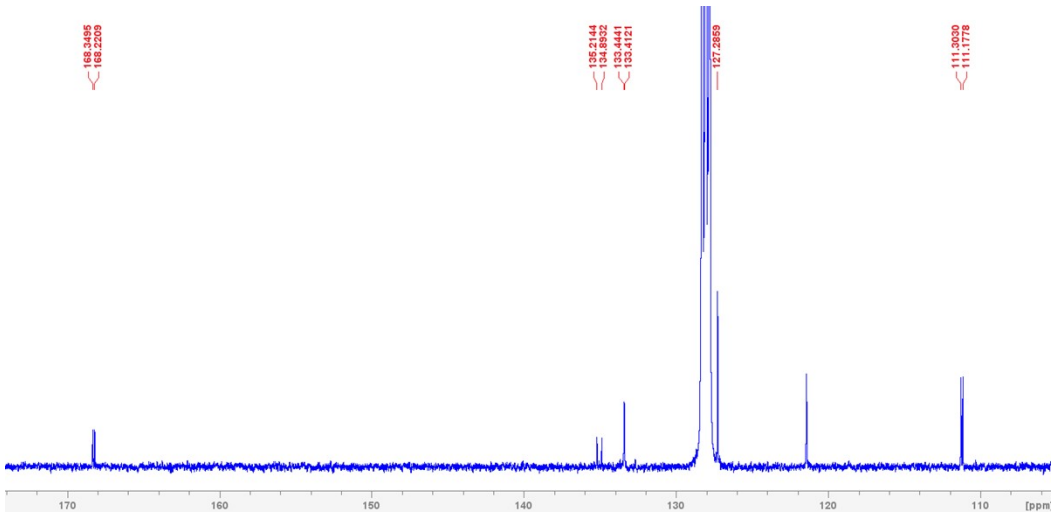

Figure S44. The expanded aromatic region of the $^{13}C\{^{1}H\}$ NMR spectrum of **5a** in C_6D_6.

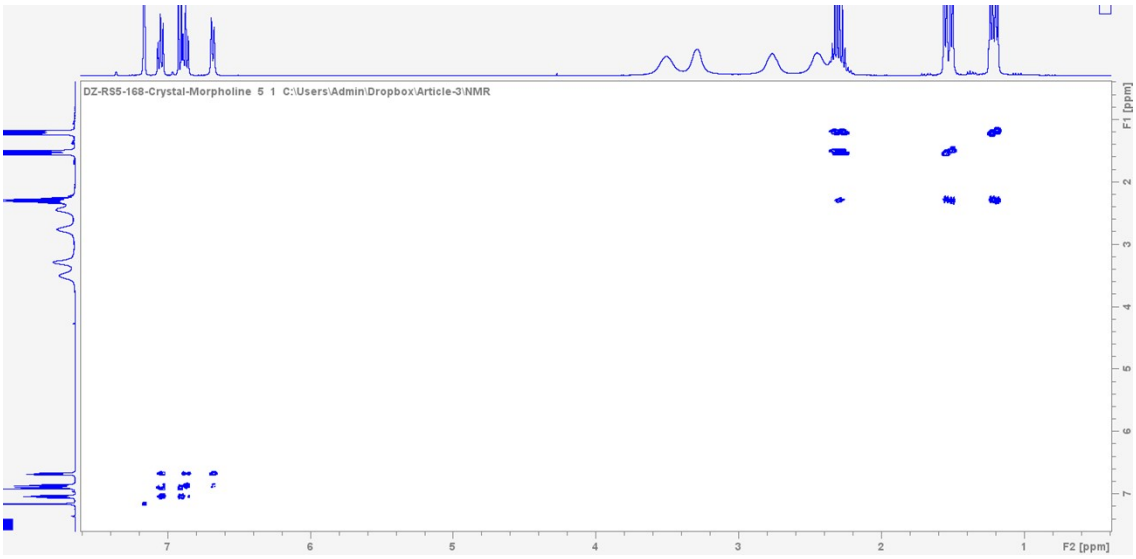

Figure S45. Full ^{1}H-^{1}H COSY NMR of complex **5a** in C_6D_6.

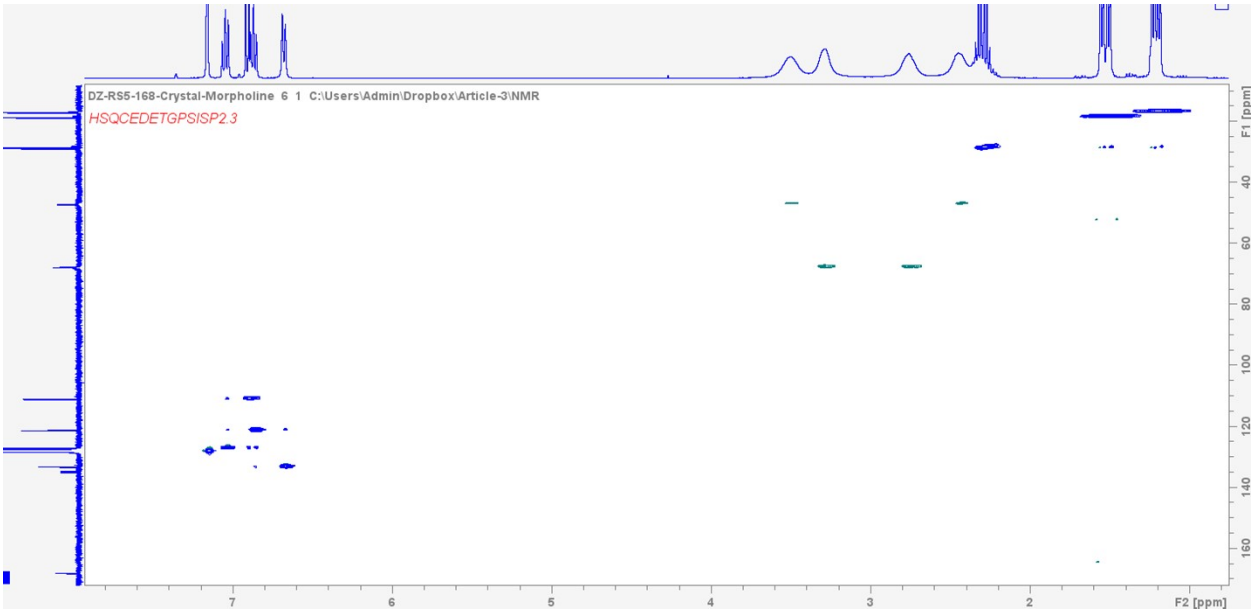

Figure S46. Full HSQC- Edited NMR of complex **5a** in C_6D_6.

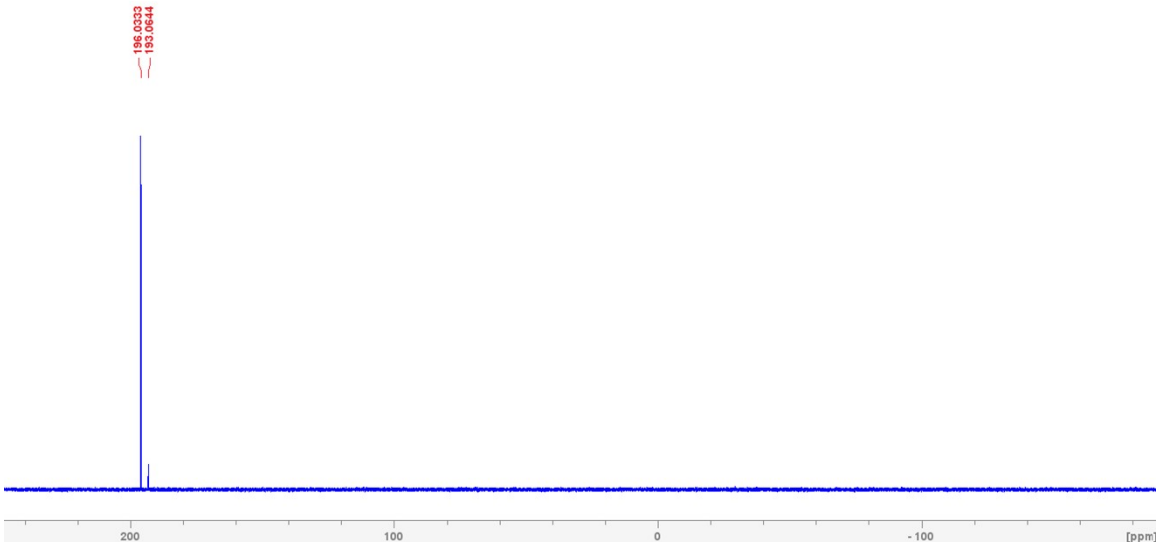

Figure S47. Full $^{31}P\{^{1}H\}$ NMR spectrum of **5a** in C_6D_6.

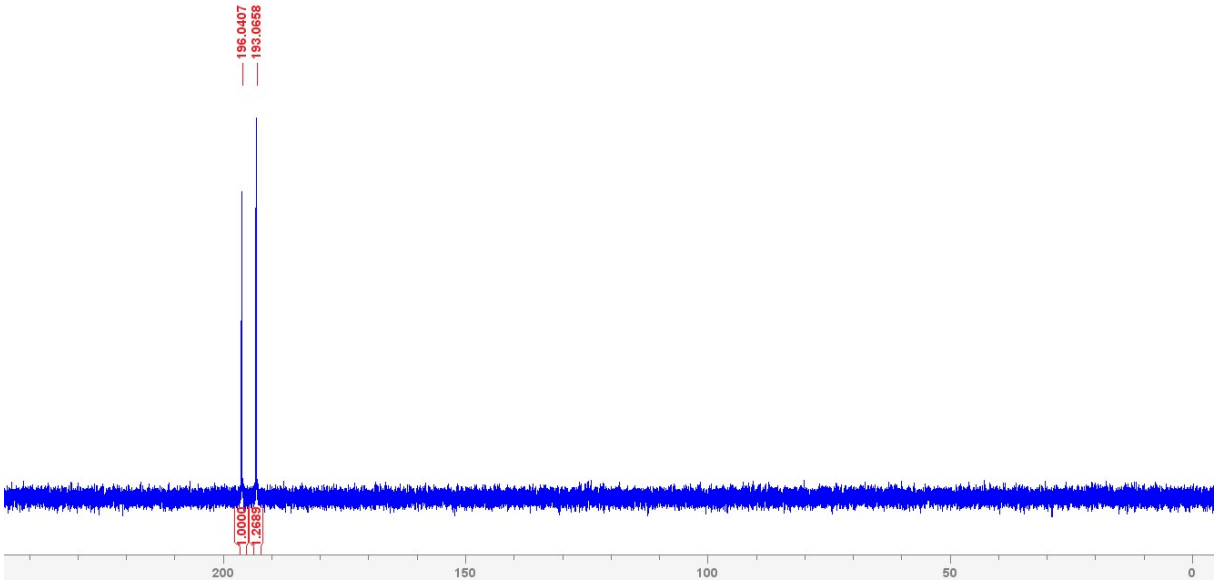

Figure 48. Full $^{31}P\{^{1}H\}$ NMR spectrum of **5a** in C_6D_6 from a different batch.

Complex **6a**

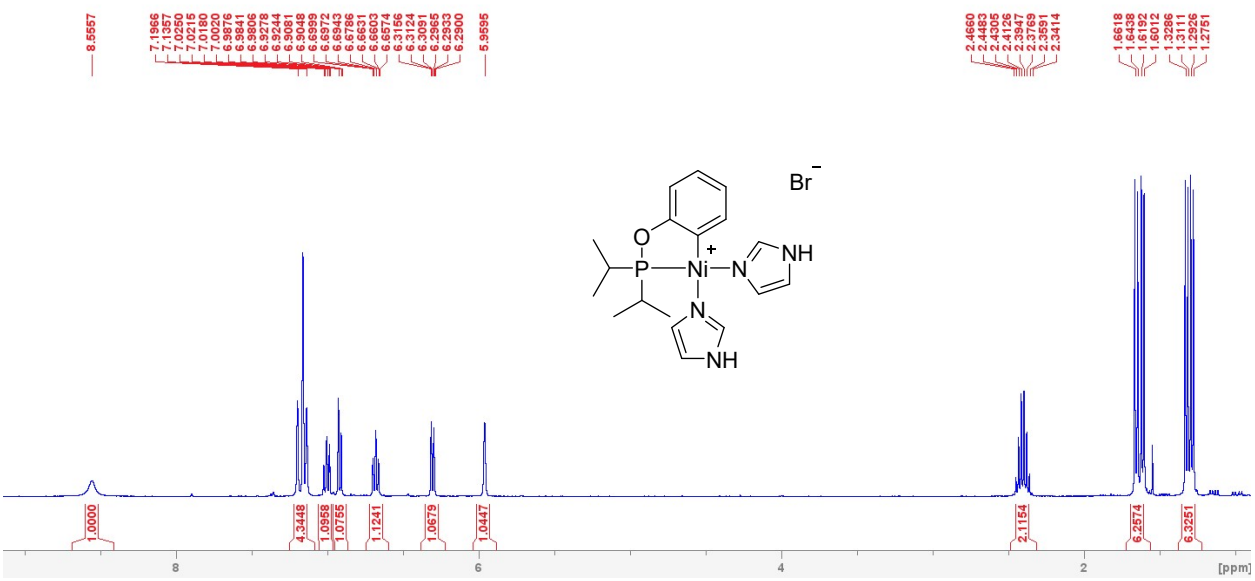

Figure S49. Full ^{1}H NMR spectrum of **6a** in C_6D_6.

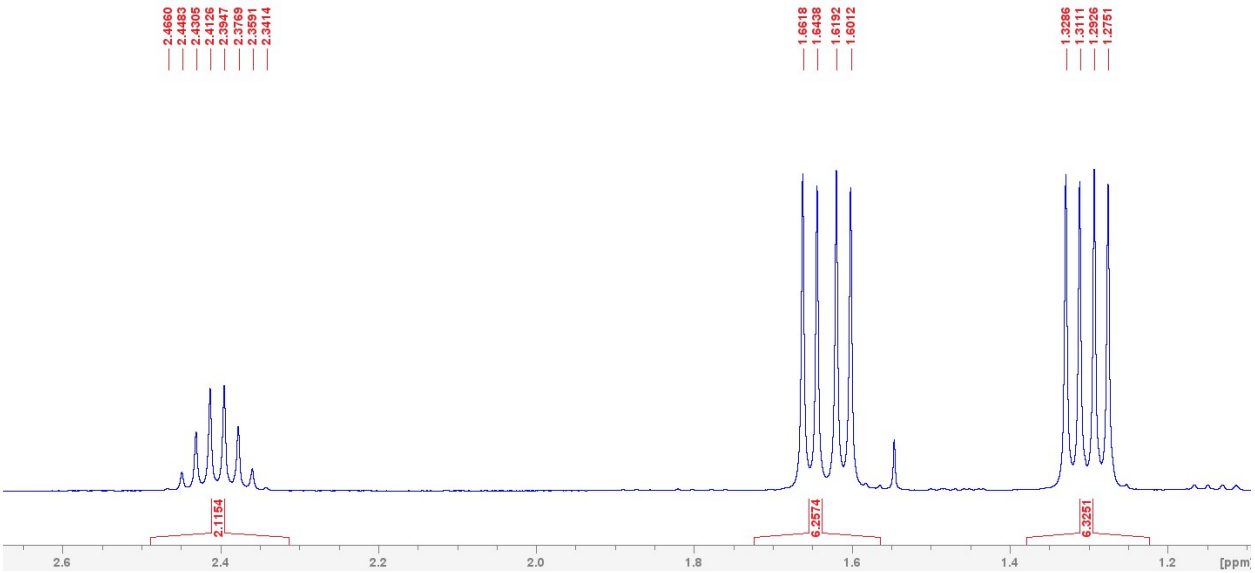

Figure S50. The expanded aliphatic region of the ^{1}H NMR spectrum of **6a** in C_6D_6.

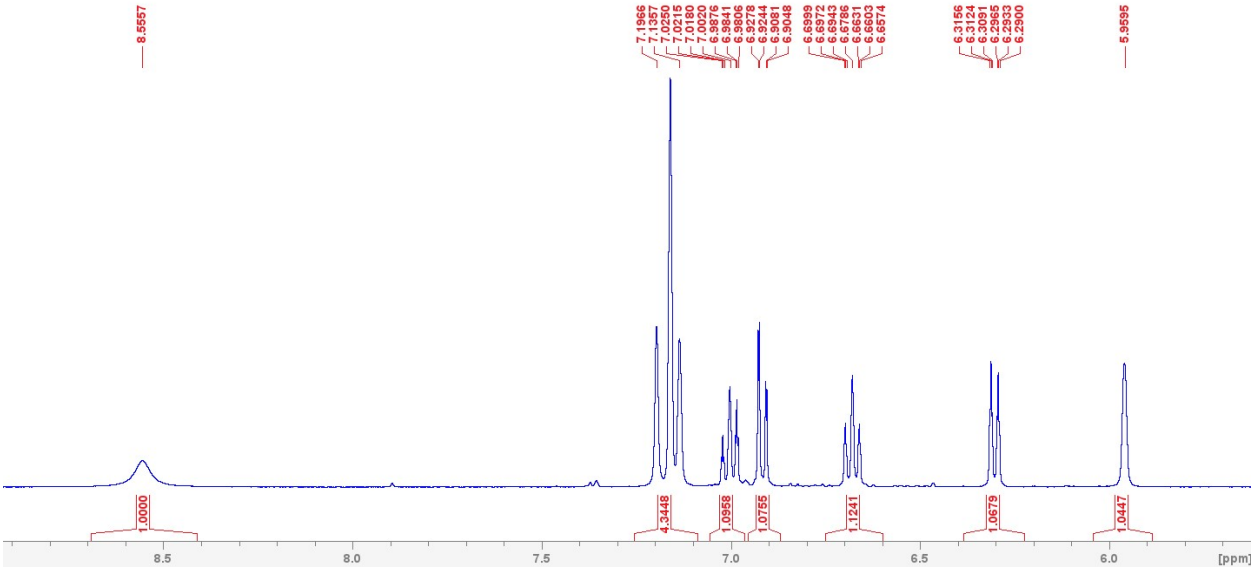

Figure S51. The expanded aromatic region of the ^{1}H NMR spectrum of **6a** in C_6D_6.

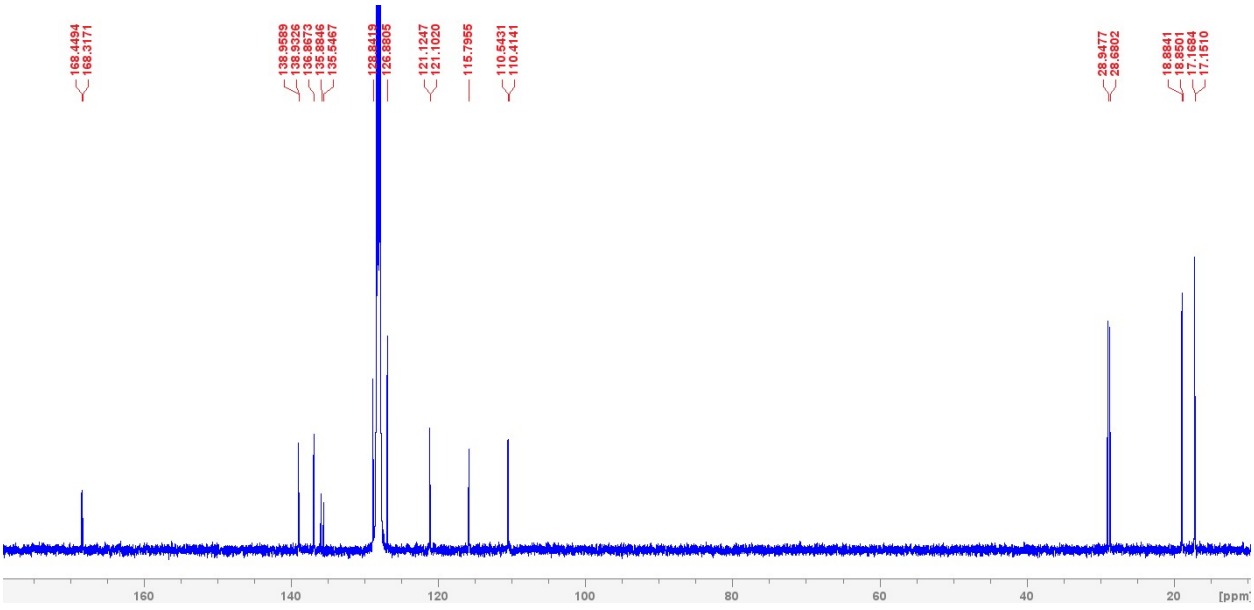

Figure S52. Full $^{13}C\{^{1}H\}$ NMR spectrum of **6a** in C_6D_6.

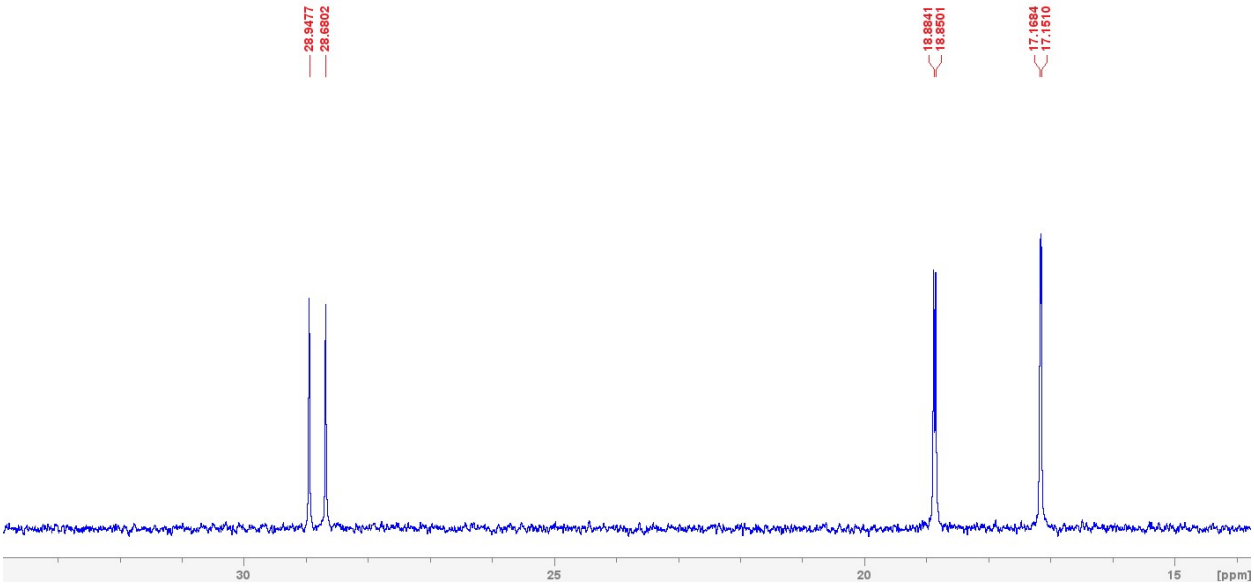

Figure S53. The expanded aliphatic region of the $^{13}C\{^{1}H\}$ NMR spectrum of **6a** in C_6D_6.

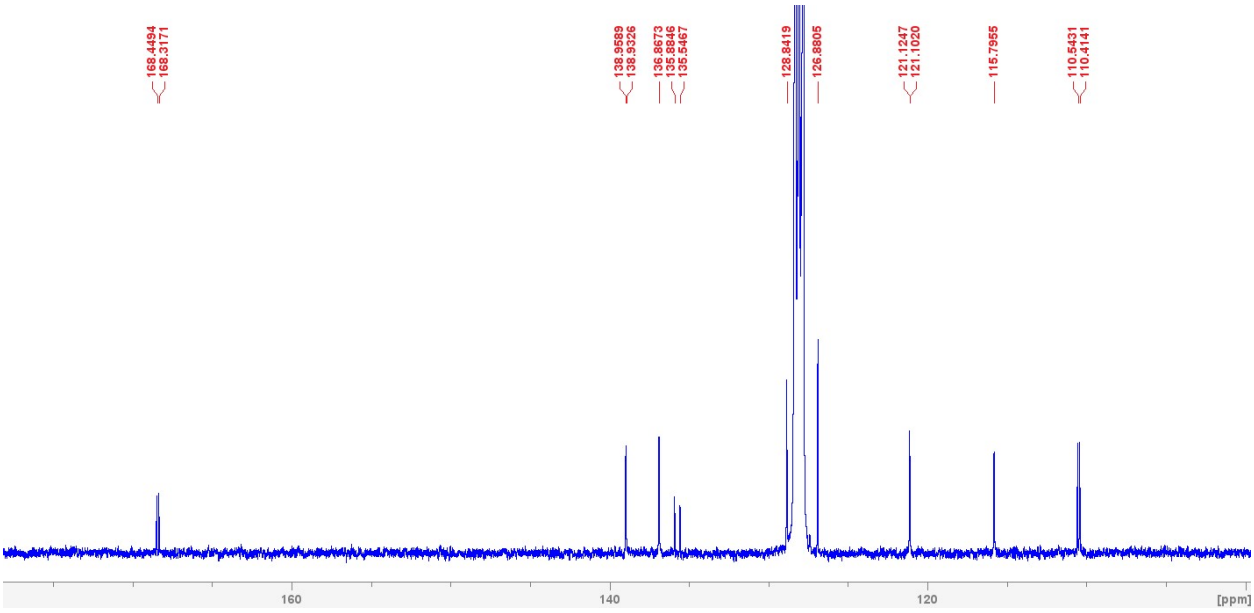

Figure S54. The expanded aromatic region of the $^{13}C\{^{1}H\}$ NMR spectrum of **6a** in C_6D_6.

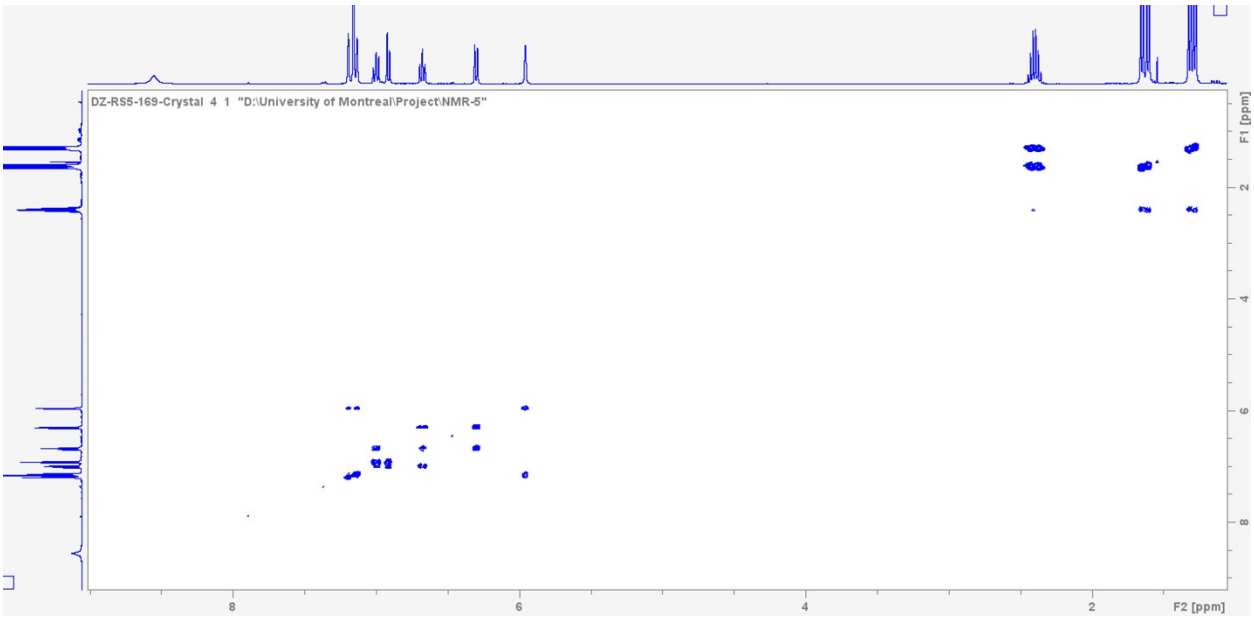

Figure S55. Full ^{1}H-^{1}H COSY NMR spectrum of **6a** in C_6D_6.

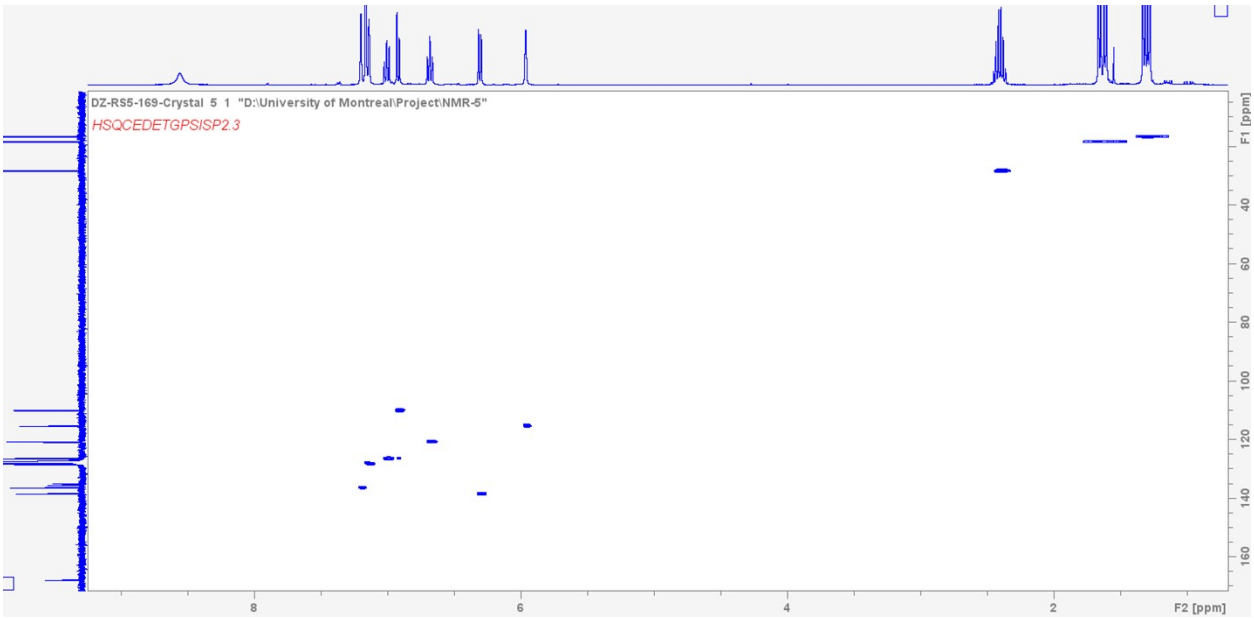

Figure S56. Full HSQC-edited NMR spectrum of **6a** in C_6D_6.

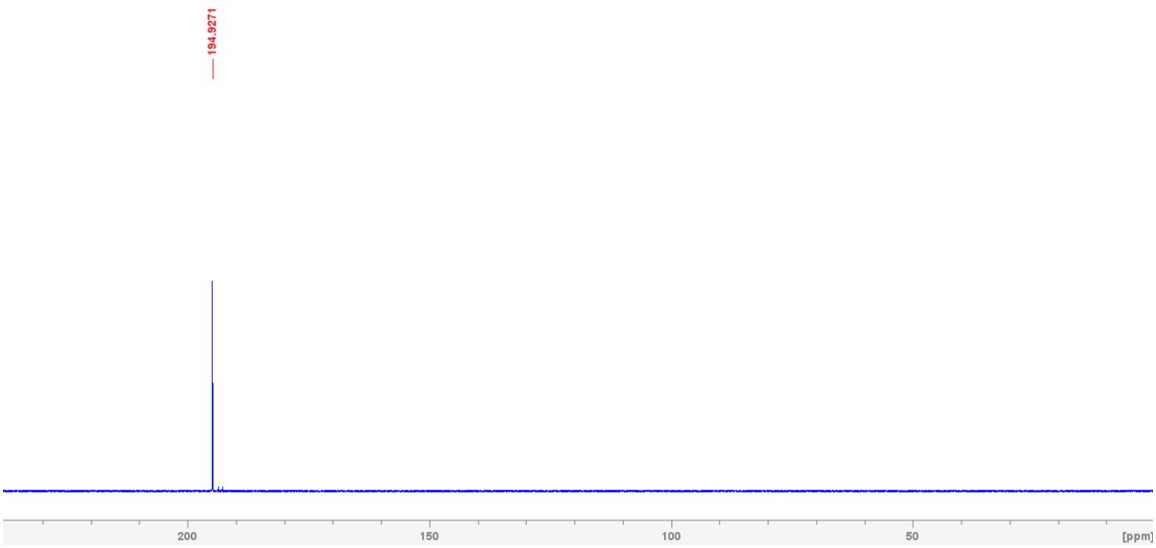

Figure S57. $^{31}P\{^{1}H\}$ NMR spectrum of **6a** in C_6D_6.

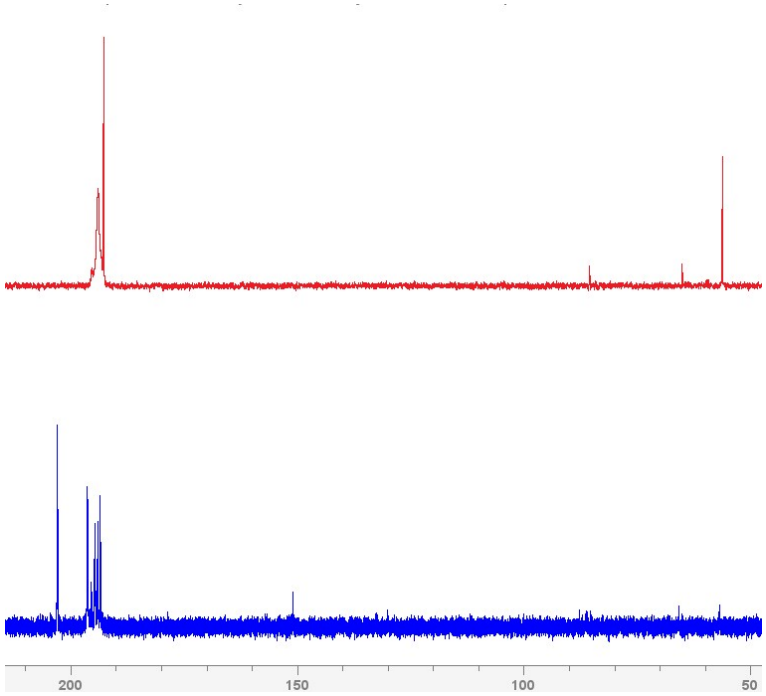

Figure S58. $^{31}P\{^{1}H\}$ NMR spectra of **3a** with 1 equiv (blue trace) and 2 equiv (red trace) of imidazole in CH_2Cl_2.

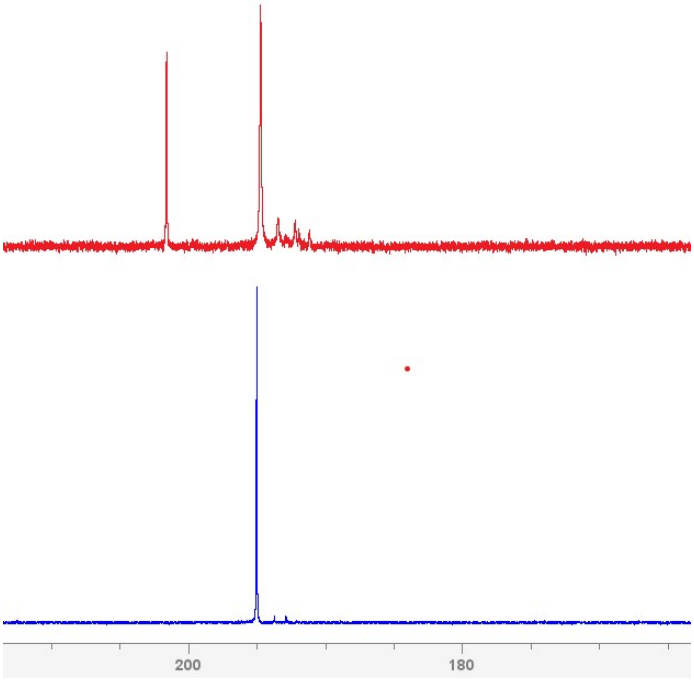

Figure S59. $^{31}P\{^{1}H\}$ NMR spectra of **1a** with 2 equiv (blue trace) of imidazole and 2 equiv (red trace) of TEMPOH (Ni:imidazole:TEMPOH= 1:1:1) in CH_2Cl_2.

Complex **7a**

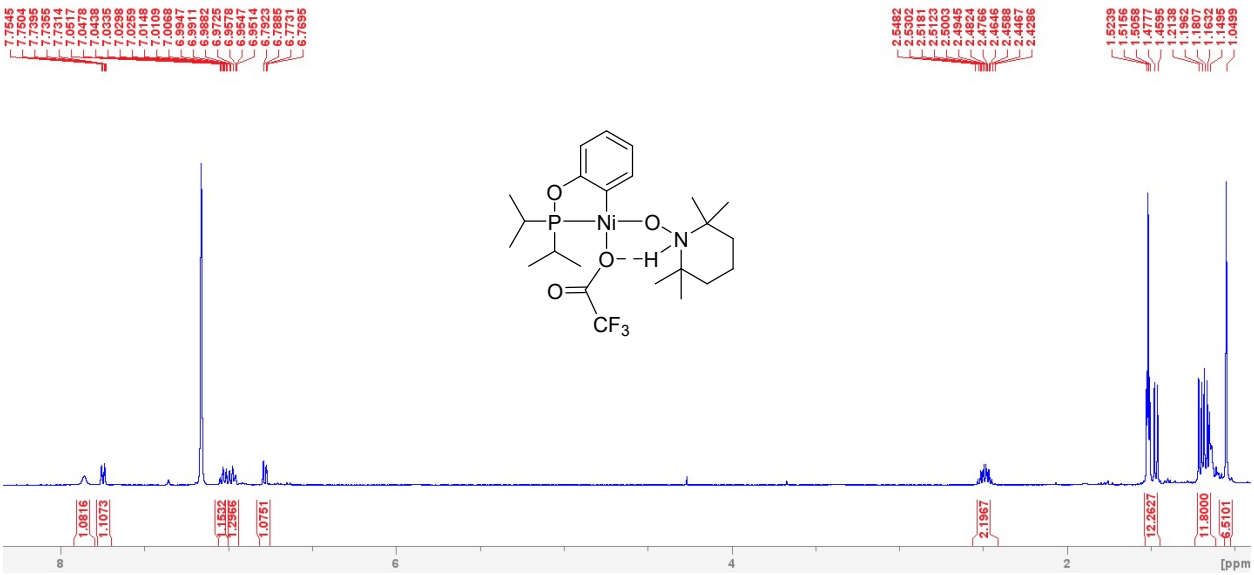

Figure S60. Full ^{1}H NMR spectrum of **7a** in C_6D_6.

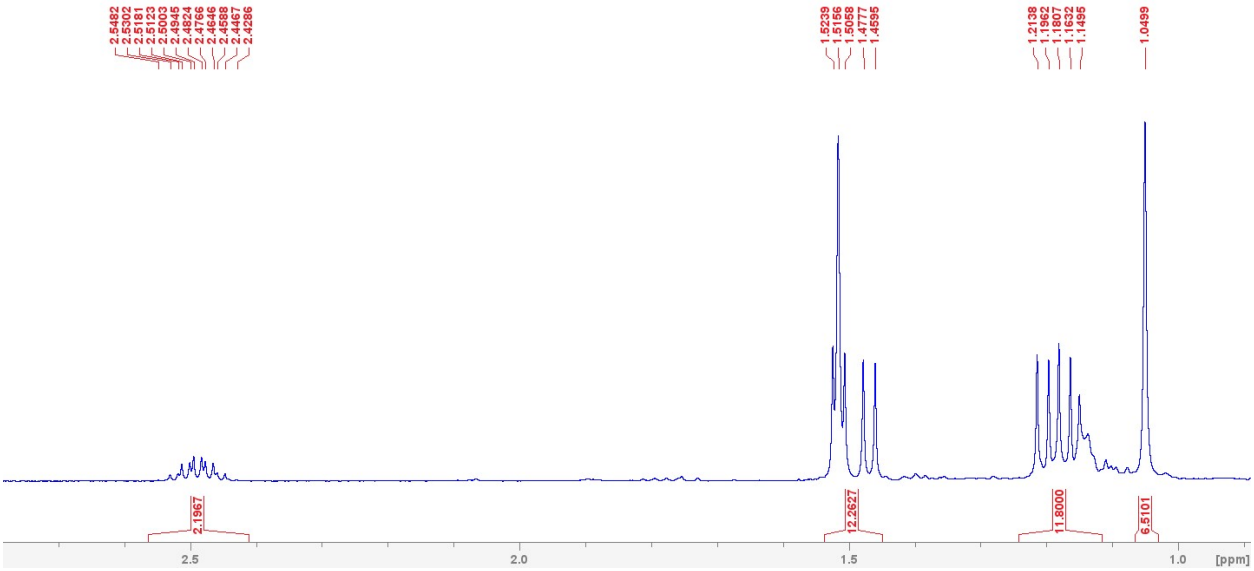

Figure S61. The expanded aliphatic region of the ^{1}H NMR spectrum of **7a** in C_6D_6.

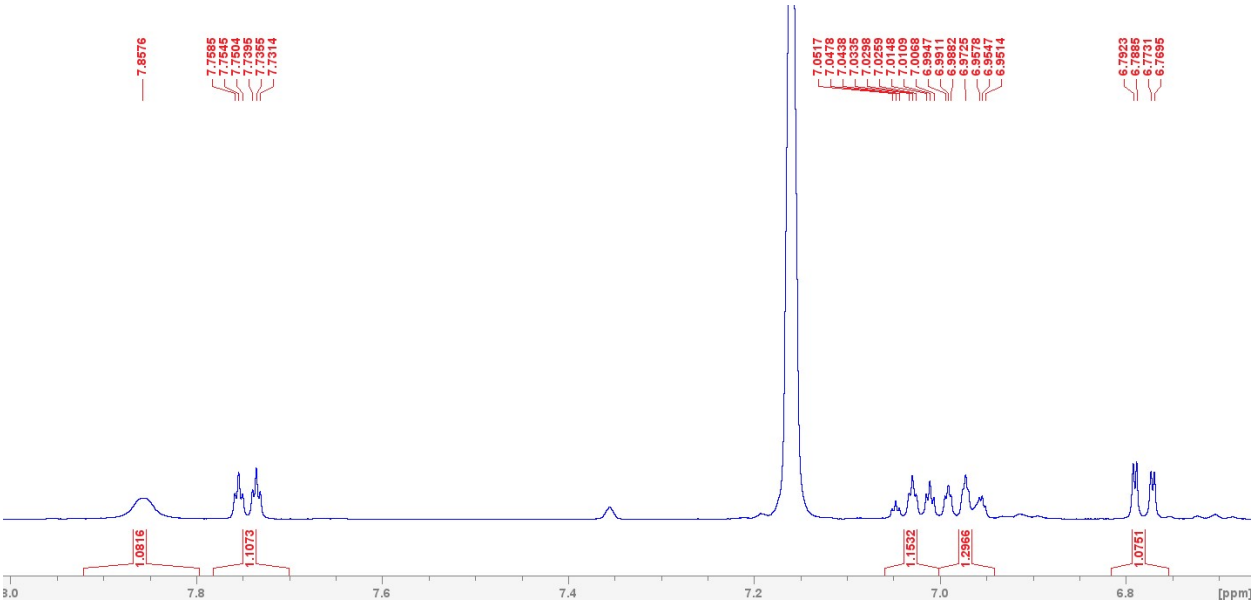

Figure S62. The expanded aromatic region of the ^{1}H NMR spectrum of **7a** in C_6D_6.

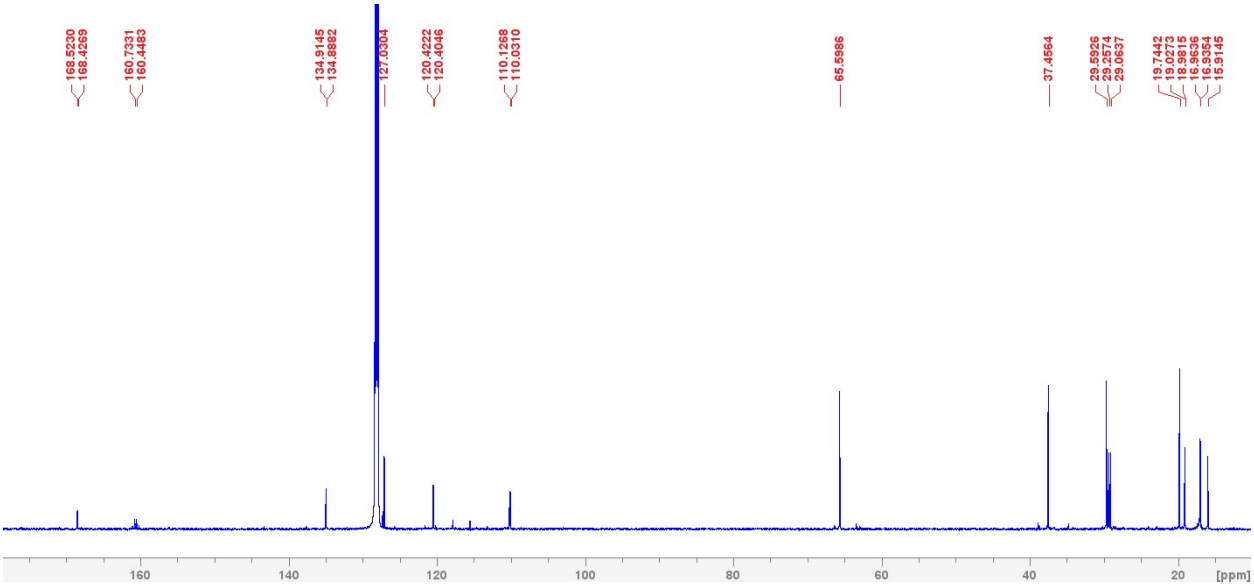

Figure S63. Full $^{13}C\{^{1}H\}$ NMR spectrum of **7a** in C_6D_6.

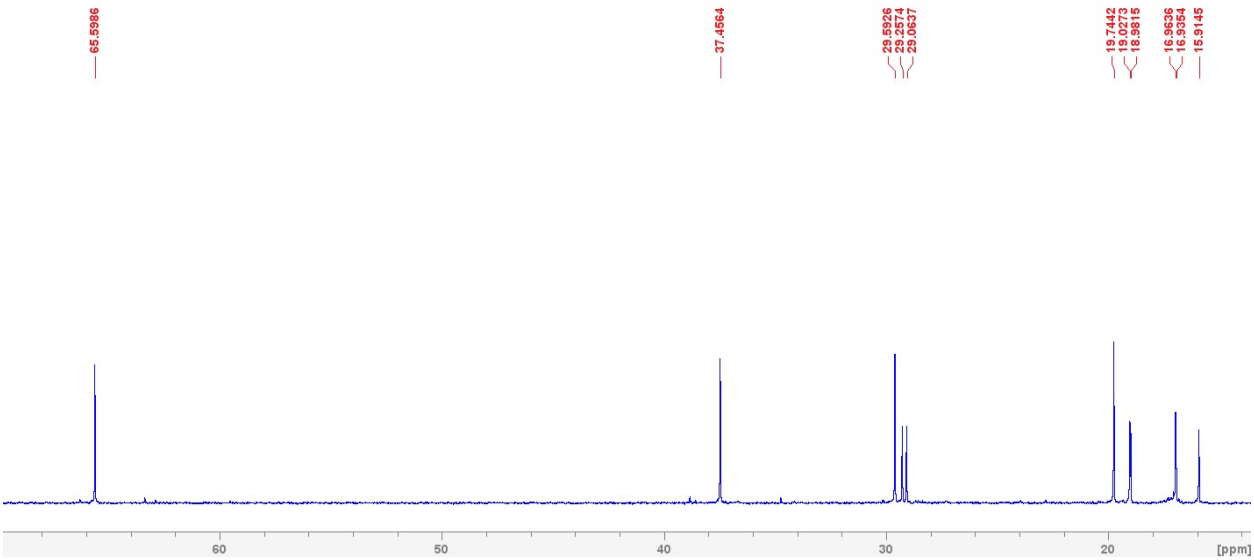

Figure S64. The expanded aliphatic region of the $^{13}C\{^{1}H\}$ NMR spectrum of **7a** in C_6D_6.

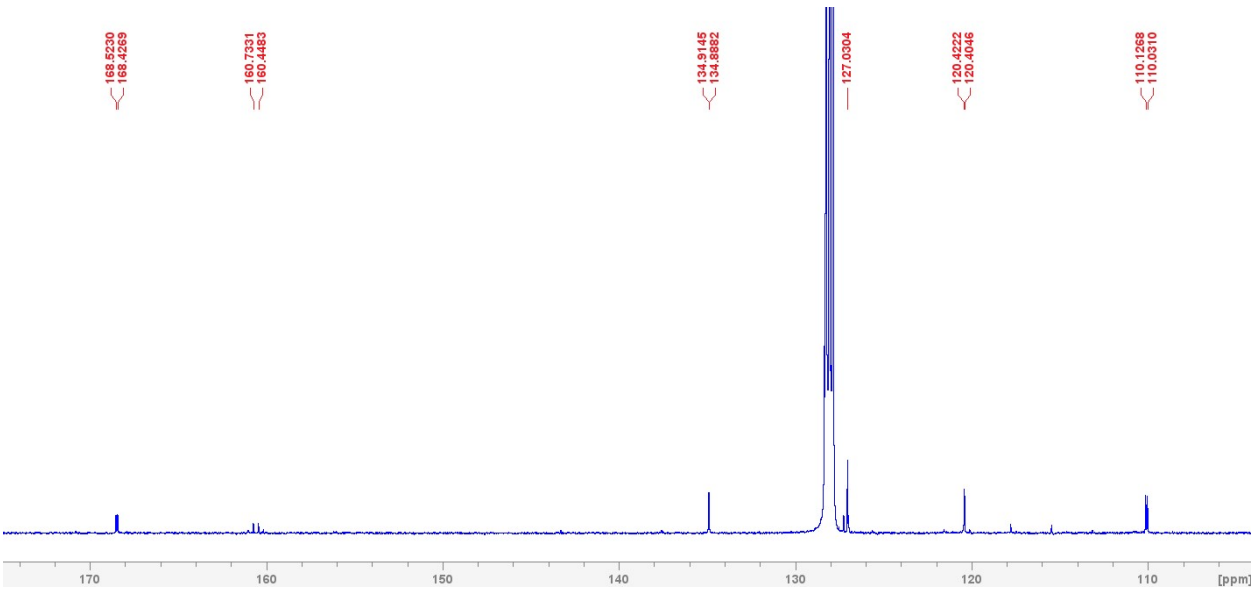

Figure S65. The expanded aromatic region of the $^{13}C\{^{1}H\}$ NMR spectrum of **7a** in C_6D_6.

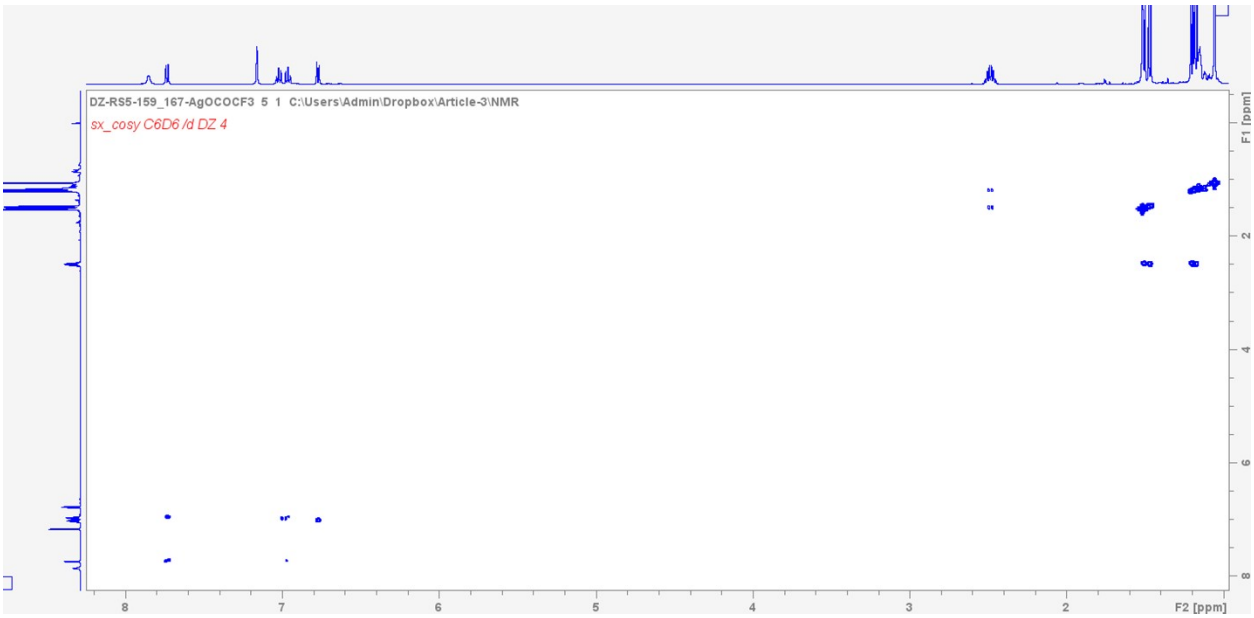

Figure S66. Full ^{1}H-^{1}H COSY NMR spectrum of **7a** in C_6D_6.

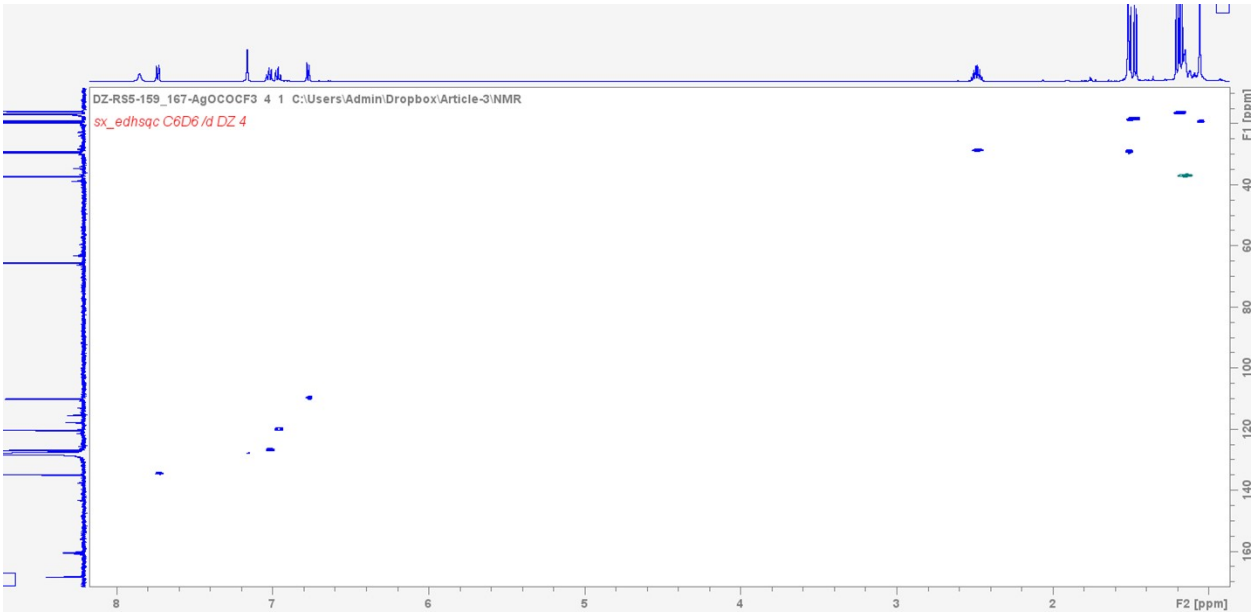

Figure S67. Full HSQC-Edited NMR spectrum of **7a** in C_6D_6.

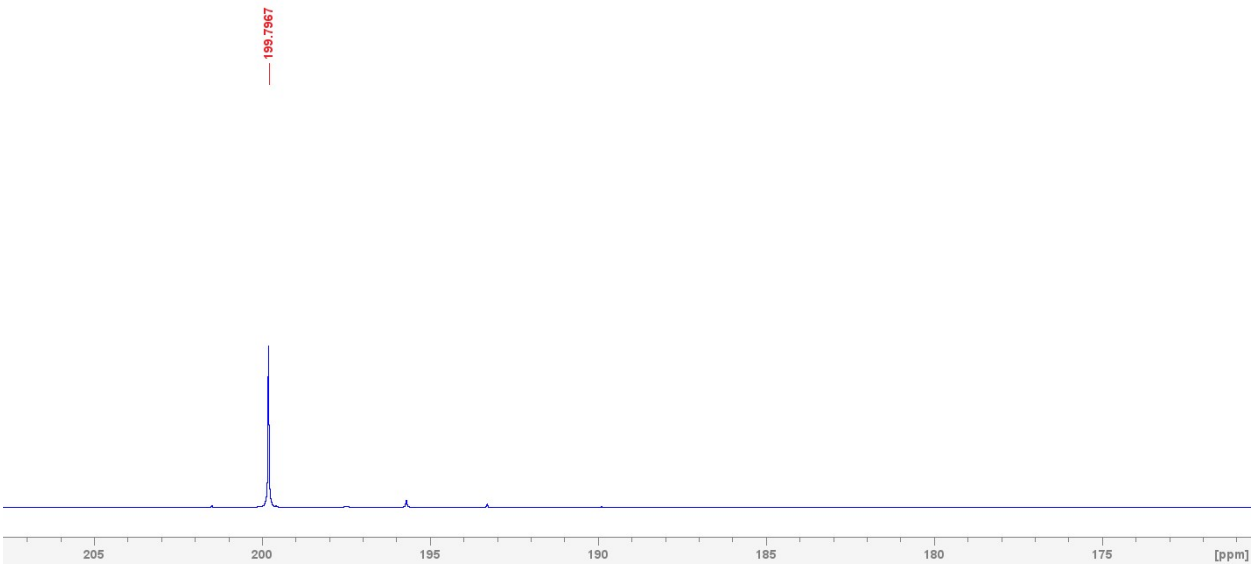

Figure S68. Full $^{31}P\{^{1}H\}$ NMR spectrum of **7a** in C_6D_6.

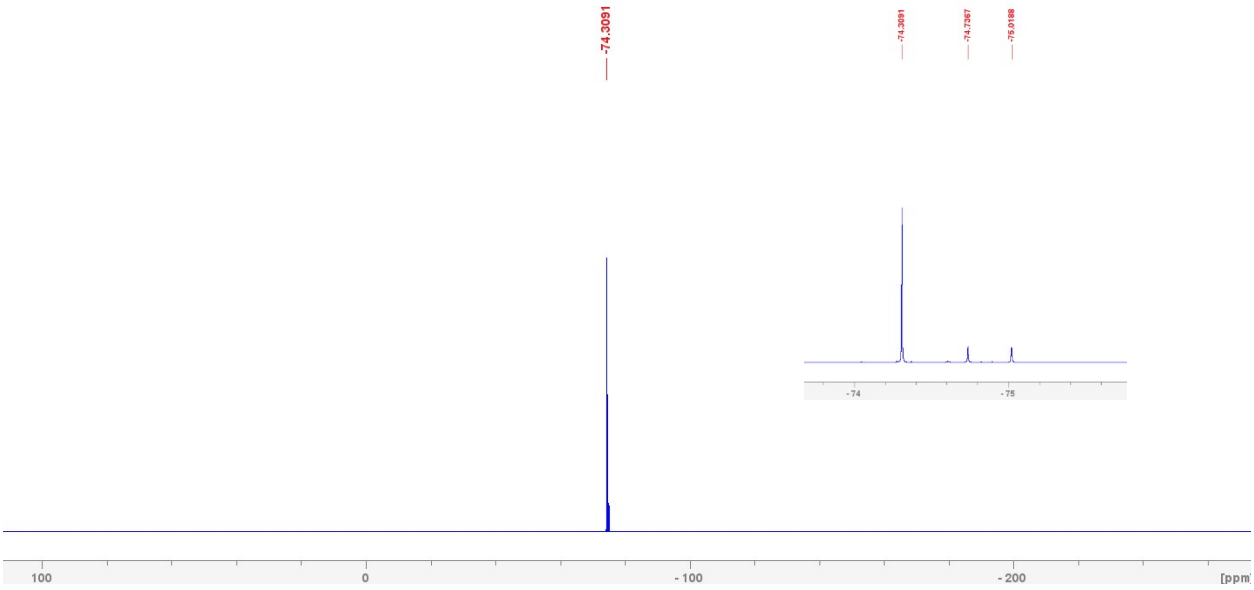

Figure S69. Full $^{19}F\{^{1}H\}$ NMR spectrum of **7a** in C_6D_6.

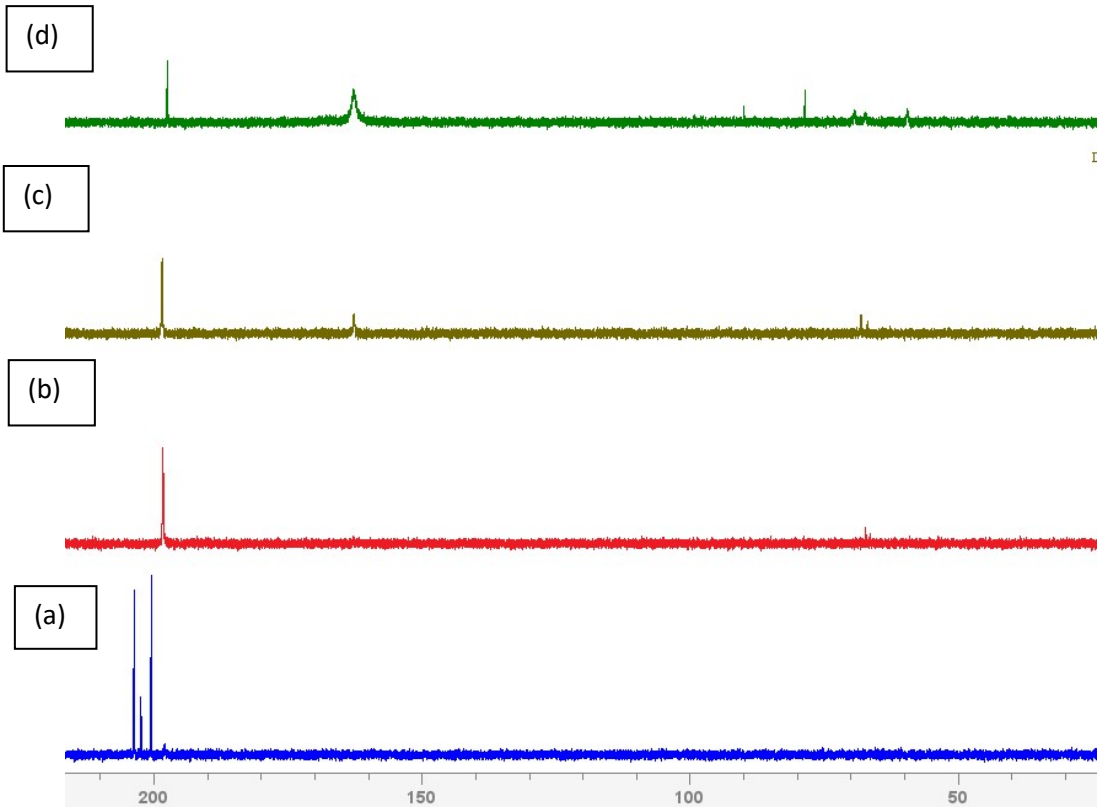

Figure S70. $^{31}P\{^{1}H\}$ NMR (CH_2Cl_2) spectra of **3a** with various amounts of $AgOCOCF_3$: blue trace, a (1 equiv), red trace, b (3 equiv), brown trace, c (3 equiv, after 24h), green trace, d (4 equiv).

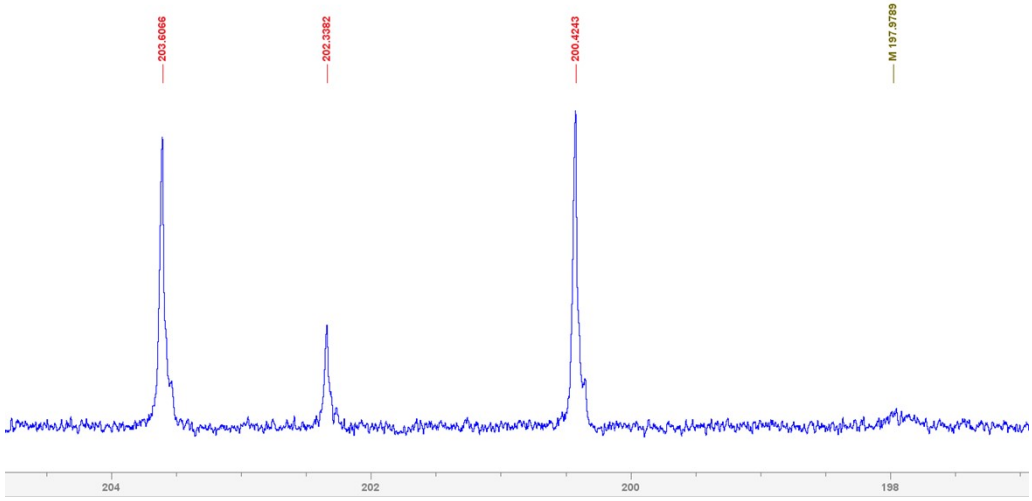

Figure S71. $^{31}P\{^{1}H\}$ NMR spectra of **3a** with 1 equivalent of $AgOCOCF_3$ in CH_2Cl_2.

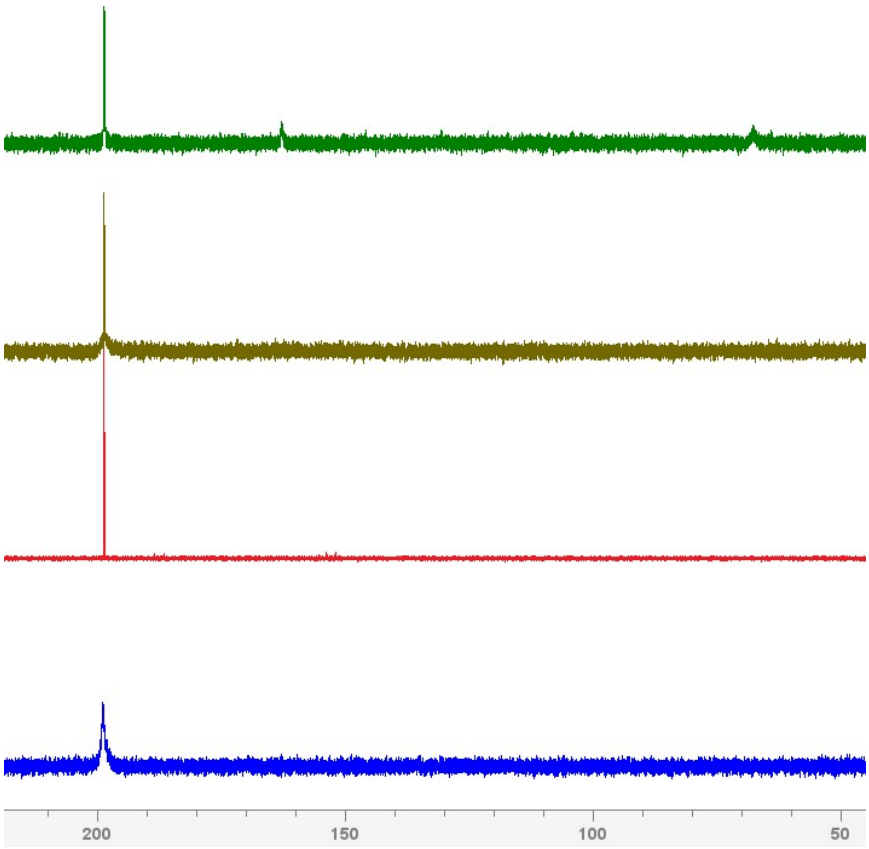

Figure S72. $^{31}P\{^{1}H\}$ NMR spectra recorded for a DCM sample of **1a** to which were added successive quantities of $AgOCOCF_3$, as follows: blue trace, 0 equiv (199 ppm, FWHM ≈ 100 Hz); red trace, 2 equiv (196 ppm, FWHM ≈ 4 Hz); brown trace, 4 equiv (196 ppm, FWHM ≈ 9 Hz); green trace, 6 equiv (198 ppm, FWHM ≈ 21 Hz).

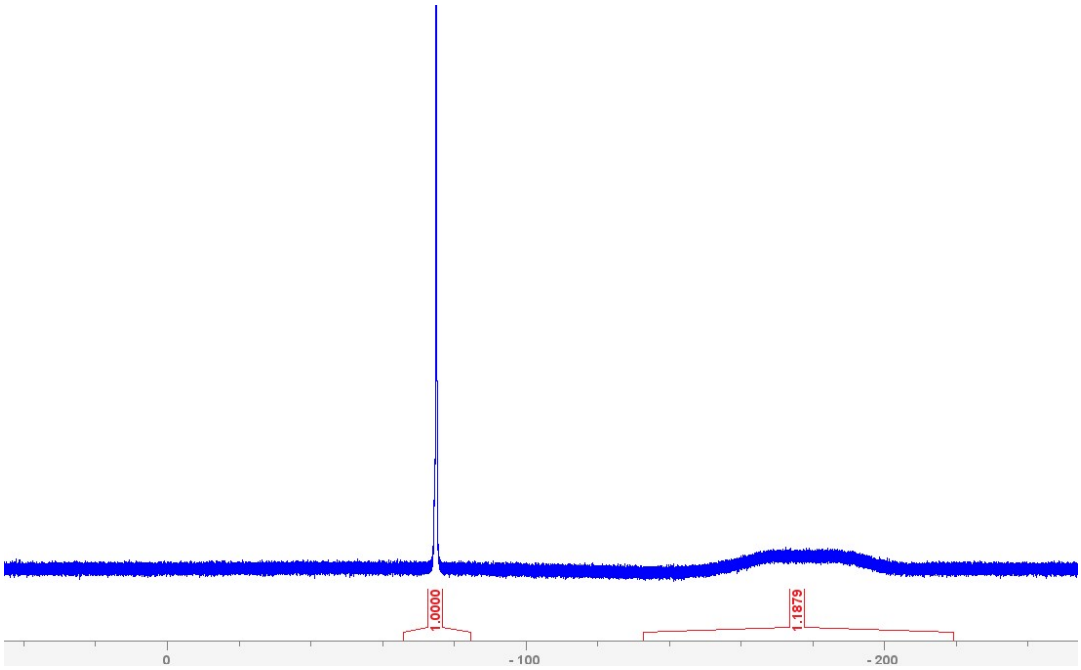

Figure S73. $^{19}F\{^{1}H\}$ NMR spectrum of crude mixture of **3a** with 3eq of $AgOC(O)CF_3$ in CH_2Cl_2.

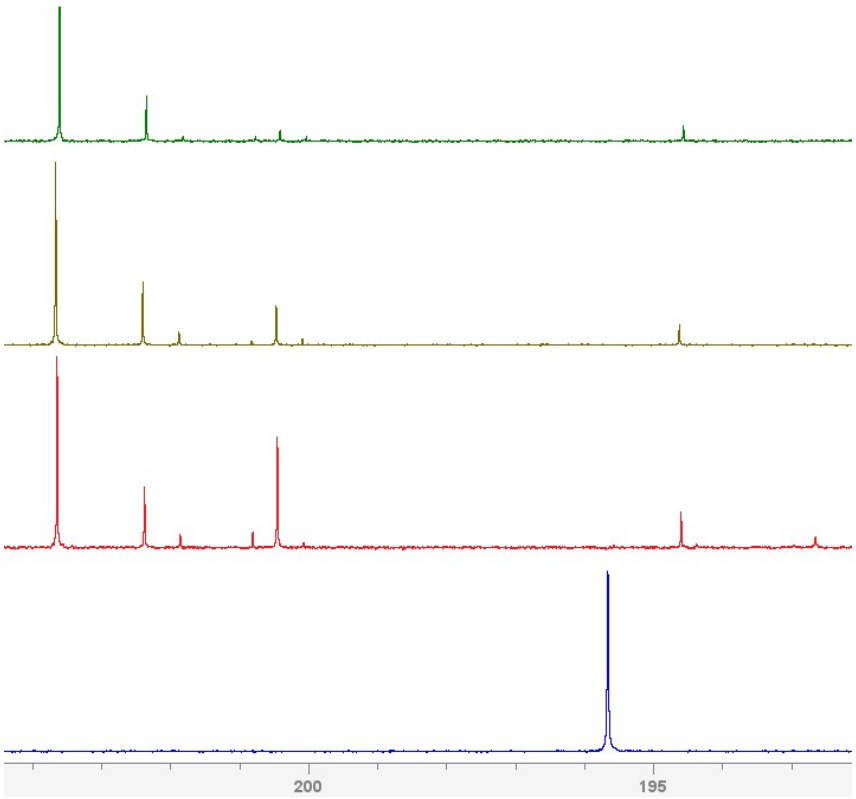

Figure S74. $^{31}P\{^{1}H\}$ NMR spectra recorded for a DCM sample containing a mixture of **1a** and 2 equiv of $AgOCOCF_3$ (to generate a 1:1 ratio of Ni : CF_3COO) to which were added successive quantities of TEMPOH, as follows (bottom to top): blue trace, 0 equiv; red trace, 1 equiv; brown trace, 2 equiv; green trace, 4 equiv.

5. Crystallographic data tables

Table S1: Crystal description and refinement indicators for compounds 3a-3c

	3a	**3b**	**3c**
chemical formula	$C_{21}H_{37}BrNNiO_2P$	$C_{21}H_{36}BrClNNiO_2P$	$C_{22}H_{39}Br_{0.25}Cl_{0.75}NNiO_3P$
crystal colour	brown	brown	brown
crystal size (mm)	0.122 × 0.175 × 0.197	0.226 × 0.331 × 0.472	0.118 × 0.149 × 0.178
index ranges	-18 ≤ h ≤ 18 -14 ≤ k ≤ 13 -18 ≤ l ≤ 18	-19 ≤ h ≤ 19 -14 ≤ k ≤ 14 -18 ≤ l ≤ 18	-14 ≤ h ≤ 14 -17 ≤ k ≤ 17 -36 ≤ l ≤ 36
***Fw*; *F*(000)**	505.10; 1056	539.55; 1120.0	501.78; 2132.0
***T* (K)**	150	150	150
wavelength (Å)	1.34139	1.34139	1.34139
space group	$P2_1/c$	$P2_1/c$	$P2_1/c$
***a* (Å)**	15.1559(3)	15.8263(4)	11.9270(5)
***b* (Å)**	11.6422(3)	11.6352(3)	14.1466(6)
***c* (Å)**	15.0239(3)	14.8354(4)	29.5812(12
α (deg)	90	90)	90
β (deg)	117.4860(10)	114.5960(10)	98.950(2)
γ (deg)	90	90	90
Z	4	4	8
***V* (Å^3)**	2351.71(9)	2483.95(11)	4930.4(4)
ρ_{calcd} (g·cm^{-3})	1.427	1.443	1.352
μ (mm^{-1})	6.320	6.654	5.623
2θ range (deg); completeness	5.718 − 113.912; 0.992	5.342 − 109.842; 0.993	5.262 − 109.846; 0.988
collected reflections; R_σ	24417; 0.0290	30401; 0.0483	45605; 0.0268
unique reflections; R_{int}	4716; 0.0404	4668; 0.0640	9244; 0.0315
R1[a]; wR2[b] [I > 2σ(I)]	0.0266; 0.0705	0.0424; 0.1060	0.0284; 0.0721
R1; wR2 [all data]	0.0278; 0.0711	0.0469; 0.1078	0.0308; 0.0734
GOOF	1.087	1.095	1.029
largest diff peak and hole	0.33 and -0.79	0.91 and -0.96	0.67 and -0.46

[a] $R_1=\Sigma(||F_o|-|F_c||)/\Sigma|F_o|$

[b] $wR_2=\{\Sigma[w(F_o^2-F_c^2)^2]/\Sigma[w(F_o^2)^2]\}^{½}$

Table S2: Crystal description and refinement indicators for compounds 3d, 5a & 6a.

	3d	**5a**	**6a**
chemical formula	$C_{26}H_{41}BrNNiO_3P$	$C_{16}H_{27}Br_{0.24}Cl_{0.76}NNiO_2P$	$C_{21}H_{30}BrN_6NiOP$
crystal colour	brown	brown	brown
crystal size (mm)	0.236 × 0.354 × 0.388	0.083 × 0.101 × 0.168	0.088 × 0.099 × 0.117
index ranges	$-15 \le h \le 15$ $-19 \le k \le 19$ $-17 \le l \le 18$	$-9 \le h \le 9$ $-30 \le k \le 30$ $-11 \le l \le 11$	$-11 \le h \le 10$ $-0 \le k \le 33$ $-0 \le l \le 12$
***Fw*; *F*(000)**	585.19; 1220.0	401.18; 841.0	552.10; 1136.0
***T* (K)**	150	150	150
wavelength (Å)	1.34139	1.34139	1.34139
space group	$P2_1/n$	$P2_1/n$	$P2_1/n$
***a* (Å)**	12.4164(6)	7.7771(3)	9.1454(4)
***b* (Å)**	16.3578(8)	24.7633(8)	27.5501(11)
***c* (Å)**	14.9046(7)	9.4301(3)	9.8982(4)
α (deg)	90	90	90
β (deg)	112.769(2)	97.0120(10)	102.159(2)
γ (deg)	90	90	90
Z	4	4	4
***V* (Å^3)**	2791.3(2)	1802.53(11)	2437.97(18)
ρ_{calcd} (g·cm^{-3})	1.390	1.478	1.504
μ (mm^{-1})	5.394	7.580	6.154
θ range (deg); completeness	7.31 − 109.844; 0.978	6.21 − 109.74; 0.969	9.048 – 109.8; 0.986
collected reflections; R_σ	20919; 0.0446	15394; 0.0252	42525; 0.0436
unique reflections; R_{int}	5133; 0.0493	3317; 0.0280	9390; 0.0664
R1[a]; wR2[b] [I > 2σ(I)]	0.0678; 0.1716	0.0275; 0.0697	0.0429; 0.1126
R1; wR2 [all data]	0.0687; 0.1735	0.0281; 0.0700	0.0445; 0.1149
GOOF	1.044	1.136	1.065
largest diff peak and hole	2.01 and -1.10	0.39 and -0.38	0.52 and -0.62

[a] $R_1=\Sigma(||F_o|-|F_c||)/\Sigma|F_o|$
[b] $wR_2=\{\Sigma[w(F_o^2-F_c^2)^2]/\Sigma[w(F_o^2)^2]\}^{½}$

Table S3: Crystal description and refinement indicators for compounds 7a.

	7a	**Piperidinium trifluoroacetate**
chemical formula	$C_{23}H_{37}F_3NNiO_4P$	$C_{11}H_{20}F_3NO_2$
crystal colour	yellow	yellow
crystal size (mm)	0.097 × 0.112 × 0.148	0.099 × 0.24 × 0.25
index ranges	-18 ≤ h ≤ 19 -15 ≤ k ≤ 15 -17 ≤ l ≤ 17	-27≤ h ≤ 25 -11 ≤ k ≤ 9 -21 ≤ l ≤ 21
***Fw*; *F*(000)**	538.21; 1136.0	255.28; 1088.0
***T* (K)**	150	150
wavelength (Å)	1.34139	1.34139
space group	$P2_1/c$	C2/c
***a* (Å)**	15.7583(5)	19.9649(14)
***b* (Å)**	12.7241(4)	8.3817(6)
***c* (Å)**	14.1830(5)	15.8150(11)
α (deg)	90	90
β (deg)	115.546(2)	91.234(4)
γ (deg)	90	90
Z	4	8
***V* (Å^3)**	2565.82(15)	2645.9(3)
ρ_{calcd} (g·cm^{-3})	1.393	1.282
μ (mm^{-1})	4.797	0.632
2θ range; completeness	5.408 – 110.106; 0.993	7.706 –131.816; 0.985
collected reflections; R_σ	24214; 0.0735	29827; 0.0318
unique reflections; R_{int}	4845; 0.0835	3447; 0.0468
R1[a]; wR2[b] [I > 2σ(I)]	0.0568; 0.1171	0.0565; 0.1566
R1; wR2 [all data]	0.0942; 0.1291	0.0673; 0.1674
GOOF	1.050	1.058
largest diff peak and hole	0.39 and -0.42	0.45 and -0.28

[a] $R_1=\Sigma(||F_o|-|F_c||)/\Sigma|F_o|$
[b] $wR_2=\{\Sigma[w(F_o^2-F_c^2)^2]/\Sigma[w(F_o^2)^2]\}^{½}$

Table S4. Pertinent bond angles and distances for complexes **3a-3d** and **5a-7a**

	Ni1–C2	Ni1–P1	Ni1–Br1 or Ni1-Cl1	Ni1–O2/O3	Ni1–N	N-O2	C2-Ni1-Br1/ Cl1/N2/O3	P1-Ni1-N/O
3a	1.9017(18)	2.0905(5)	2.3897(3)	1.9045(12)		1.3973(18)	170.76(5)	171.64(4)
3b	1.9026(16)	2.0927(5)	2.373(8)	1.9132(11)		1.400(2)	174.0(2)	171.90(4)
3c	1.907(2)	2.0924(6)	2.3872(4)	1.8918(16)		1.3902(19)	172.14(8)	169.73(5)
3d	1.896(3)	2.0995(8)	2.3775(5)	1.908(2)		1.399(3)	173.99(9)	171.23(7)
5a	1.9076(18)	2.1026(5)	2.380(11)		1.9921(17)		168.6(3)	164.72(5)
6a	1.918(2)	2.1210(7)			1.944(2) 1.930(2)		175.45(9)	176.01(6)
7a	1.904(4)	2.1138(12)		1.945(3) 1.902(3)		1.390(4)	174.86(16)	169.95(9)

Table S5. Pertinent bond angles and distances for complexes **3a-3d** and **7a**

	Br-N/ O3-N	N1–H1–Br1/ N1-H1-O3
3a	3.167	144.462
3b	3.167	144.121
3c	3.136	144.097
3d	3.190	139,480
7a	2.665	140.149

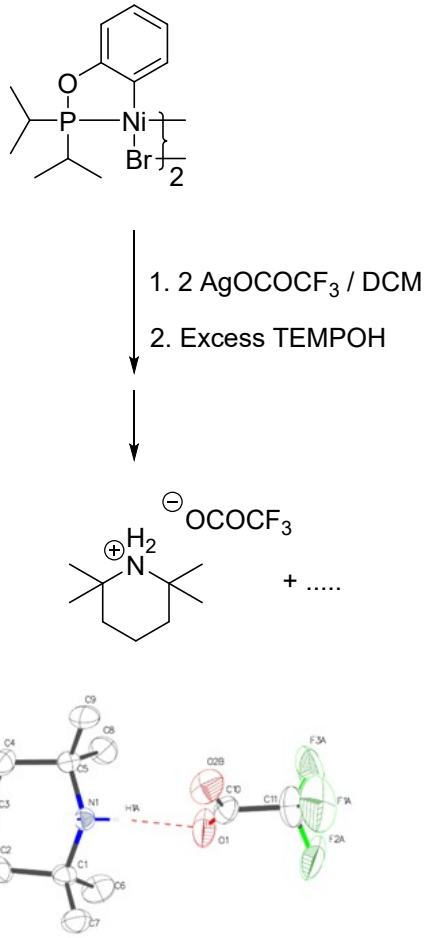

Figure S75. Reaction scheme for formation of piperidinium trifluoroacetate and its molecular diagram. Thermal ellipsoids are shown at the 50% probability level. Hydrogen atoms have been omitted for clarity.

Scheme S1: Anticipated reactivity of title complexes with hydroxylamines and TEMPO

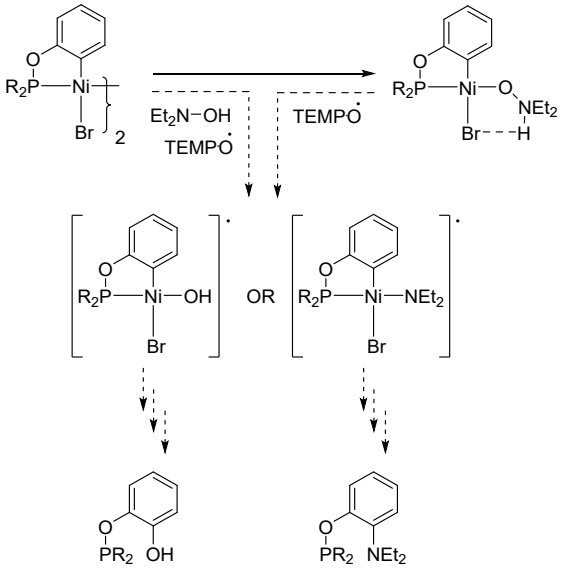

Scheme S2. Proposed reactivity of 3a with AgOC(O)CF3.

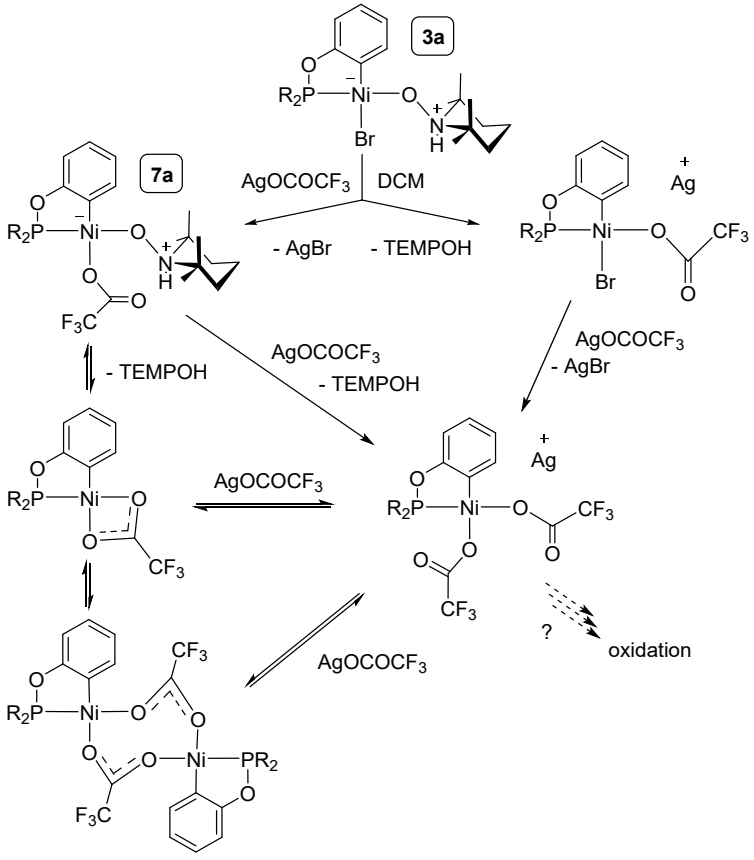

Cyclic voltammetry traces for isolated nickelacycle complexes 3a and 7a.

Conditions: 5 mM solutions of [Ni] in 0.1 M NBu_4SbF_6 in CH_2Cl_2; scan rate 100 mV/s, scanning oxidatively. Potentials are calibrated against the Fc/Fc^+ couple.

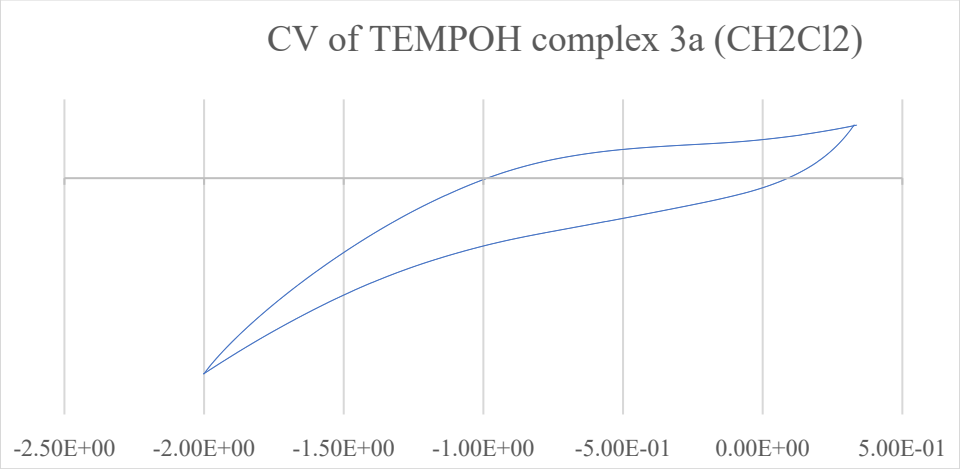

Figure S76.

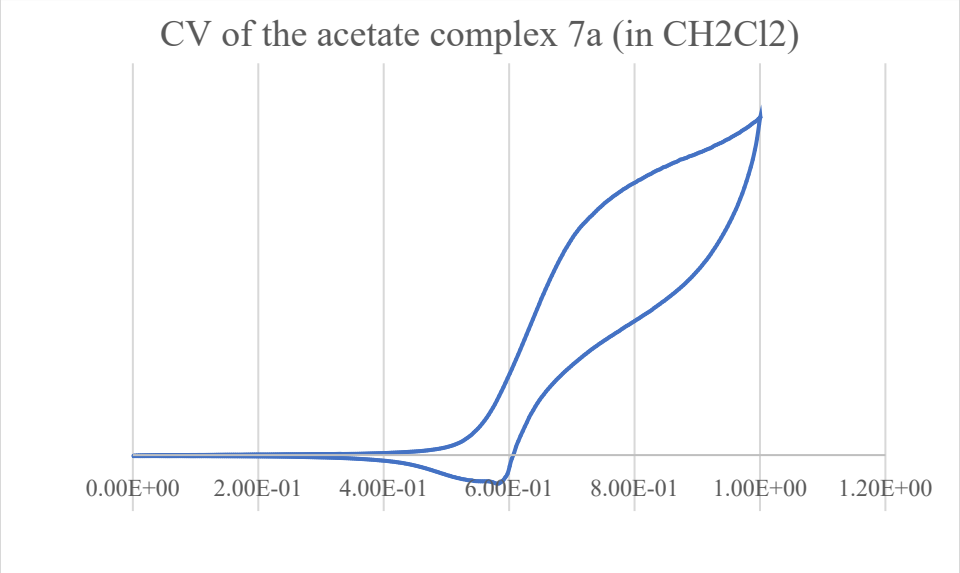

Figure S77.

References

(1) Post-facto calibration of the 100-1000 µl micropipette with 20 ∈ 500 µl aliquots of deionized H_2O revealed that we must allow an accuracy (systematic error) of +4 µl and a precision of ±3 µl for our measurements, with > 99% confidence. The 20-200 µl micropipette was calibrated by the same procedure, with 150 µl aliquots, and revealed an accuracy of +0.3 µl and a precision of ±3 µl for our measurements, with > 99% confidence.

(2) Vabre, B.; Spasyuk, D. M.; Zargarian, D. Impact of Backbone Substituents on POCOP-Ni Pincer Complexes: A Structural, Spectroscopic, and Electrochemical Study. *Organometallics* **2012**, *31* (24), 8561–8570. https://doi.org/10.1021/om3009475.

(3) Vabre, B.; Lindeperg, F.; Zargarian, D. Direct, One-Pot Synthesis of POCOP-Type Pincer Complexes from Metallic Nickel. *Green Chemistry* **2013**, *15* (11), 3188–3194. https://doi.org/10.1039/c3gc40968f.

(4) Bruker (2012). APEX2 / Bruker (2016) APEX3, Bruker AXS Inc., Madison, WI, USA.

(5) Bruker (2012). "SAINT Integration Software for Single Crystal Data", Bruker AXS Inc., Madison, WI, USA. (a).

(6) (A) G. M. Sheldrick (1996). SADABS/TWINABS. University of Göttingen, Germany. (b) Bruker (2001). SADABS/TWINABS. Bruker AXS Inc., Madison, Wisconsin, USA. Bruker (2012). Data Preparation and Reciprocal Space Exploration Program, Bruker AXS Inc., Madi-Son, WI, USA.

(7) Bruker (2012). Data Preparation and Reciprocal Space Exploration Program, Bruker AXS Inc., Madison, WI, USA.

(8) A: O. V. Dolomanov, L. J. Bourhis, R. J. Gildea, J. A. K. Howard and H. Puschmann. "OLEX2: A Com-Plete Structure Solution, Refinement and Analysis Program". J. Appl. Cryst., 2009, 42, 339-341. https://doi.org/10.1021/acs.inorgchem.3c01236.

(9) Sheldrick, G. M. SHELXT - Integrated Space-Group and Crystal-Structure Determination. *Acta Crystallogr A* **2015**, *71* (1), 3–8. https://doi.org/10.1107/S2053273314026370.